RELIABILITY EVALUATION OF A WIND INTEGRATED POWER SYSTEM WITH COMPRESSED AIR ENERGY STORAGE

A Thesis Submitted to the College of

Graduate and Postdoctoral Studies

In Partial Fulfilment of the Requirements

For the Degree of Master of Science

In the Department of Electrical and Computer Engineering

University of Saskatchewan

Saskatoon, Canada

By

Damilola Fadele

PERMISSION TO USE

In presenting this thesis in partial fulfilment of the requirements for a Postgraduate degree from the University of Saskatchewan, I agree that the Libraries of this University may make it freely available for inspection. I further agree that permission for copying of this thesis in any manner, in whole or in part, for scholarly purposes may be granted by the professor or professors who supervised my thesis work or, in their absence, by the Head of the Department or the Dean of the College in which my thesis work was done. It is understood that any copying or publication or use of this thesis or parts thereof for financial gain shall not be allowed without my written permission. It is also understood that due recognition shall be given to me and to the University of Saskatchewan in any scholarly use which may be made of any material in my thesis.

Requests for permission to copy or to make other use of material in this thesis in whole or part should be addressed to:

Head of the Department of Electrical and Computer Engineering
57 Campus Drive
University of Saskatchewan
Saskatoon, Saskatchewan S7N 5A9
Canada

OR

Dean
College of Graduate and Postdoctoral Studies
University of Saskatchewan
116 Thorvaldson Building, 110 Science Place
Saskatoon, Saskatchewan S7N 5C9
Canada

ABSTRACT

World-wide environmental concerns about green-house gas emissions from conventional generation sources have led to an increase in renewable energy penetration in electric power systems. Wind energy as a form of renewable power generation is environmentally friendly and suitable for bulk power generation. Wind power sources however, are intermittent and stochastic in nature and their increased penetration in the electric power system will introduce major challenges to reliable planning and operation of electric power systems. Energy storage systems are receiving considerable attention as potential means to adequately harness the benefits from wind power by absorbing the variability and reducing or eliminating the uncertainty in renewable power generation.

This thesis is focused on compressed air energy storage (CAES) which has a high potential to be used on a grid scale. The ability of the CAES to absorb the variability and mitigate the uncertainty associated with wind energy is explored. The development of a suitable reliability model for the operation of the CAES is presented which proposes a hybrid approach by integrating a Monte Carlo Simulation (MCS) method with an analytical technique. The MCS technique is used to model the state of charge (SOC) of the CAES during the charging operation while recognizing the time chronology and the correlation between the variation in the wind, the load and the SOC of the storage. The analytical technique utilizes a period analysis to quantitatively assess the system adequacy for the diurnal and seasonal sub-periods under consideration. The diurnal analysis with sub-periods within a day captures the operation of the CAES on a daily cycle. The assumption is made that a seasonal period consists of a number of days with similar diurnal profile.

This thesis presents the reliability and economic benefits of CAES being utilized in a number of ways to meet different objectives. The CAES can be operated in coordination with the wind

resources to absorb the variability of wind power to promote renewable energy utilization in the system. A merchant owned CAES operated in an electricity market tries to exploit short term price difference to maximize profit from energy arbitrage. Different scenarios and operating strategies are used to investigate these objectives in this thesis.

An energy management strategy for an annual study is developed and tested using appropriate data. The strategy divides the year into different seasons, and low-cost energy is transferred from the off-peak season to the peak season. The effect of energy management is examined with respect to monetary profit and reliability improvement. Results obtained in this thesis and the conclusions drawn can be a valuable source of information to help utilities in effective and efficient planning of their systems considering CAES.

ACKNOWLEDGEMENTS

I would like to express my sincere and deepest gratitude to my supervisor, Dr. Rajesh Karki, for the mentorship and guidance I received throughout my research work as well as during the preparation of this thesis. I'm so grateful for increasing my depth of understanding in engineering and power system reliability. His patience, time, technical depth and contributions to the success of my studies and this thesis are deeply appreciated. I would also like to thank the College of Graduate Studies and Research, the Department of Electrical and Computer Engineering and NSERC for providing the financial support for my graduate program.

I would like to sincerely thank my committee members for their valuable suggestions and inputs which has greatly improved the quality of this thesis. I am also very grateful to my graduate studies professors. Dr. Sherif O. Faried, Dr. Ramakrishna Gokaraju and Dr. Nurul A. Chowdhury for deepening my knowledge of Power system analysis, power system protection and economic system operation. I would also like to thank all my colleagues in the Power Systems Research Group for their support and the discussions we had in the pursuit of clarity.

To my parents, Pastor & Pastor (Mrs.) F.O. Fadele, your labour of love and prayers cannot be forgotten. Thanks for always believing in me even when I doubted myself. To my siblings Bukky, Funmi, Opeoluwa and Joseph. You guys are the best. Thanks for your patience and understanding. To my Uncle, Pastor (Dr.) James O. Fadel, who played the role of a father to me in Canada, all of this might not have been possible without you. I'm grateful for everything.

My deepest love and appreciation goes to my wife Olumide Olanike Fasakin, thank you for your understanding, love, patience and commitment. There are still so many mountains to climb, the best is yet to come. Thanks for being amazing.

DEDICATION

To the ONE whose strength is inexhaustible and whose wisdom is infinite.

TABLE OF CONTENTS

LIST OF TABLES

LIST OF FIGURES

Figure Page

LIST OF ABBREVIATIONS

A	Availability
AESO	Alberta Electric System Operator
ARMA	Auto Regressive and Moving Average
CAES	Compressed Air Energy Storage
CAPT	Capacity Available Probability Table
COPT	Capacity Outage Probability Table
DPLVC	Daily Peak Load Variation Curve
ESS	Energy Storage System
FOR	Forced Outage Rate
GW	Gigawatt
HL-I	Hierarchical Level I
HL-II	Hierarchical Level II
HL-III	Hierarchical Level III
hrs	Hours
IEEE	Institute of Electrical and Electronics Engineers
IEEE-RTS	IEEE- Reliability Test System
Km	Kilometer
LDC	Load Duration curve
LOEE	Loss of Energy Expectation
LOLE	Loss of Load Expectation
M	Million
MCR	Maximum Continuous Rating
MCS	Monte Carlo Simulation
MTTF	Mean Time to failure
MTTR	Mean time to Repair
MW	Megawatt
MWh	Megawatt Hour
NID	Normally and Independently Distributed
NoCI	Number of Class Interval
pd	Period
PHES	Pumped Hydro Energy Storage
SIPS	Small Isolated Power System
SOC	State of Charge
U	Unavailability
WIPS	Wind Integrated Power System
WTG	Wind Turbine Generator

INTRODUCTION

1.1 Power System Reliability Evaluation

Electric power systems have evolved over the years and have become more complex. The deregulation of the electric power system has introduced major changes to the electric power system in terms of its operation and structure. In deregulated electricity market, different parts of the electric power system are owned by different entities, and therefore there are challenges in accurately synchronising the operation of the independent power producers, transmission system operators, and the distribution system owners. The primary objective of an electric power system is to provide a supply of electrical energy to its customers as economically as possible with an acceptable degree of continuity and quality [1]. The failure in meeting this objective can have very severe consequences to the customers. Spare or redundant capacities in generation and network facilities are often needed to maintain the reliability of the system. Having and maintaining a high level of reliability usually requires a high level of investment. The incremental reliability due to additional investment however decreases as the system reliability is improved. Reliability studies are therefore done to determine the optimal investment in a system, and to find out the incremental reliability for the next dollar invested in the system [1]. Human daily lives are highly dependent on the availability of electric power supply and it is expected that the demand for electric power will keep increasing. As this demand increases, there will be an increasing need to find ways of providing electric power as reliable and economically as possible.

Power system reliability in a general sense is the ability of the electric power system to continuously satisfy the customer demand for electrical energy. It can be divided into basic concepts of security and adequacy as shown in Fig. 1.1.

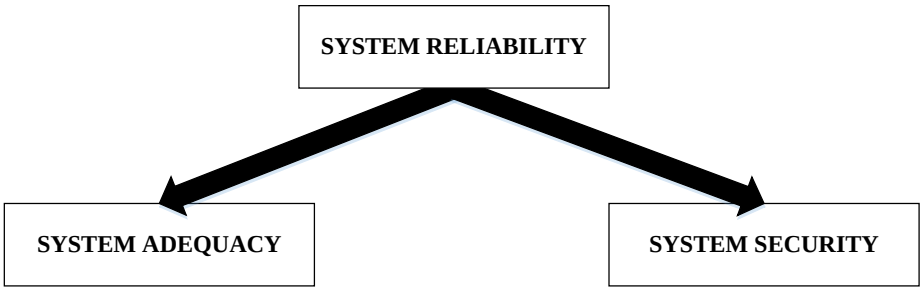

Fig. 1.1: Subdivision of electric power system reliability

The concept of adequacy is generally considered to be the existence of sufficient facilities within the system to satisfy consumer demand. The basic aim of generating capacity adequacy evaluation is to determine if the power system has enough generating facilities to meet the system load demand [1]. Adequacy is associated with static conditions which do not include system disturbances. Security, on the other hand, is considered to relate to the ability of the system to respond to disturbances arising within that system. Security is therefore associated with the response of the system to whatever disturbance they are subjected to. These are considered to include conditions causing local and widespread effects and loss of major generation and transmission facilities [1]. The scope of the work presented in this thesis is restricted to the area of adequacy studies of electric power systems.

A modern electric power system is complex, highly integrated and very large. It is therefore, very impractical to attempt to analyse the system as a whole; not only will the amount of computation be excessive, but the results are likely to be so vast that meaningful interpretations will be difficult, if not impossible [1]. The most convenient approach is to divide the whole system into its three main functional zones of generation, transmission and distribution. These functional zones are combined to create the three hierarchical levels as shown in Fig. 1.2.

The reliability assessment at the hierarchical level 1 (HLI) refers to the generation facilities and their ability on a pooled basis to satisfy the pooled system demand. Research at this level is usually done to determine the future generation capacity requirements of an electric system. HLI analysis is the most basic type of reliability study that can be done and a lot of research work has been done in this area. Ref. [2-5] contain large number of work done in this area. The second level

(HLII) refers to the composite generation and transmission system, or the bulk power system, and its ability to deliver energy to the bulk supply points. HLII studies are relatively more complex compared to HLI and considerable amount of work [2-7] have been done in this area as well. HLIII study on the other hand refers to the complete system including distribution and its ability to satisfy the capacity and energy demands of individual consumers. HLI and HLII studies are frequently performed but a complete HLIII studies is usually not done because of its scale and impracticality, instead, the distribution functional zone can be assessed independently and results analysed. The research work described in this thesis is restricted to HLI.

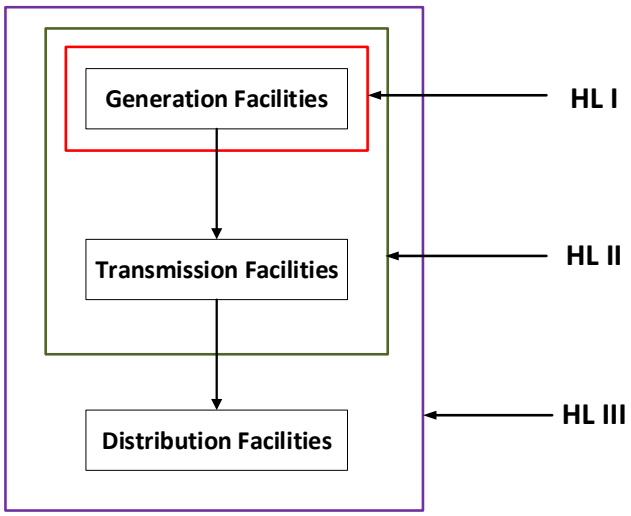

Fig. 1.2: Hierarchical level

1.2 Wind Energy and Power System Reliability Evaluation

Conventional method of generating electricity has adverse effect on the environment as it introduces greenhouse gases to the atmosphere, and because of this, a lot of attention has been turned towards renewable electrical energy supply. A Renewable Portfolio Standard (RPS) [8, 9] is a policy which requires that a certain portion of the total electrical generation comes from renewable energy sources within a certain time limit. Many countries have adopted this policy. In Canada, the province of Saskatchewan has set an objective to develop wind, solar and geothermal power to meet up to 50% renewable target by 2030. Today, about 25% of Saskatchewan's generation capacity comes from renewable sources – 20% from hydro and 5% or 220 megawatts

(MW) from wind. Three new wind power projects already approved or in development will add another 207 MW of renewable generation by 2020 [10]. Other provinces in Canada have adopted various forms of RPS. Wind energy is one of the most widely adopted technology of renewable energy due to its huge potential for large scale power production and its minimal environmental pollution.

Wind energy is one of the fastest growing renewable energy source. By the end of year 2015, global installed wind power capacity was more than 430 GW, total installed wind capacity in Canada was over 11 GW while it was over 74 GW and 147 GW in the USA and Europe respectively [11]. Fig. 1.3 shows the global cumulative installed wind capacity from year 2000 to 2015, it clearly shows a rising trend in wind capacity installed and this increase in high levels of wind power penetration in the electric grid is expected to continue in the foreseeable future. Fig. 1.4 also shows the total installed wind capacity in Canada with the province of Ontario having the largest installed wind capacity among all the provinces and territories and the province of Saskatchewan having 221 MW installed wind capacity [12].

Conventional generating units (CGU) are quite different from wind energy sources in that they can generate constant power outputs at all time with the few exceptions of when they undergo partial or complete failures. Wind energy sources are variable in nature, and even at a site with a high wind power potential, the wind can blow and stop frequently in a short period and can be totally absent when it is most needed [13]. Electricity generated from wind can be highly variable at several time scales; hourly, daily, seasonal and annually. Because instantaneous electrical generation and consumption must remain in balance to maintain grid stability, this variability can present substantial challenges to incorporate large amounts of wind power into a grid [14]. Evaluation models to represent wind energy sources are quite different from the models used in conventional sources because of their variable nature.

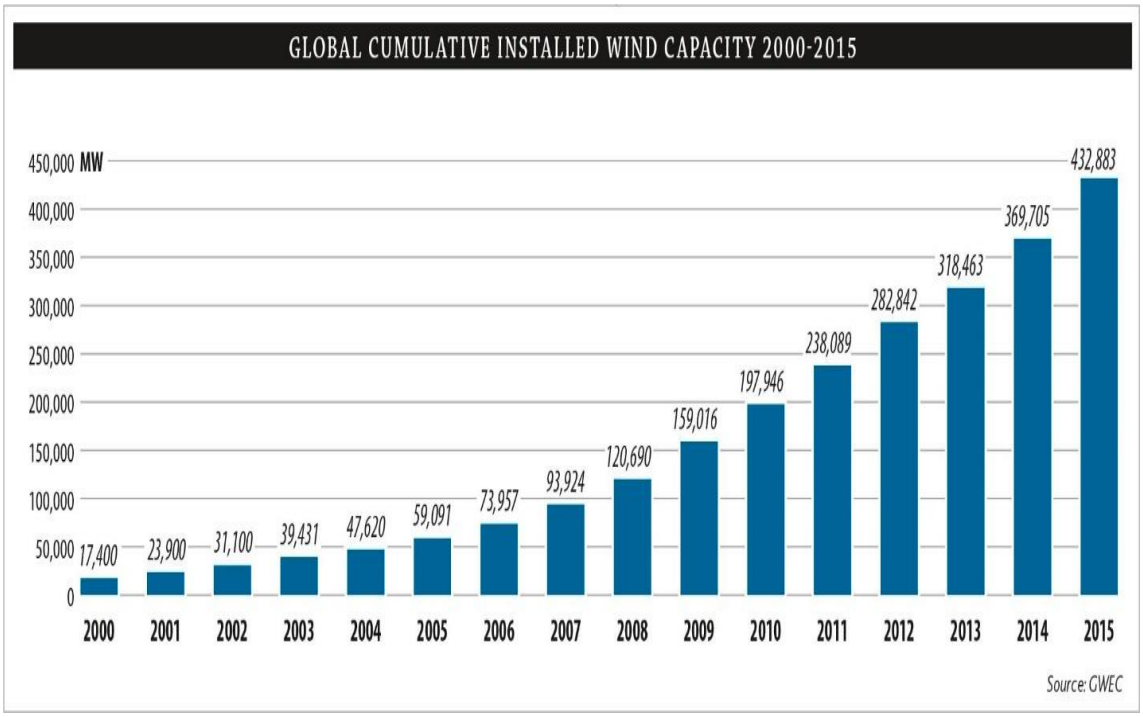

Fig. 1.3: World wind electricity-generating capacity, 2000-2015. (Source: *global wind energy council*, *www.gwec.net*)

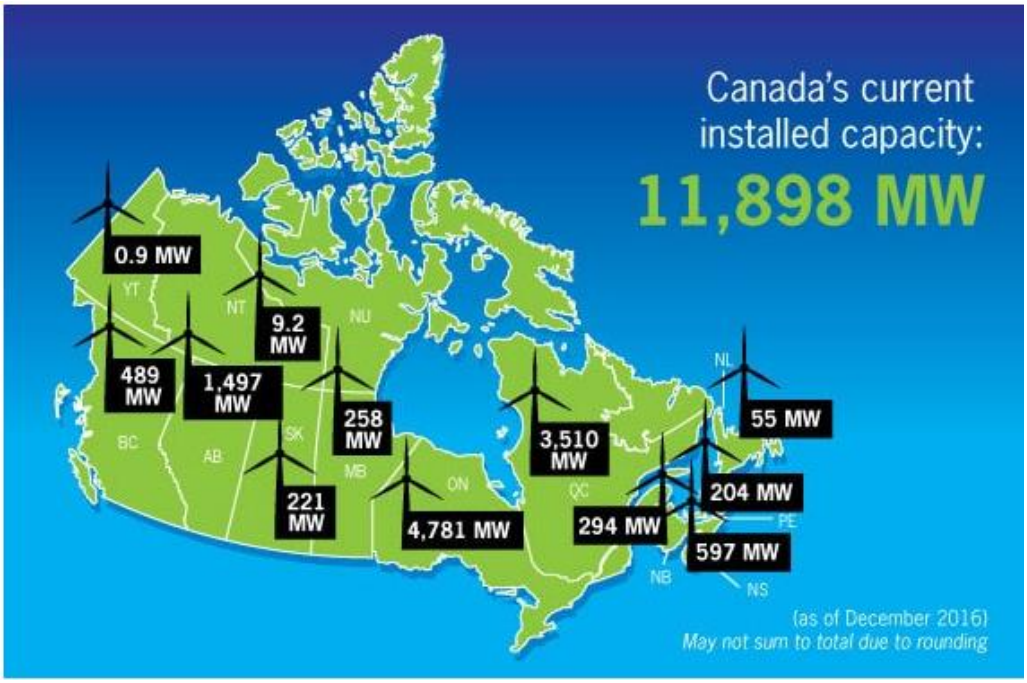

Fig. 1.4: Total installed wind capacity in Canada as of December 2016. (Source: *Canadian wind energy association*, *www.canwea.ca*)

The wind turbine generator (WTG) is the main component in converting wind speed to wind power and its design characteristics can determine how much power can be harnessed from various wind speeds. Important parameters in performing an adequacy evaluation of a wind integrated power system are the WTG characteristics and the wind speed regime at the particular wind site. The relationship between the wind speed and the output of the WTG is usually provided by the wind turbine manufacturers in the form of a non-linear relation known as the wind power curve [15]. The variation in electric power generation from wind energy sources and the uncertainty associated with the power output levels causes significant challenges in the planning and operation of a power system to meet the projected demand with an acceptable level of reliability. The system risk associated with these uncertainties is significant at high level of wind energy penetration in the power system.

Significant research has been done in the area of power system reliability including wind energy in the past years. A procedure to incorporate the WTG power for determining the impact of wind generation on system reliability is developed in [15]. An algorithm is developed in [16] to model the reliability characteristics of large electric utility with WTG and the application of this model to determine the annual energy output of a grid connected wind farm. Ref. [17] presents a technique to obtain multi-state power output models of WTG units for reliability evaluation. Ref. [18] presents a simplified multi-state wind power generation model with reasonable accuracy for reliability evaluation. This model was used to develop a common wind speed model applicable to multiple wind farm locations. A simplified wind speed model was developed in [19] that can generate wind speed probability distributions for multiple wind farm sites if their annual mean wind speed and standard deviations values are known. The model developed combined with the WTG characteristics to obtain the wind farm generation model was modified to incorporate the effect of the transmission line on wind power delivery system.

1.3 Reliability Considerations in Generating Systems Containing Wind Energy and Energy Storage

Large scale integration of wind power in an electric grid produce large power fluctuations

and result in increased challenges in providing a continuous power supply [20]. There are serious reliability and stability concerns in a power system with high degree of wind penetration. The variability and intermittency of wind can be absorbed using an energy storage system (ESS). Energy can be stored in a variety of forms, such as solid-state batteries, flow batteries, flywheels, compressed air energy storage (CAES), pumped hydro storage (PHES) and thermal storage [21]. Lithium Ion (LI-ION) batteries, Nickel-Cadmium (NI-CD) batteries, Sodium Sulfur (NAS) batteries are some examples of common solid-state batteries. Redox Flow batteries, Iron-Chromium (ICB) Flow batteries, Vanadium Redox (VRB) Flow batteries and Zinc-Bromine (ZNBR) Flow batteries are examples of flow batteries [21].

The magnitude of the energy the ESS can store, and the time scales involved are especially important in the operation of an energy storage system [22]. As an example, flywheels would be particularly well suited to provide large amount of power for short periods of seconds to minutes. When larger amounts of electrical energy are needed for periods of hours or longer, PHES or CAES would be the more suitable energy storage systems [22]. PHES and CAES systems could be referred to as grid scale energy storage systems because of their ability to store large amount of energy for long periods. Various applications of ESS include peak shaving, load levelling, renewable energy integration, energy management, standby power etc. The focus of this research will be on the CAES and its contribution to the reliability of the power system, utilizing as much wind as possible in conjunction with CAES. Some review of the works done utilizing CAES include [23] which presents comparative technical and cost data associated with 25 MW - 220 MW CAES technology used as a load levelling tool on the utility side of the meter during intermediate and peaking time periods. The data included steady-state and dynamic load following characteristics. The performance of a CAES plant is presented in [24], and its generated energy, energy ratio (ER) and primary energy efficiency was evaluated over a wide range of pressure ratio and load, which depended on the rate of air discharged. A computer program was specially designed to evaluate these performances. The results obtained show that the CAES plant produces about 30% more power than that consumed during the off- peak period. It also produced about three times the power of a conventional gas turbine plant and enjoyed economic superiority at part

load. Ref. [25] evaluated the potential values and benefits that CAES can bring to Midcontinent Independent System Operator (MISO), and the revenue/cost that CAES will get from both energy and ancillary service market by using production cost simulation software (PLEXOS). This was done by comparing the CAES with a combine cycle (CC) unit and appropriate evaluations were carried out. Ref. [26] investigated and compared two scenarios; one without CAES and a second with CAES as an additional resource in the 2020 Irish power system using power system and market modelling tool PLEXOS. It was concluded that a 270 MW CAES plant can displace a significant fraction of coal and natural gas generators. In [27], a study was done on how to find the optimum tank volume, associated with the minimum mass of the tank and the maximum time of feeding diesel generator with CAES. In the area of reliability evaluation, not much research has been done. Part of this research will focus on using CAES as an energy storage and doing a reliability evaluation of it.

1.4 Problem Statement and Research Objectives

An increasing need to protect the environment from harmful emissions has led to the adoption and implementation of RPS by different countries and jurisdictions, and therefore, there has been a rapid growth of wind power in electric power systems. The increase in power fluctuations because of high wind power penetrations in power systems has caused increased challenges in maintaining the system reliability at an acceptable level. It is expected that this trend of wind penetration increase in electric power systems is set to continue, and with this increase, the reliability of the electric power system may further deteriorate. Refs. [15-19] show the research done in the area of power system reliability incorporating wind energy using analytical and simulation techniques. As wind penetration increases, there is a need to have accurate models that can recognize the variation of wind, its absorption in the system and incorporate the correlation between the load and the wind characteristics as described in [9]. Energy storage is receiving considerable attention in recent time as a potential technology that can be used to absorb the variability of the wind and smooth out the wind fluctuations to improve the continuity of supply

and to maintain the electric power system at an acceptable reliability level.

Adequacy evaluation of a wind integrated power system using analytical technique is usually done on an annual basis [1] but to incorporate the correlation between wind and load, a period analysis is used. The wind speed characteristics of a wind farm site exhibits a variation pattern on a seasonal basis as well as on a diurnal basis. The load also generally has an inherent seasonal and diurnal variation. A certain level of correlation exists between the wind speed and the load and this must be factored in when operating the ESS.

This research work focuses on quantifying the contribution of the CAES in integrating wind variations and maintaining system reliability. Some works have been done in the area of reliability assessment of power system incorporating other storage technologies using generalised storage characteristics, and the battery energy storage system (BESS). The research works include [28] which presents a simulation technique that extends the conventional well-being approach to generating systems using energy storage. This technique is applied to several small stand-alone power systems. Ref. [29] presents a time series simulation technique to evaluate the system adequacy of a small stand-alone wind energy conversion system with battery storage. An application of energy storage in small isolated power systems (SIPS) was discussed in [30]. The paper describes a sequential Monte Carlo simulation (MCS) method for incorporating energy storage capability in generating capacity adequacy evaluation of such systems. Ref. [31] investigates the benefits obtained from utilizing wind energy for electric power generation using reliability and economic evaluation techniques. This paper presents a reliability cost/worth evaluation method that can incorporate the impacts of wind energy and energy storage utilization in electric power systems. A novel analytical approach of reliability evaluation for wind-diesel hybrid power system with battery bank for power supply in remote areas was proposed in [32]. The proposed approach is developed on the basis of the discrete wind speed frame analysis of the Weibull wind speed distribution. Ref. [13] presents a simulation technique to assess the long-term reliability benefits of energy storage considering different scenario such as storage capacity and operating constraints, wind energy dispatch restrictions, wind penetration level and wind farm location on the reliability benefits from energy stored. Ref. [13] introduces an energy storage

model that can include the energy storage operating constraints for reliability evaluation using the MCS method. Ref. [33] presents assessment of the generation adequacies of power systems including WTG and ESS using Monte Carlo simulation, taking account of two different objectives of installing wind farms. One objective is to replace the conventional power plant by WTGs while the other is installing them to meet the load growth and maintain the system adequacy. Refs [14, 34] both present an analytical method to evaluate the reliability of power systems with WTGs and energy storage. Also, the impacts of energy storage on reliability of power systems with WTGs was analyzed. The expected energy not supplied (EENS) index was used to investigate the impacts of the rated capacity of energy storage and charging/discharging rate.

The CAES as the choice of energy storage in electric power system operation and planning is gaining momentum, and some research work has been carried out in this regard. The role of CAES in addressing the issue of transmission constraint in power systems was presented in [35-37]. The idea that distributed energy storage technologies, with next-generation storage devices, are most likely to fill the role for energy storage in solving the current problems of stressed electricity supply systems especially in the area of transmission was discussed in [35]. Ref. [36] considered the estimation of the values of benefits and costs for applying energy storage to three situations on the Niagara Mohawk Power Corporation system with the third situation being a case of thermal overload on a transmission line to a growing load in an environmentally sensitive location while a real-time optimal dispatch algorithm was proposed in [37] by formulating a mixed integer linear programming problem to determine dispatch quantities for a privately-owned ESS operating in an open electricity market and how to relief transmission congestion using CAES as an energy storage.

Refs. [38-41] studied the role CAES plays in grid voltage stability. A comprehensive ESS application design for regulating wind power variation and increasing wind energy integration and grid voltage stability was discussed in [38]. The design included a method for calculating a reference output profile, a charge-discharge scheme for directing the ESS operation, and an optimization-based method for determining ESS optimal rating. Ref. [39] investigated the use of these CAES and PHES to increase wind farms transient stability by dynamic reactive

compensation. In [40], a generalized energy storage system model for voltage and angle stability analysis was presented. The proposed solution allows modeling most common energy storage technologies through a given set of linear differential algebraic equations. The issue of power system security and stability analysis was discussed and a CAES model was developed in [41].

Refs. [27, 42-46] present work in the area power system operation, planning and optimization. In [42], a co-optimization approach to determine the optimum operation and planning of a wind generation-CAES system using particle swarm optimization was presented. Two optimization methodologies were used to optimize the short-term operation and long-term planning of the wind generation-CAES system in [42]. Ref. [43] deals with the optimal placement of the energy storage units within a deregulated power system to minimize its hourly social cost. The optimal operation of CAES without considering renewable generation was studied in [44]. Ref. [45] shows how the amount of energy dispatched and the profit may be improved by adding CAES to wind generation. CAES was incorporated to enhance the operation of grid-integrated wind generation, considering the electricity market prices in [46] while [27] studied how to find the optimum tank volume, associated with the minimum mass of the tank and the maximum time of feeding diesel generator with CAES

Refs. [23, 25-26, 47] studied the economics involved in utilizing CAES with a power system. In [47], a stochastic electricity market model is applied to estimate the effects of significant wind power generation on system operation and on economic value of investments in compressed air energy storage. Ref. [23] presents technical and cost data associated with the compressed air energy storage technology which is a load levelling tool on the utility side of the meter during intermediate and peaking time periods. Ref. [25] evaluated the potential values that CAES can bring to Midcontinent Independent System Operator, and the revenue/cost that CAES will get from both energy and ancillary service market by using production cost simulation software (PLEXOS) while [26] investigated economic feasibility of two scenarios; one without CAES and a second with CAES as an additional generator in the 2020 Irish power system using power system simulation software PLEXOS.

A number of research works studied the modeling of CAES as seen in [42, 48-53]. In [42],

a model of a wind generation-CAES system which can generate, store, and sell electricity to the grid was developed. The authors in [50] provided a model for CAES considering the mass and energy balance inside the reservoir. Some of these studies include the intermittency of wind generation in their models as well [51-53].

In the reliability assessment of electric power system incorporating wind energy and CAES, little research work has been done and one of the major contribution of this thesis is creation of a simple and appropriate CAES hybrid reliability model that can be used for electric power system reliability assessment. The operating strategy of the CAES can have significant impact on the electric power system reliability. Different scenarios and operating strategies are utilised, results compared, and valuable information is provided for power system reliability evaluation, planning and decision making.

The scope of this research work is concentrated on the development of HLI adequacy evaluation model for an electric power system including wind energy and CAES, and assessing different scenarios and operating strategies for the different operation of the CAES and their corresponding reliability contributions.

The objective of this research work is summarized below;

- To develop a technique to incorporate seasonal as well as diurnal correlations between wind speed and load.
- To develop a simplified CAES state of charge (SOC) reliability model using suitable methods.
- To investigate the possible impacts of CAES on the reliability of relatively large electric power systems with high wind penetration.
- To incorporate market scenarios and operating strategies in reliability evaluation of CAES integrated power systems.
- To assess the reliability contribution of CAES under different operating scenarios.

1.5 Outline of the Thesis

This thesis consists of six chapters. The main content of each chapter is described below.

Chapter 1 introduces the basic concept regarding generating systems reliability and the incorporation of wind in HLI reliability assessment. The challenges faced with the increase in wind power penetration is discussed. A brief review of the available literature on reliability assessment of power systems containing wind power and energy storage is presented. The chapter describes the problem and outlines the research objective of the thesis, scope and the outline of the thesis.

Chapter 2 reviews the basic reliability concepts and techniques for generating system adequacy evaluation. Basic generation models, load models and the convolution of these two models to obtain the risk model using probabilistic methods are introduced. Incorporating wind model to the available generation model is also discussed. Analytical techniques and Monte Carlo simulation methods widely used in probabilistic power system reliability evaluation are discussed as well.

Chapter 3 introduces the compressed air energy storage, its operation and the different units that make up the CAES. The existing and proposed CAES plants are highlighted. Different advancements in the CAES technology are discussed and mathematical models for converting flow of atmospheric air into power in MW are discussed.

Chapter 4 looks at the development of the reliability model of the CAES using a hybrid technique of both analytical and Monte Carlo simulation. The periodic analysis of the load model and wind model is done for the diurnal, seasonal and yearly period. Three different scenarios of the CAES interconnection are considered and two different operating strategies of the CAES from is discussed as well.

Chapter 5 presents an approximate technique to assess the strategy of the merchant when operating the CAES. A 3-period analysis is considered, and studies are done on a seasonal basis. Cost-Benefit estimation of the 3-period analysis for the winter season is estimated. An annual analysis is done with the objective of implementing energy management; transferring energy from a season with very low load demand to a season with very high load demand and recommendations

are made.

Finally, Chapter 6 summarises and concludes the thesis.

2. BASIC CONCEPTS AND TECHNIQUES FOR GENERATING SYSTEM ADEQUACY ASSESSMENT FOR WIND INTEGRATED SYSTEMS

2.1 Introduction

The determination of the required amount of system generating capacity to ensure an adequate supply is an important aspect of power system planning and operation. A suitable reliability evaluation technique is therefore required in planning an electric power system to ensure a continuous power supply in the future planning horizon. A major objective in reliability evaluation is to create appropriate techniques to assess the continuity of supply. The primary purpose of adequacy evaluation at the HL-1 level is to assess the ability of the generating facilities to meet the total system load demand. In an HL-1 reliability evaluation, the reliability of the transmission facility and its ability to deliver the available generation to the different load points is not considered. The system representation in a conventional HL-1 study is shown in Fig. 2.1 [1]. The HL-1 model considers the entire system generation supplying the aggregated system load.

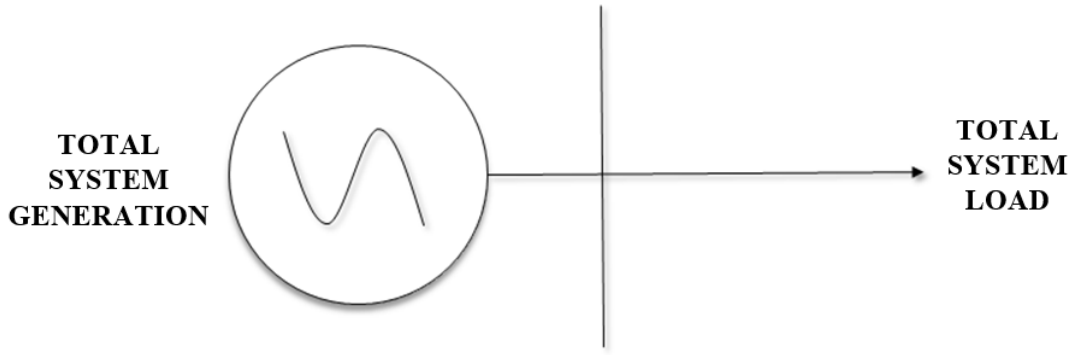

Fig. 2.1: Basic system model for HL-1 generating system adequacy assessment

In determining the total available generation to meet the total system load demand, certain factors have to be put in consideration such as uncertainty in load variation, generating unit failures and repairs and the periodic maintenance of the generating units. Different techniques have been

used by electric power utilities to carry out HL-1 reliability studies of the electric power system. In the past, HL-1 reliability studies were done using deterministic techniques [1]. These techniques are still used in some SIPS and in some large power systems as well. In most modern large electric power systems, probabilistic techniques are used instead. These two techniques are described below.

2.2 Deterministic Evaluation Techniques

Electric power system planning has been done in the past by applying deterministic techniques [54]. The common deterministic techniques are highlighted below:

1. Capacity Reserve Margin (CRM)

Capacity reserve margin is defined as the amount of excess generation capacity over the system peak load (PL). The capacity reserve margin is expressed as a percentage of the system PL or the total installed capacity (IC) as seen in Equation (2.1). A fixed percentage of CRM is used as the criterion for capacity requirement in this method. The percentage value is chosen based on past experience.

$$CRM = \frac{IC-PL}{IC} * 100\% \quad (2.1)$$

2. Loss of the Largest Unit (LLU) or (N-1)

The LLU is a commonly used deterministic technique for assessing the reliability of an electric power system [1]. This technique requires that a reserve should be maintained equivalent to the capacity of the largest unit in the generation system. This is also known as the "N-1" method. The capacity reserve margin is at least equal to the largest generation unit. This method is being used in SIPS.

3. Loss of Largest Unit and a Percent Margin

This method combines the above two methods and has also been used in the past. Here the capacity reserve should not be less than the capacity of the largest unit in the system plus a fixed percentage of either the system PL or total IC.

The deterministic techniques evaluate the system adequacy largely based on past experiences and personal judgments and can be used to easily evaluate the total capacity required in the overall power system. This method is however incapable of accounting for the stochastic nature of power system behavior [55]. The three deterministic techniques mention above cannot determine the true risk of the electric power system because of their failure to recognize and incorporate the inherent random nature of generating unit failures and uncertainty in load variations. As a result of this deficiency, their applications to generation planning for very complex power systems are severely limited. Probabilistic methods, on the other hand can recognize the inherent random nature of electric power system. Table 2.1 presents a summary of a survey taken from 1964-1987 showing the criteria in use at the time by different Canadian utilities for capacity reserve planning [54, 56].

Table 2.1: Criteria used in capacity reserve planning

Criterion Used	**Number of Utilities in Year**					
	1964	**1969**	**1974**	**1977**	**1979**	**1987**
Percent Margin	1	4	2	2	3	1*
Loss of Largest Unit	4	1	1	1	-	-
Combination of 1 and 2	3	6	6	6	2	-
Probability Methods	1	5	4	4	6	6
Other Methods	2	1	-	-	-	-

* With supplementary checks for probabilistic index LOLE

As can be seen from Table 2.1, only one utility indicated that it used a probabilistic approach in 1964. By 1987, most utilities have turned to probabilistic technique with the exception of one utility using a deterministic criterion with supplementary checks for probabilistic index [54].

2.3 Probabilistic Adequacy Evaluation Models

There are fundamentally two approaches used in calculating the reliability indices in a probabilistic evaluation; (1) analytical method and (2) simulation method, commonly called the Monte Carlo Simulation (MCS) [1, 57]. Analytical techniques represent the system by a mathematical model and evaluate the reliability indices from this model using direct numerical solutions. The advantage of this approach is the fast computation time. The disadvantage is that assumptions are frequently required because of the inability of the analytical technique to model and incorporate complex systems and operating procedures. Simulation methods estimate the reliability indices by simulating the actual process and random behaviour of the system. The reliability indices are obtained by observing the simulated operating history of the system. The advantage of the MCS method is its ability to model very complex system while its disadvantage is the high computation time and system resources involved.

2.3.1 Analytical Techniques

The analytical evaluation of generating capacity adequacy can provide information on the likelihood that the available generation will be unable to serve the system load. The generation model in most analytical technique is developed using convolution of probability density functions to obtain a capacity outage probability table (COPT) [1]. The COPT is a simple array of capacity levels and the associated probabilities of their occurrences. The creation of a COPT is an important procedure in generating capacity reliability evaluation using an analytical technique.

Various methods have been proposed for constructing a capacity model [1, 58-59]. A recursive technique can be utilised to construct the COPT by adding a multi-state generating unit

in the COPT one at a time in a loop process until all the units in the system have been considered as seen in [1].

A generating unit with a capacity of C MW is considered to be either fully up or fully down in a two-state model. The cumulative probability of a particular capacity outage state of X MW after a unit of capacity C MW and forced outage rate U is added given by (2.2) [1].

$$P(X) = (1 - U)P'(X) + (U)P'(X - C) \tag{2.2}$$

Where, P'(X) and PP(X) denote the cumulative probabilities of the capacity outage state of X MW before and after the unit is added. Equation (2.2) is initialised by setting P'(X) =1.0 for $X \leq 0$ and P'(X) =0 otherwise [1]. For a generating system with generating units that has derated states. Equation (2.3) is a more general recursive algorithm that can incorporate multi-state units [1].

$$P(X) = \sum_{i=1}^{n} p_i \, P'(X - C_i) \tag{2.3}$$

Where;

n = the number of unit states

C_i = capacity outage of state i for the unit being added

p_i = probability of existence of the unit state i.

The COPT is combined with an appropriate load model such as the load duration curve (LDC) or the daily peak load variation curve (DPLVC) to evaluate the system risk indices such as the loss of load expectation (LOLE). Fig. 2.2 shows the method of combining the different system capacity states in a generation model with the DPLVC load model.

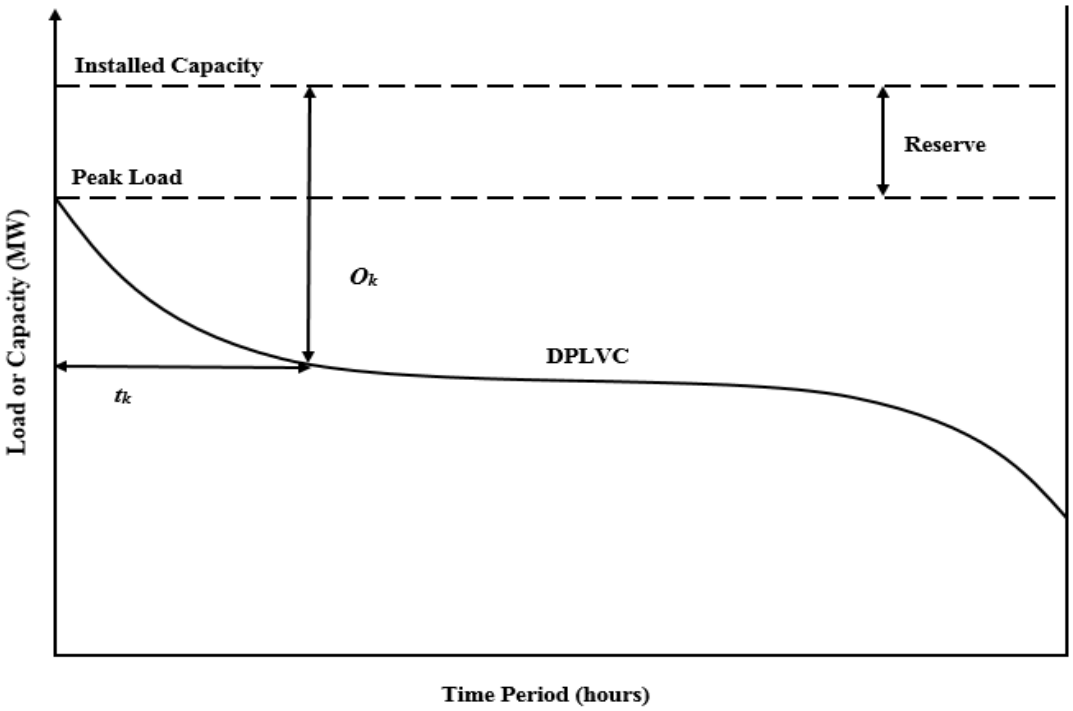

Fig. 2.2: Loss of load method

It can be seen from Fig. 2.2 that any capacity outage less than the reserve will not contribute to system LOLE. Outage of capacity in excess of the reserve will result in varying numbers of time units during which loss of load could occur. It is also seen that a capacity outage O_k in excess of the reserve will cause a loss of load for a time duration t_k. Expressed mathematically, the system LOLE for a specified time is seen in equation (2.4).

$$LOLE = \sum_{k=1}^{n} p_k * t_k \qquad (2.4)$$

Where;

n = the number of capacity outage states in the COPT.

p_k = probability of the existence of the capacity outage O_k.

t_k = duration of outage if the loss of load occurs due to outage O_k.

The p_k values in Equation (2.4) are the individual probabilities associated with the capacity

outage states. Equation (2.5) is used to calculate the LOLE when cumulative state probabilities are used.

$$LOLE = \sum_{k=1}^{n} P_k * (t_k - t_{k-1}) \tag{2.5}$$

Where P_k is the cumulative outage probability for capacity state O_k.

The evaluation period is usually a year. The LOLE is expressed in days per year when the DPLVC is used as the load model. The LOLE is measured in hours per year when the LDC is the load model. The area under the LDC curve represents total system energy requirement in a given period. Fig. 2.3 shows that any outage of generating capacity which exceeds the reserve can result in system load curtailment. The energy curtailed is given by the shaded area in Fig. 2.3.

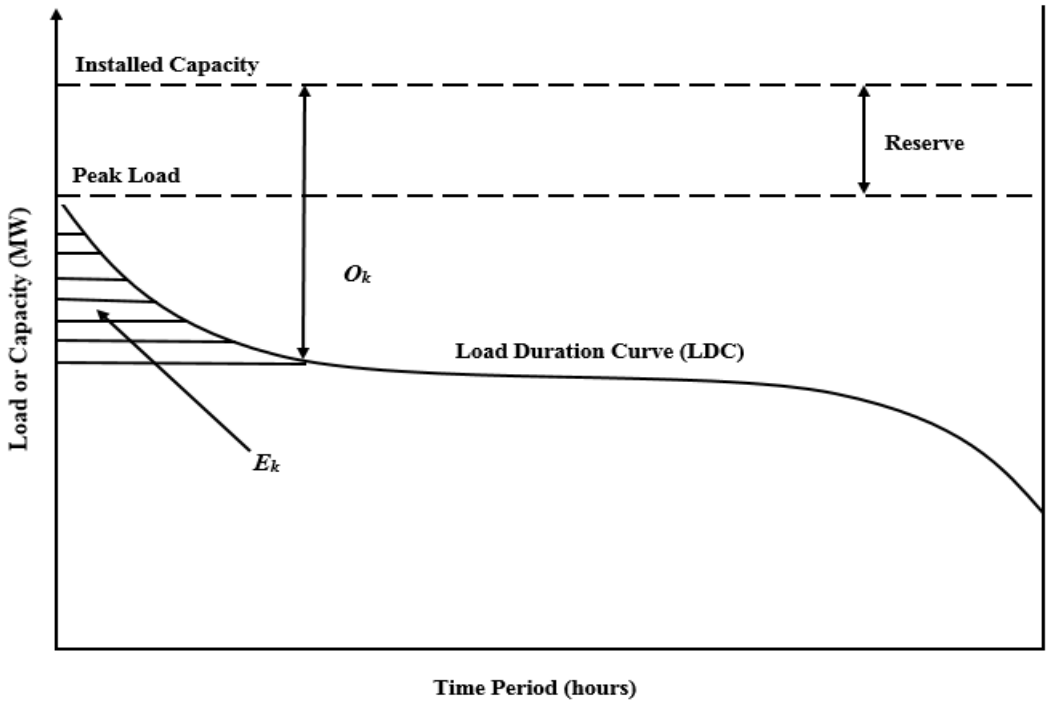

Fig. 2.3: Loss of energy method

If O_k is the magnitude of the capacity outage, p_k is the probability of the capacity outage, and E_k is the energy curtailed by the outage, the total expected energy curtailed or LOEE can be calculated as seen in equation (2.6).

$$LOEE = \sum_{k=1}^{n} p_k * E_k \tag{2.6}$$

It is difficult to compare the reliability of systems with different sizes using the LOEE index as the LOEE of the large system will generally be greater than that of the small system regardless of their reliability levels. Therefore, LOEE can be normalised by the total energy demand of the system or the system peak to obtain reliability indices which can be utilised to compare various power systems. The units per million (UPM) index is obtained when the LOEE index is normalised by the annual energy demand [1]. The resulting number is multiplied by one million as shown in (2.7).

$$UPM = \frac{LOEE}{Annual\ energy\ demand} * 10^6 \tag{2.7}$$

The Saskatchewan Power Corporation (Saskpower) uses a reliability criterion of 200 UPM [54] for HL-I adequacy analysis.

Another reliability index which can be derived from LOEE is system minutes (SM) [1]. This is obtained by normalising the LOEE by the system annual peak load as shown in (2.8).

$$SM = \frac{LOEE}{Annual\ peak\ load} * 60 \tag{2.8}$$

There exist various alternative methods for the analytical approach for HL-1 adequacy assessment. Examples include the load modification method and the frequency and duration (F&D) approach. The frequency and duration method uses Markov models to represent the generating units and the system load. Additional data such as the state transition rates for the generating units and the load are required for the F&D calculations. The basic concepts for this method are presented in [56] while its application in adequacy evaluation is seen in [1]. For complex systems, analytical technique for adequacy evaluation may not suffice and results obtained might be inaccurate based on assumptions made in order to simplify the complex system. The MCS approach will be appropriate for such systems, and this technique is discussed in the

next section.

2.3.2 Monte Carlo Simulation Method

A simulation technique provides an alternative method to evaluate the adequacy indices. This technique can easily take into account virtually all aspects and contingencies inherent in the planning, design, and operation of a power system. These include random events such as outages and repairs of elements represented by general probability distributions, dependent events and component behaviour or failure, queuing of failed components, load variations, variations of energy input for hydrogenation, as well as all different types of operating policies [1].

In the case of modelling energy storage such as CAES, it will be difficult to model the chronological variation in the SOC dependent on load variation and renewable generation during charging or discharging period using analytical approach. Failure is a random event and can occur anytime, this has an effect on how much we have in storage during charging and how much we can put out during discharge. The past history has an effect on present conditions. Stochastic simulation can take care of this challenge easily and is a practical technique for systems that contain a large number of time dependent random variables [1].

The main disadvantage of the simulation methods is that it requires extensive amount of computation time and computing resources. The rapid development of computer technology has, however, made this less of a problem in modern times.

Generally, stochastic simulation methods for power system reliability assessment are known as Monte Carlo simulation (MCS). The simulation process can be broadly categorised into two namely; state sampling and sequential methods [60].

2.3.2.1 State Sampling Method

A system state depends on the combination of all component states and each component state can be determined by sampling the probability that the component appears in that state. The state sampling method is carried out by assuming that the behaviour of each component can be

described by a uniform distribution between [0, 1] denoting that the component is either in the success state or failure state, and the system available capacity can be obtained by summing the individual capacity of each available generating unit [60]. Another uniform random number is generated to determine the system load level using the DPLVC or LDC. The total available system generation is compared with the system load to determine if a loss of load event has occurred. This process is simulated for large number of sample years to achieve convergence or until a specified stopping rule indicates that the process has converged.

Time chronology is not a factor in this simulation process and the system behaviour at each time interval is considered to be independent. This approach can be used if the previous state i.e. the history has no effect on the future state and generally, on the overall impact on system reliability indices.

When an electric power system contains non-conventional sources such as wind power and energy storage facilities, chronology becomes very critical in assessing the reliability of the system because the chronology of events is time dependent and correlated. The state sampling method will be inadequate to carry out this kind of evaluation. The sequential simulation method will be an appropriate technique in such cases.

2.3.2.2 Sequential Monte Carlo Simulation Method

The sequential MCS method can be used to examine and simulate each basic time interval for the simulated period in a chronological order with the recognition that the system state in a given time period can be dependent with that in the previous time period. An operating history of each generating unit can be simulated in time chronology using random number generators. Using this method, the system capacity model is obtained by aggregating the operating history of all the generating units in the system. This system generation model is then superimposed on the load model to form the system risk model [1].

The mean time to failure (MTTF) and the mean time to repair (MTTR) are the main parameters used to create an operational history for each individual generating unit [1, 60]. These parameters in conjunction with random numbers between [0, 1] are used to produce a state history consisting of a series of random up and down times called state residence times for each generating unit in the system. The state residence time is sampled from its probability distribution. An exponential distribution is assumed for the times to failures and repairs in this thesis. The operating history of a typical generating unit is shown in Fig. 2.4 modelled as a two-state unit [61].

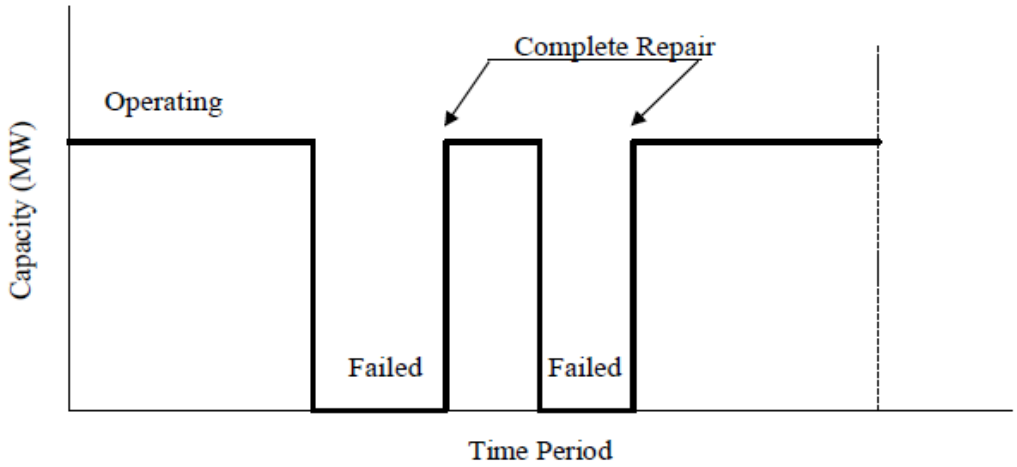

Fig. 2.4: Operating history of a conventional generating unit

If the state residence time is represented by an exponentially distributed random variable *t*, the corresponding probability density function is given by equation (2.9) [60],

$$f(t) = xe^{-xt} \tag{2.9}$$

Where x is the reciprocal of the mean value of the distribution. Its cumulative probability distribution function is given in equation (2.10)

$$F(t) = 1 - e^{-xt} \tag{2.10}$$

The inverse transform method [59] is utilised and random variable t can be obtained as seen in equation (2.11)

$$t = F^{-1}(U) = -\frac{1}{x}1n(1-U) \tag{2.11}$$

Since (1-*U*) distributes uniformly in the same way as *U* in the interval [0, 1]

$$t = -\frac{1}{x}1n(U) \tag{2.12}$$

The load model in a sequential MCS is usually a chronological hourly load model as seen in Fig. 2.5, and is generally modelled in hourly time steps. The overall system adequacy indices are assessed by aggregating the individual generating unit operating states and durations to form the total system capacity model and superimpose this on the load model as seen in Fig. 2.6 [61]. This approach will be very useful in modelling the operation of the CAES while incorporating failures and repairs in the overall process.

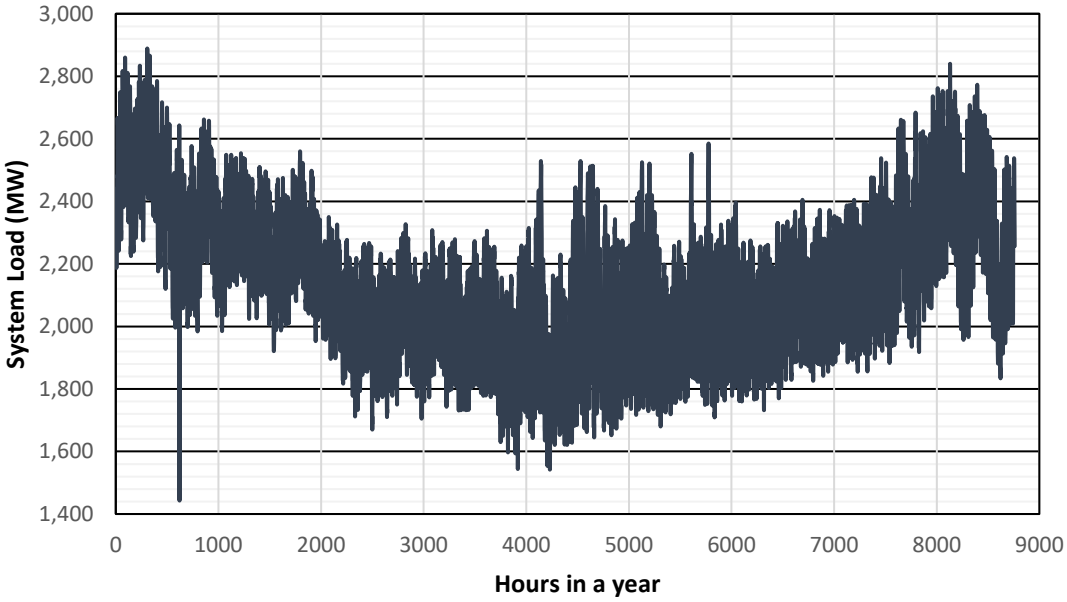

Fig. 2.5: Chronological hourly load model for a sample year in Saskatchewan

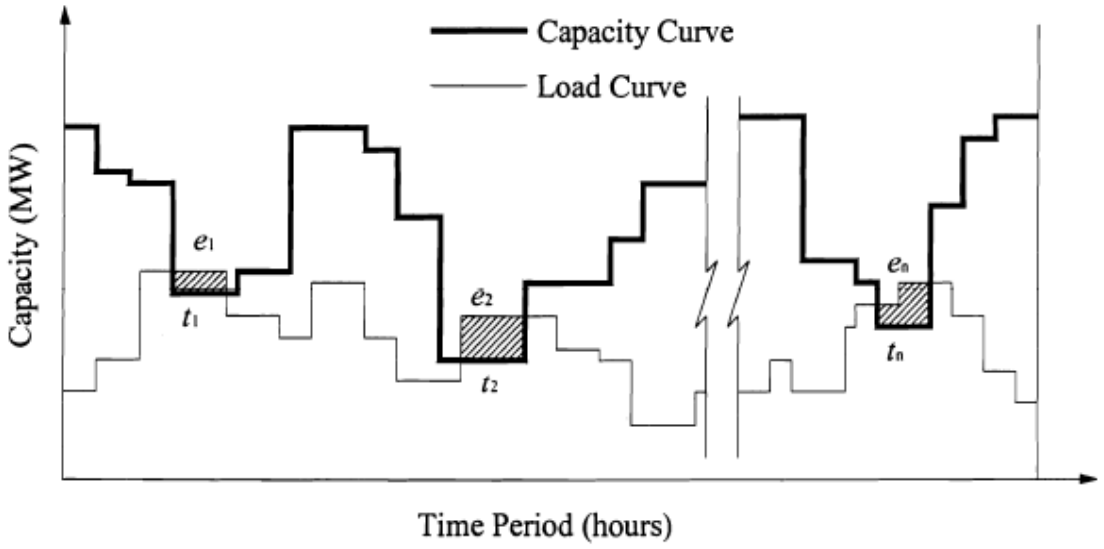

Fig. 2.6: Superimposition of generation capacity states and the chronological load

2.4 System Modelling Using Probabilistic Methods

Electric power system behaviour is stochastic in nature, and therefore it is logical to consider that the assessment of such systems should be based on probabilistic techniques. This has been acknowledged since the 1930s, and there have been numerous publications dealing with the development of models, techniques, and applications of reliability assessment of power systems [3-7]. In the past, the challenges in using probabilistic techniques included lack of data, limitation of computational resources, lack of realistic reliability techniques, aversion to the use of probabilistic techniques and a misunderstanding of the significance and meaning of probabilistic criteria and risk indices [1]. These reasons are not valid anymore since most utilities have valid and applicable data, reliability evaluation techniques are highly developed, and most engineers have a working understanding of probabilistic techniques [1, 54]. As discusses earlier, probabilistic techniques can be broadly categorised under two main approaches; analytical and simulation approach [1, 57].

The basic approach in evaluating the probabilistic adequacy of a particular generation

configuration is fundamentally the same for any technique. It consists of three main parts as shown in Fig. 2.7 [1]. The generation and load model shown in Fig. 2.7 are convolved to form the appropriate risk model. The calculated indices do not consider transmission constraints or transmission reliabilities. Adequacy evaluation, therefore consists of the following three steps [1, 61]:

1. Build a generation model based on the operating characteristics of all the generating units in the system.
2. Construct an appropriate load model.
3. Obtain a risk model by combining the generation model with the load model.

Appropriate risk indices can be utilised in the risk model to provide a quantitative measure of system reliability. The three models are described in the following sub-sections.

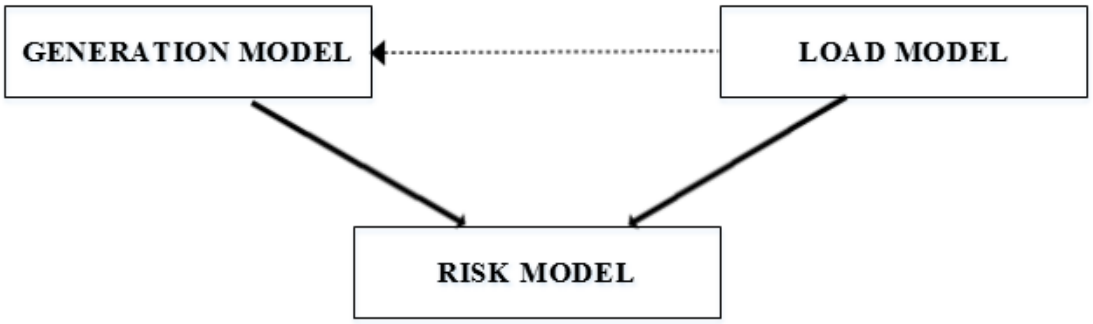

Fig. 2.7: Conceptual tasks in generating capacity reliability evaluation

2.4.1 Conventional Generation Model

Each generating unit in a power system can be represented by a multi-state Markov model. A two-state Markov model of a single generating unit is shown in Fig. 2.8. This model represents a generating unit that can reside either in the up (operating) state or the down (outage or forced out of service) state. The component failure rate (λ) and the repair rate (μ) are the transition rates between the two states [1]. For a generating unit that has partial outputs states, i.e. more than two states, the appropriate Markov model can be derived showing the different states and the transitions

between them. The MTTF is the average time a unit spends in the "up" state. The failure rate (λ) is equal to the reciprocal of the MTTF and can be obtained for a generating unit using equation (2.13). The MTTR is the average time a unit spends in the "down" state. The repair rate (μ) is equal to the reciprocal of the MTTR and can be obtained for a generating unit using equation (2.14)

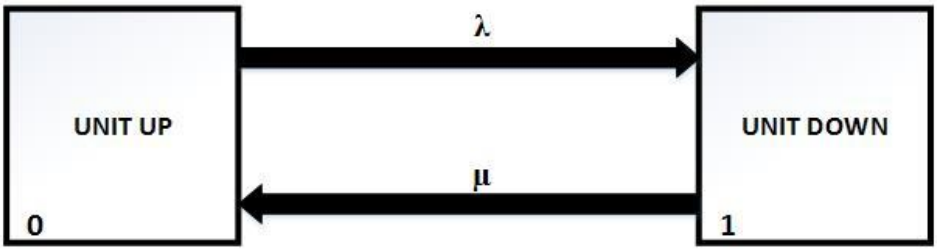

Fig. 2.8: Two-state model for a generating unit

$$\lambda = \frac{1}{MTTF} = \frac{\text{numbers of failures of a component in the given period of time}}{\text{total period of time the component was operating}} \quad (2.13)$$

$$\mu = \frac{1}{MTTR} = \frac{\text{numbers of repairs of a component in the given period of time}}{\text{total period of time the component was under repair}} \quad (2.14)$$

The basic generating unit parameter used in adequacy evaluation is the probability of finding the unit on forced outage at some distant time in the future. The probability is defined in [56] as the unit unavailability, and historically in power system applications, it is known as the unit forced outage rate (FOR). The FOR is a key parameter in power system reliability studies [1]. Equations (2.15) and (2.16) can be used to obtain the unavailability and availability of a generating unit if the unit failure rate (λ) and the repair rate (μ) are known. Equations (2.15) and (2.16) are obtained from the two-state Markov model shown in Fig. 2.8. The general unit FOR is usually calculated from the unit operational data using (2.15) [1]. In the case of generating equipment with relatively long operating cycles, the unavailability or the FOR is an adequate estimator of the probability that the unit under similar conditions will not be available for service in the future.

$$U = FOR = \frac{\lambda}{\lambda + \mu} = \frac{\sum[\text{down\_time}]}{\sum[\text{down\_time}] + \sum[\text{up\_time}]} \tag{2.15}$$

$$A = 1 - U = \frac{\mu}{\lambda + \mu} = \frac{\sum[\text{up\_time}]}{\sum[\text{down\_time}] + \sum[\text{up\_time}]} \tag{2.16}$$

In Canada, data on generation unit outage statistics are collected and normally reported by the Canadian electrical association - equipment reliability information system (CEA-ERIS). Table 2.2 shows a simple electric power system with data from the CEA-ERIS containing 5 generating units with their corresponding FOR. The MCR is the maximum continuous rating [62].

Table 2.2. CEA-ERIS generation equipment status

Unit #	**Type**	**MCR Class (MW)**	**MCR (MW)**	**FOR (%)**
1	Fossil unit (coal)	60-99	60	2.93
2	Fossil unit (coal)	100-199	150	4.92
3	Fossil unit (coal)	200-299	200	5.19
4	Hydraulic unit	24-99	50	2.08
5	Hydraulic unit	100-199	120	2.47

Equation (2.2) in Section 2.3.1 is used to obtain the generation model of the generation system shown in Table 2.2. The algorithm combines the generating unit one at a time to create overall system model shown in Table 2.3.

Table 2.3. Total conventional generation model

Capacity out (MW)	Probability	Cumulative probability
0	0.8356761	1
50	0.01775128	0.1643239
60	0.02522438	0.14657262
110	0.00053582	0.12134824
120	0.02116394	0.12081242
150	0.04324282	0.09964848
170	0.00044956	0.05640566
180	0.00063882	0.0559561
200	0.04666435	0.05531728
210	0.00130526	0.00865293
230	0.00001357	0.00734767
250	0.00097173	0.0073341
260	0.00140853	0.00636237
270	0.00109515	0.00495384
310	0.00002933	0.00385869
320	0.0011818	0.00382936
330	0.00003306	0.00264756
350	0.00236715	0.0026145
370	0.00002461	0.00024735
380	0.00003567	0.00022274
400	0.00005029	0.00018707
410	0.00007145	0.00013678
430	0.00000074	0.00006533
460	0.00000152	0.00006459
470	0.00005995	0.00006307
520	0.00000127	0.00000312
530	0.00000181	0.00000185
580	0.00000004	0.00000004

The first column in Table 2.3 shows the capacity outage states of the total generation of the electric power system, the second column shows the corresponding probabilities of occurrence while the third column shows the cumulative probabilities.

2.4.2 Wind Power Model

Wind energy sources are variable in nature, as the power output varies with time depending

on the wind speed. The wind can blow and stop frequently in a short period and can be totally absent when it is most needed resulting in a wide variation in the wind power output [13]. The power output profile of a wind farm is therefore different from that of a conventional power plant and the modelling must be factored in this variation. The generation capacity profile of a wind farm is usually represented by a multistate capacity model with its output varying from zero to rated capacity. The capacity output states in a wind generation model will therefore be significantly more than that of the conventional generation in order to account for the wide variation in output. A 100 MW wind farm represented by an 11-state capacity model is shown in Table 2.4. A detailed explanation of the wind power modelling is presented in the latter part of this section.

Table 2.4. Example of a wind farm capacity model

Capacity Out (MW)	**Probability**
0	0.3251342
10	0.2588843
20	0.117133
30	0.0822426
40	0.0593306
50	0.0385852
60	0.0305636
70	0.0212901
80	0.0158562
90	0.0188439
100	0.0321373

The explanation given so far for the wind modelling assumes that the wind power is modelled as a generation for a wind integrated power system (WIPS). This wind power model is added to the conventional generation to get the overall generation in the system as seen in Fig. 2.9(a). Wind power can also be modelled as a negative load as shown in Fig. 2.9(b) where the hourly wind power output is subtracted from the corresponding hourly load to obtain a modified

system load which can be used to build a modified system load model. This modified load is then convolved with the conventional generation to derive the appropriate risk indices.

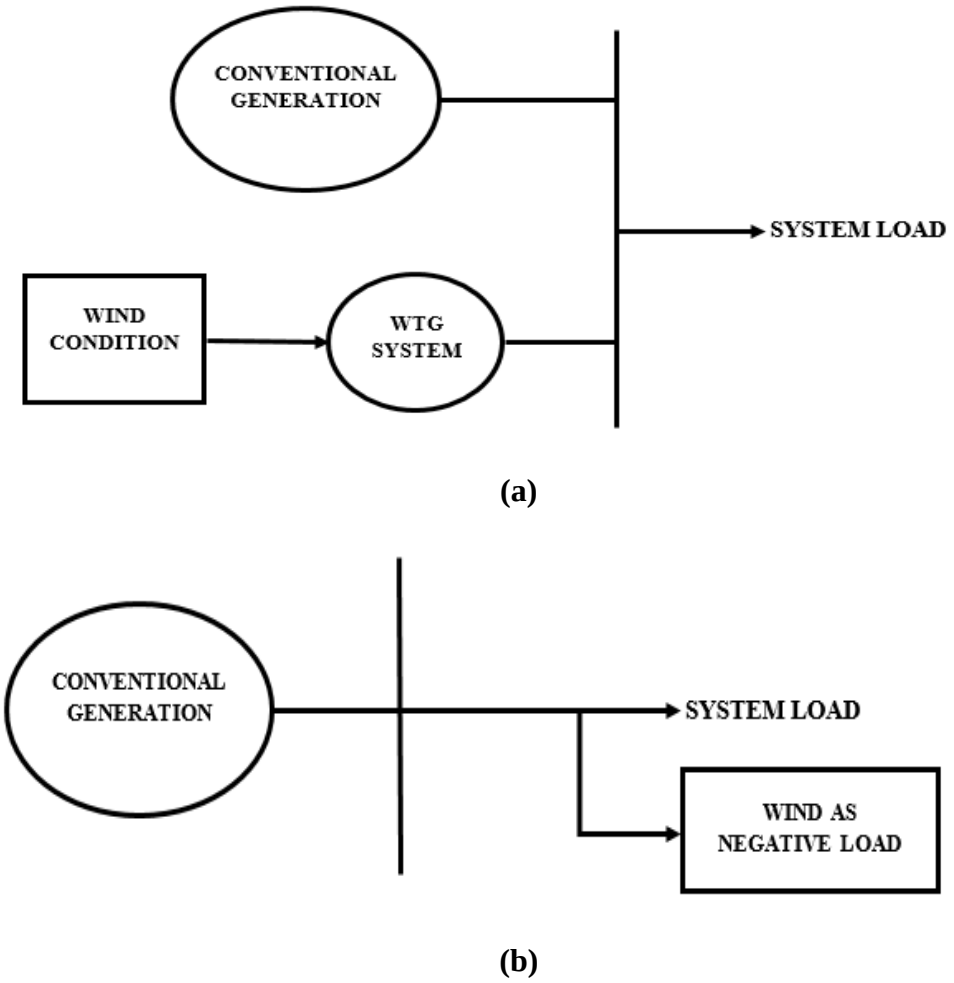

Fig. 2.9: Wind-integrated power system model for generating system adequacy assessment with wind capacity modelled as (a) generation and (b) negative load

In Fig. 2.9b, the wind-integrated system model for generating system adequacy assessment is depicted with the wind capacity modelled as a negative load. An illustration of how the load is modified when the wind is modelled as a negative load is shown in Table 2.5. An hourly load model for a period of 12 hours is used in the illustration using a hypothetical power system, the hourly wind power output for the twelve hours is subtracted from the corresponding hourly load to obtain a modified load for each hour of the twelve hours. Table 2.5 shows the hourly peak load,

the hourly wind power output and the hourly modified load when the wind is used as a negative load.

Table 2.5: Hypothetical electric power system with wind modelled as a negative load

Hour	Load (MW)	Wind power output (MW)	Modified Load (MW)
0	70	8	62
1	88	12	76
2	93	5	88
3	77	0	77
4	100	7	93
5	110	9	101
6	105	7	98
7	112	15	97
8	98	9	89
9	76	1	75
10	83	2	81
11	67	5	62

Data on wind power outputs are not always available. This is usually the case in system planning when considering new potential wind farm sites. The wind power can be estimated in such cases using wind speed data collected for the sites of interest.

The development of an appropriate and suitable wind model for the reliability evaluation of a WIPS requires historical wind speed data collected over a large number of years [9]. The chronological characteristics of wind speed and its effects on wind power output cannot be easily recognized while representing wind regime of a site by a particular probability distribution. A technique using MCS is used in [63] and can be used to incorporate this consideration. Wind speed data for a selected site can be simulated for a desired number of sample years using an Auto Regressive Moving Average (ARMA) model [9, 63] and can be represented in the form shown in (2.17). An ARMA model with p autoregressive terms and q moving average terms is denoted as ARMA (p, q).

$$y_t = \varphi_1.y_{t-1} + \varphi_2.y_{t-2} \ldots + \varphi_s.y_{t-s} + \alpha_t - \theta_1.\alpha_{t-1} - \theta_2.\alpha_{t-2} - \cdots \theta_m.\alpha_{t-m} \quad (2.17)$$

Where φ_i (i= 1, 2, 3, … s) and θ_j (j= 1, 2, 3, … m) are auto-regressive and moving average coefficients of the wind model respectively. These coefficients can be calculated using the historical data of a particular site [63]. α_t is a normally and independently (NID) Gaussian white noise process with zero mean and σ^2 variance generally expressed in the form $\alpha_t \epsilon NID\ (0, \sigma^2)$. Equation (2.17) represents a times series for y, which can be generated using the value of α_t randomly generated for each time interval and the previous values of y and α. A time interval of an hour is used in this study. The time series of y obtained using (2.17) can then be used to calculate the simulated hourly wind speed using (2.18).

$$SW_t = \mu_t + \sigma_t.y_t \quad (2.18)$$

Where,

SW_t= Simulated wind speed for hour t.

μ_t= Hourly mean wind speed for hour t.

σ_t= Hourly standard deviation of wind speed for hour t.

The hourly mean wind speed and hourly standard deviation is gotten from the historical set of data and used repetitively in the sequential simulation process. There are 8760 hours in a year, so 8760 hourly mean wind speeds and 8760 hourly standard deviations are computed from the historical data and used in developing the future artificial data. An ARMA (4, 3) model for the Swift Current site located in the Province of Saskatchewan in Canada is presented in [64] and expressed in (2.19).

$$y_t = 1.1772\, y_{t-1} + 0.1001\, y_{t-2} - 0.3572\, y_{t-3} + 0.0379\, y_{t-4} + \alpha_t - 0.5030\alpha_{t-1} - 0.2924\alpha_{t-2} + 0.1317\alpha_{t-3} \quad (2.19)$$

$$\alpha_t \in NID(0, 0.524760^2)$$

α_t is generated using a normal random number generator and the initial four preceding values of y are assumed to be zero. i.e. y_1 to y_4 are assumed zero. The hourly mean and standard deviation of the Swift Current wind speed was developed using 5000 sample years of simulated data, and is shown in Fig. 2.10.

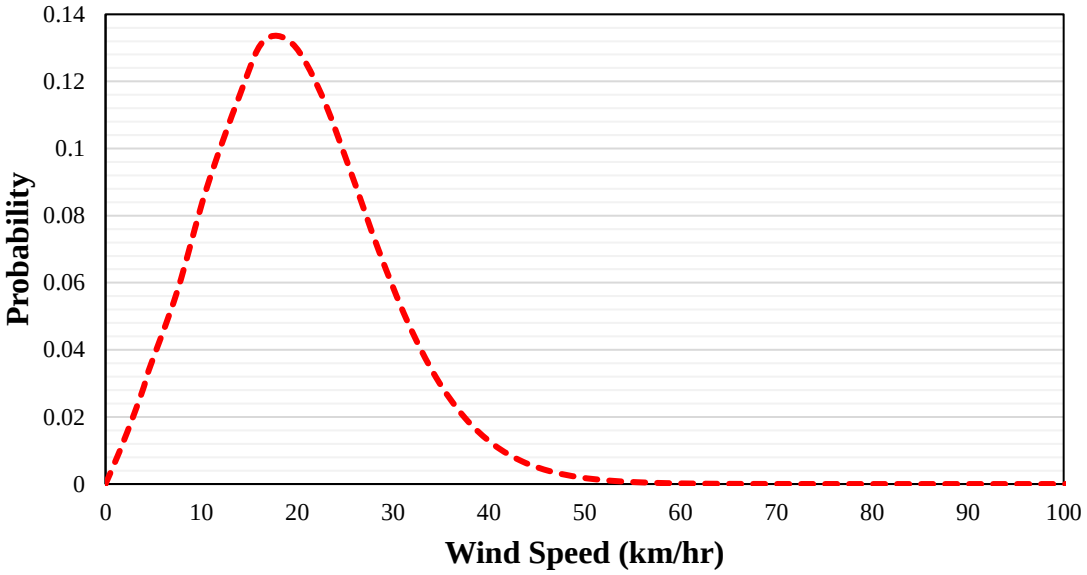

Figure 2.10: Wind speed probability distribution

There are three factors which affect the output of a WTG at any given time; the wind speed at the time, the forced outage rate (FOR) of the WTG, and the WTG characteristics defined by the cut-in (V_{ci}), rated (V_r) and cut-out wind speeds (V_{co}). The cut-in (V_{ci}) wind speed is the minimum speed at which the WTG will produce power, the WTG will not produce at speed lower than this. The rated wind speed (V_r) is the wind speed required for a WTG to produce rated power. The cut-out wind speed (V_{co}) is the maximum wind speed the WTG can handle safely, the WTG will shut down at any speed above the cut-out speed for safety reasons [14]. The power output of the WTG as a function of wind speed is shown graphically in Fig. 2.11, and is called the WTG power curve as outlined in [14] and its expression is seen in (2.20).

$$p(v) = \begin{cases} 0, & 0 \le v \le V_{ci} \\ (A + Bv + Cv^2)P_r, & V_{ci} \le v \le V_r \\ P_r, & V_r \le v \le V_{co} \\ 0, & v \ge V_{ci} \end{cases} \quad (2.20)$$

Where P_r is the rated power of the WTG and the constants *A*, *B* and *C* are function of *Vci*, V_r and V_{co} as outlined in [14]. For this research work, a *Vci* of 15 km/h, a V_r of 50 km/h and a *Vco* of 90 km/h is used.

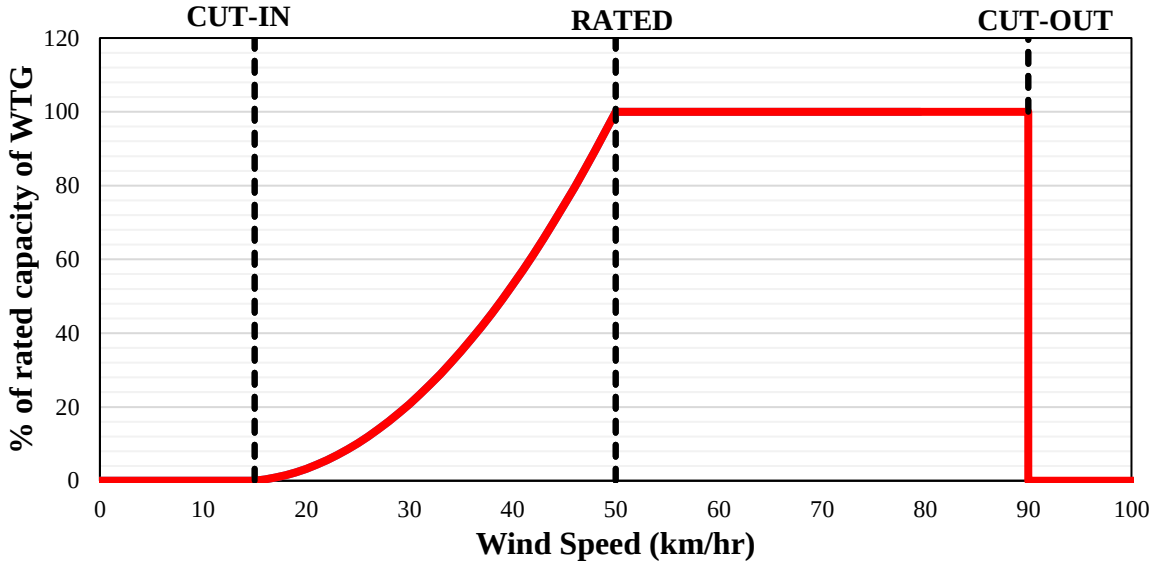

Fig. 2.11: WTG power curve

The FOR of the WTG is considered in the evaluation of the power output model of a wind farm. It has however been shown in [65] that the WTG FOR can be neglected in many practical applications without creating significant error in the reliability evaluation. The effect of the FOR has been omitted in this study in order to simplify the wind model. Also, the assumption is that all the WTGs in the wind farm experience the same wind speed in any given hour.

The anemometer height at which most wind speed data are collected is at a standard minimum height of 10 m [66]. Most WTGs have hub heights ranging from 60 m to 80 m. A hub height of 67 m was used in this study. The available wind speed was therefore scaled to the hub height of 67 m by extrapolation before deriving the wind power. The extrapolation is achieved by a logarithmic velocity profile which assumes the atmosphere to be adiabatic [67], and is shown in

(2.21)

$$\overline{u}_x(h_h) = \frac{u_*}{k} ln \frac{h_h}{z_o} \quad (2.21)$$

Where, $u_* = \frac{k}{ln\frac{h_r}{z_o}} * \overline{u}_x(h_r)$

H_h = hub height

H_r = reference height (10 m in this case)

Z_0 = surface roughness length

k ~ 0.4(von Karman constant)

The wind power output obtained using (2.20) for each hour for the entire simulation is used to obtain the wind capacity model in the form of a capacity availability probability table (CAPT). This is done by grouping the hourly generation into a suitable number of class intervals in ascending or descending order. This model is basically a probability distribution showing the different power levels and their probability of occurrence. Sturges' rule [68] was used to determine the appropriate number of class interval (NoCI) as shown in (2.22).

$$NoCI = 1 + 3.322 \log_{10}(8760 * \mathrm{N}) \quad (2.22)$$

Where N is the number of sample years and (8760*N) is the total number of data points considered.

For 4000 sample years, the number of class interval is therefore 26, the class size (CS) of each of the class interval is calculated using (2.23) [69]:

$$CS = TIC/NoCI \quad (2.23)$$

Where,

TIC= the totalled installed capacity of the wind farm under consideration.

The CAPT shows the different wind power capacity available and their respective probabilities of occurrence. If there are *NoCI* available capacity states, then the capacity available, CA_i for a state *i* is given by (2.24) while the probability of CA_i available state $P(CA_i)$ is given by

(2.25).

$$CA_i = (i-1)CS + CS/2 \tag{2.24}$$

$$P(CA_i) = (DP_i) \,/\, (8760 * N) \tag{2.25}$$

Where DP_i is the number of wind data is points in the interval I [69].

The CAPT for the Swift Current wind farm site obtained using the above method for 4000 years of simulated hourly data is shown in Fig. 2.12.

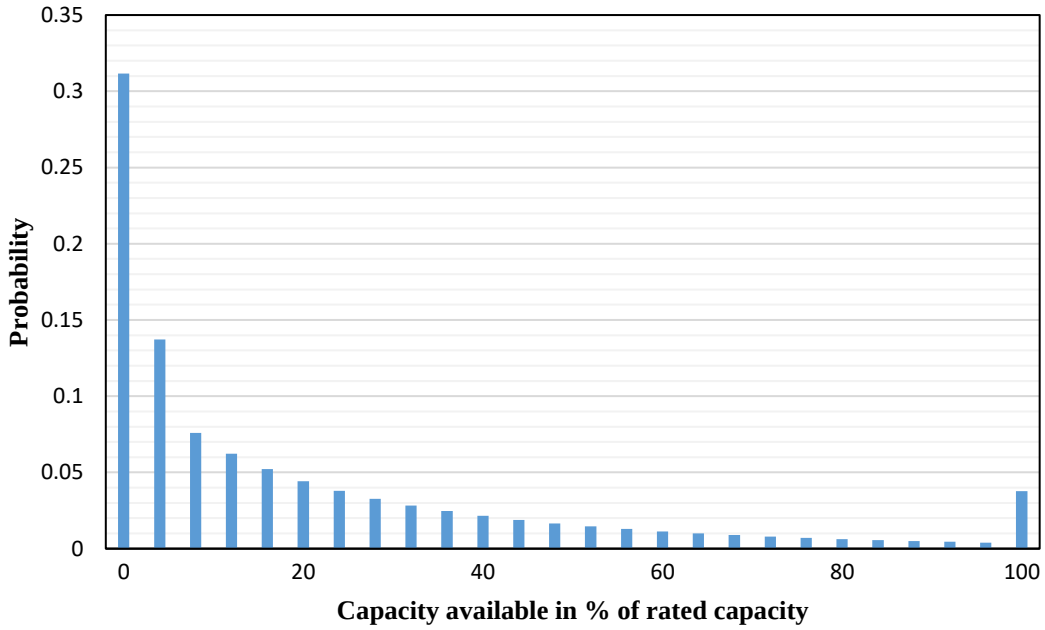

Figure 2.12: Annual CAPT for Swift Current wind site.

This large number of states can be reduced further using the apportioning techniques as described in [1]. The annual CAPT model in Fig. 2.12 was reduced to 11 states using the method described in [1] and is shown in Fig. 2.13.

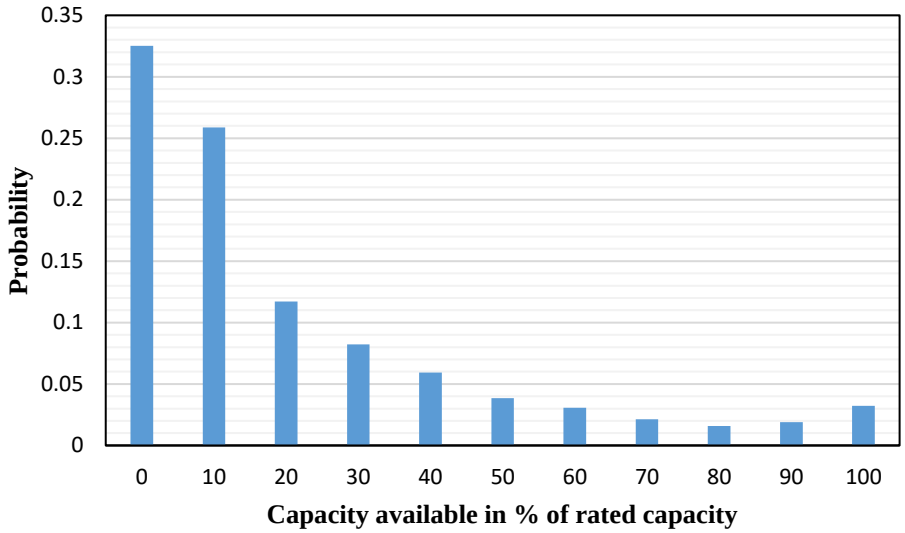

Fig. 2.13: 11-state annual CAPT for Swift Current wind site

2.4.3 Load Model

The load model incorporates the variation in system load level with time in a specified period. A period of one year is usually considered in evaluating reliability indices in power system planning. There are various kinds of load models that can be used to represent the system demand over time. On a basic level, the simplest load model is to use a fixed load for the entire period under study. The system peak load is mostly used to represent the fixed load. As discussed in Section 2.3.1, a load model can also be represented as a DPLVC or a LDC. Each day is represented by its daily peak load to create a DPLVC. The individual daily peak loads are arranged in descending order to form a cumulative load model as shown in Fig. 2.2. For the LDC, the individual hourly load values are used, and in this case the area under the curve represents the energy required in the given period, usually a year [1]. The LDC gives a more complete representation of the actual system load demand than the DPLVC. The DPLVC and LDC are widely used load models in adequacy evaluation of generation systems. The DPLVC and LDC of the IEEE-RTS are shown in Fig. 2.14.

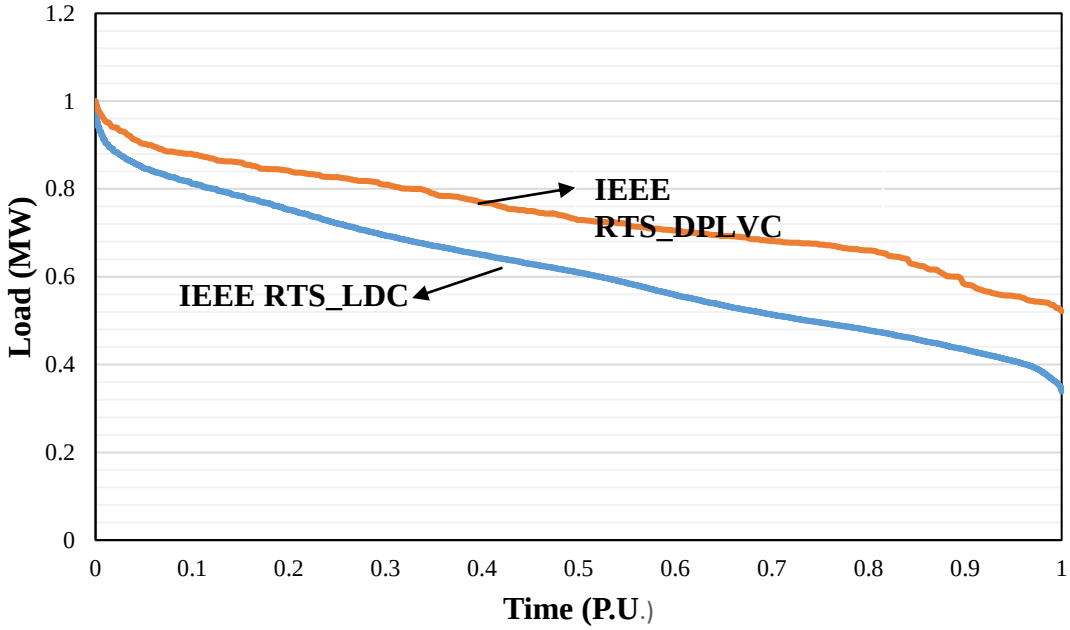

Fig. 2.14: DPLVC and LDC of the IEEE-RTS

2.4.4 System Risk model

The system risk model is obtained by convolving the system generation model with the system load model. The system risk indices can be obtained from this risk model. The most common and widely used adequacy indices are the loss of load expectation (LOLE) and the loss of energy expectation (LOEE). The LOLE is the expected number of hours or days in a year that the total system generation will not be able to satisfy system load demand. A "loss of load" will occur only when the available generating capacity in the system is exceeded by the system load in a given time. The LOEE is the expected energy that will not be supplied by the generating system due to those occasions when the load demand exceeds the available capacity.

2.5 Period Analysis

Power system risk evaluation is done based on the assumption that the total generation model and the load model are applicable for the evaluation period; usually a year. Many situations

can occur in which the generation and load models vary within the period of analysis. Factors such as seasonal deratings of the generating units, scheduled maintenance, seasonal variation of wind speed and system load, and also the correlation between the wind speed and system load contribute to the variability of the models within the period of analysis [1]. A period analysis can be used to incorporate these different factors for reliability evaluation. A period analysis is the process of splitting the analysis period into smaller sub-periods, developing separate system models for each sub-period, evaluating the required risk for each sub-period, and finally combining the risk indices of each sub-period to obtain the risk indices of the entire period as shown in (2.26) [70].

$$I_p = \sum_{p=1}^{n} I_s \tag{2.26}$$

Where;

n=number of sub-periods within the total period

I_s= reliability index for sub-period *s*

I_p= reliability index for the entire period

The concept of the period analysis will be utilised in the incorporation of the CAES to the electric power system in this research work, with charging occurring in one period and discharging occurring in another period. Period analysis is usually done in order to incorporate seasonal variability and the correlation of different factors such as wind, load and generation. Period analysis will also be used to incorporate the operation of the CAES. The CAES has the ability to act as both a generator that supplies electric power to the system and as a load that consumes electric power from the system. The period for charging and discharging of the CAES will play a critical role in the overall assessment of the reliability of the electric power system.

2.6 Conclusion

The basic concepts and techniques for generating system adequacy evaluation of a po

wer system is briefly introduced in this chapter. The adequacy evaluation of a wind integrated power system is discussed as well. The chapter describes the process of modelling the different component of the power system; the load, the conventional generation, wind power and the overall system risk model. A detailed method for generating synthetic wind speed using ARMA model is explained and its modelling described. The wind power can be modelled as a generation or as a negative load, and an example is to illustrate this behaviour as a negative load using a hypothetical system. The different techniques used to carry out an HL-1 reliability evaluation of an electric power system is discussed. The different methods of carrying out the probabilistic reliability evaluation of a power system is explained. The method of conducting sequential Monte Carlo simulations and obtaining the basic reliability indices are also discussed in the chapter. The concept of the period analysis, the reason for employing the period analysis in incorporating the CAES into the electric power system are highlighted in this chapter.

3. COMPRESSED AIR ENERGY STORAGE (CAES)

3.1 Introduction

An increase in wind penetration in the electrical power system leads to increase in power fluctuations causing increased challenges in maintaining an acceptable level of reliability in an electric power system. The increased risk introduced by having high wind penetration in the power system can be mitigated by using energy storage. Energy storage is operated by storing energy during high wind /low demand period and using it during low wind or no wind period or during peak load period.

Today, a wide array of technologies has been developed and deployed to ensure that the electrical grid can meet our everyday energy needs. Energy can be stored in a variety of forms; from scalable banks of advanced chemistry batteries and magnetic flywheels, to pumped hydro-power and compressed air energy storage [21]**.** Various types of energy storage technology available include; Solid state batteries which stores energy in form of chemical energy such as electrochemical capacitors, Lithium Ion (LI-ION) batteries, Nickel-Cadmium (NI-CD) batteries, Sodium Sulfur batteries (NAS); flow batteries such as Redox Flow batteries, Iron-Chromium (ICB) flow batteries, Vanadium Redox (VRB) flow batteries and Zinc-Bromine (ZNBR) flow batteries; flywheels which stores energy in form of kinetic energy, Compressed Air Energy Storage (CAES) and Pumped Hydro Electric Energy Storage (PHES) which store energy in form of potential energy and thermal which stores energy in form of heat [21]**.** Fig. 3.1 shows the different storage technologies available and their relative advantage over one another, it shows the amount of energy they can store and power ranges for which these storage types are designed for and can operate [71], while Fig. 3.2 shows the operating cost in $/kWh against the capital cost per unit of power ($/kW) for all the different energy storage types available [72].

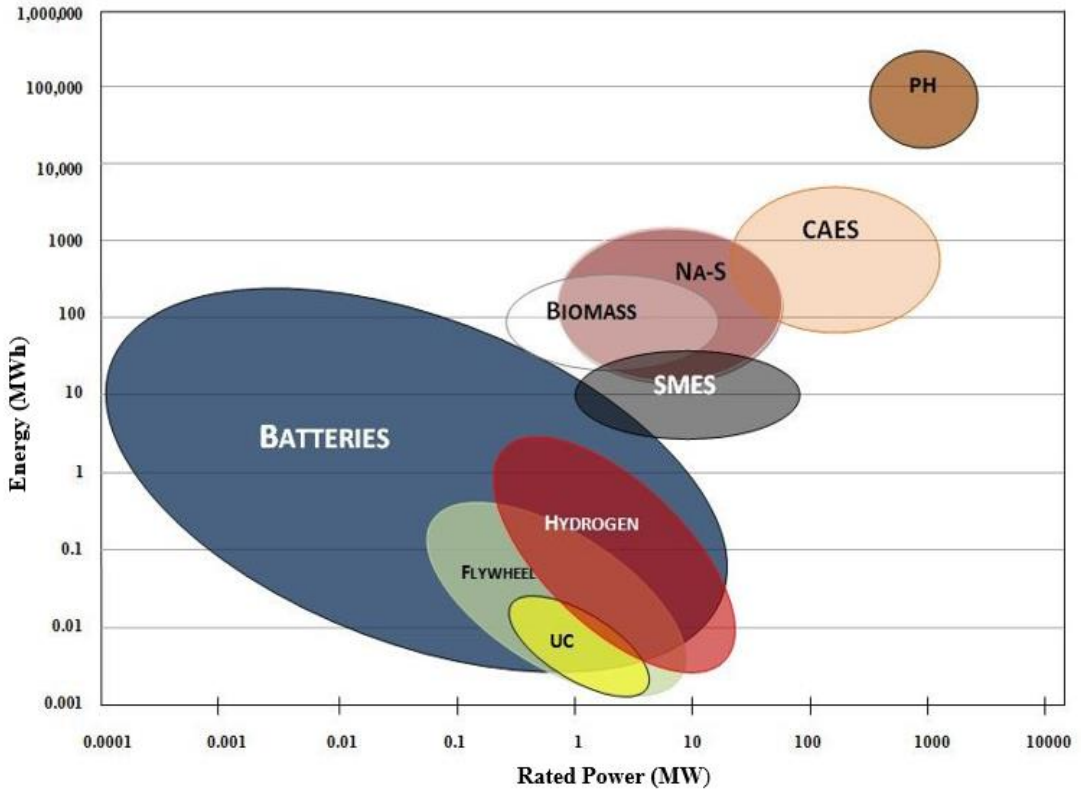

Fig. 3.1: Comparison of different energy storage technologies. *(Source: EPRI DOE Handbook of Energy Storage for Transmission and Distribution Applications)*

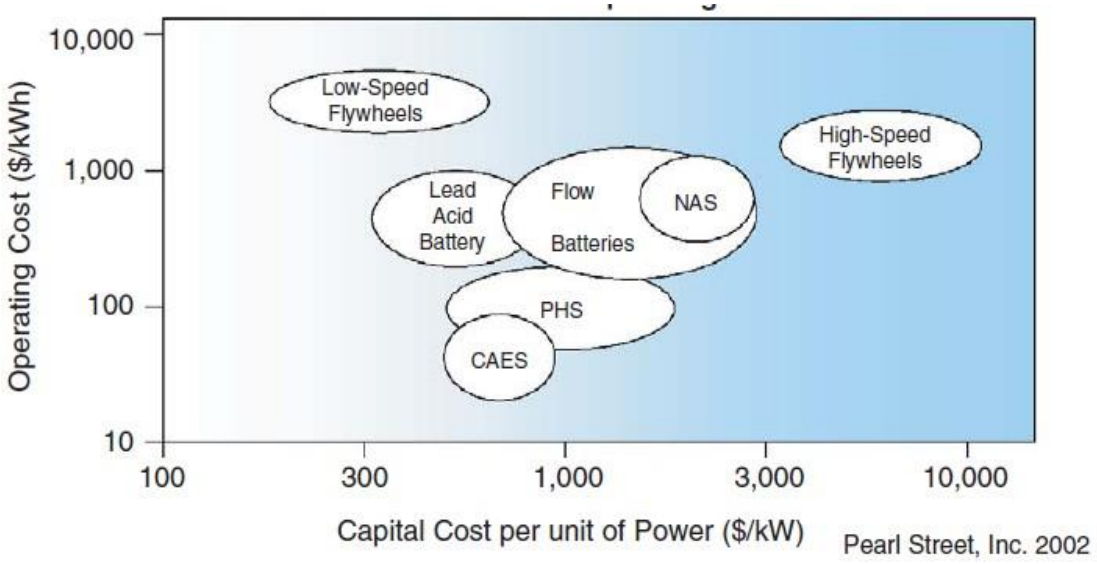

Fig. 3.2: Energy storage installation costs vs. operating costs; (Source*: Pearl Street Inc., 2002*) [72]

It can be seen from Fig. 3.1 that CAES and PHES can both be used for high energy storage and large power applications getting to the 1000 MW power and 1000 MWh energy range. They are both useful for grid-scale applications. It can be seen from Fig. 3.2, that CAES has the lowest operating cost among all the storage technologies present today falling in the $25/kWh to $90/kWh range. CAES is also competitive among other storage technologies in terms of installation costs which are about $500/kW to $950/kW. Based on the data given in Fig. 3.1 and 3.2. CAES can be proven as the most suitable storage technology in terms of the contrast of cost and performance. Also for the research described in this thesis, where the incorporation of large amount of wind is a major objective, the use of CAES will be appropriate because of its ability to store large amount of energy. Fig. 3.3 shows the comparison of the discharge time of each energy storage to their power ratings. It can be seen that CAES and pumped hydro are capable of discharge times in tens of hours, with correspondingly high sizes that reach 1000 MW [73].

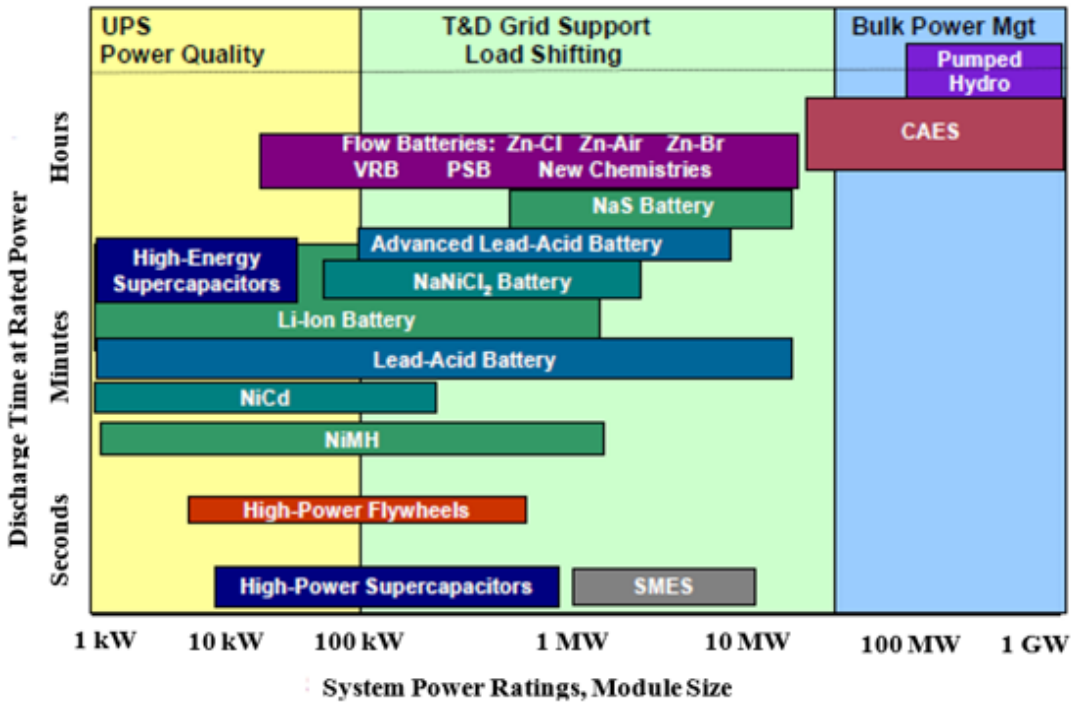

Fig. 3.3: Comparison between ES technologies in terms of rated power and discharge time. (Source: *DOE/EPRI 2013 Electricity Storage Handbook in Collaboration with NRECA*)

3.2 Operation of the CAES

The concept of CAES was first introduced in 1949 when Stal Laval filed the first patent of CAES using an underground cavern to store the compressed air. Its principle is based on the operation of the conventional gas turbine generator. In contrast to the operation of the gas turbine, the CAES decouples the compression and expansion cycle into two separate processes and stores the energy in the form of the elastic potential energy of compressed air [74]. The CAES consists of three main sections:

1. Compressor/Electric motor
2. Air storage
3. Turbine/Electric generator

Secondary sections of the CAES include the equipment controls for operating the combustion turbine, compressor, and auxiliary equipment and also for regulating and controlling changeover from generation mode to storage mode. Another secondary section of the CAES is the auxiliary equipment of fuel storage and handling, and mechanical and electrical systems for various heat exchangers required to support the operation of the facility [74]. For the purpose of this research, we assume the three main sections for simplification. Its components and operation are seen in Fig. 3.4a and 3.4b respectively.

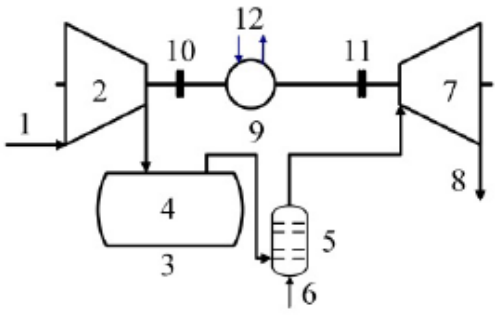

1.Air, 2.Compressor, 3.Reservoir, 4.Compressed air,
5.Combustor, 6.Fuel, 7.Turbine, 8.Exhaust,
9.Motor/Generator, 10 and 11.Clutch, 12.Electricity

Fig. 3.4a: Schematic diagram of a CAES system. (Source: *INTECH; Energy storage-technologies and applications*)

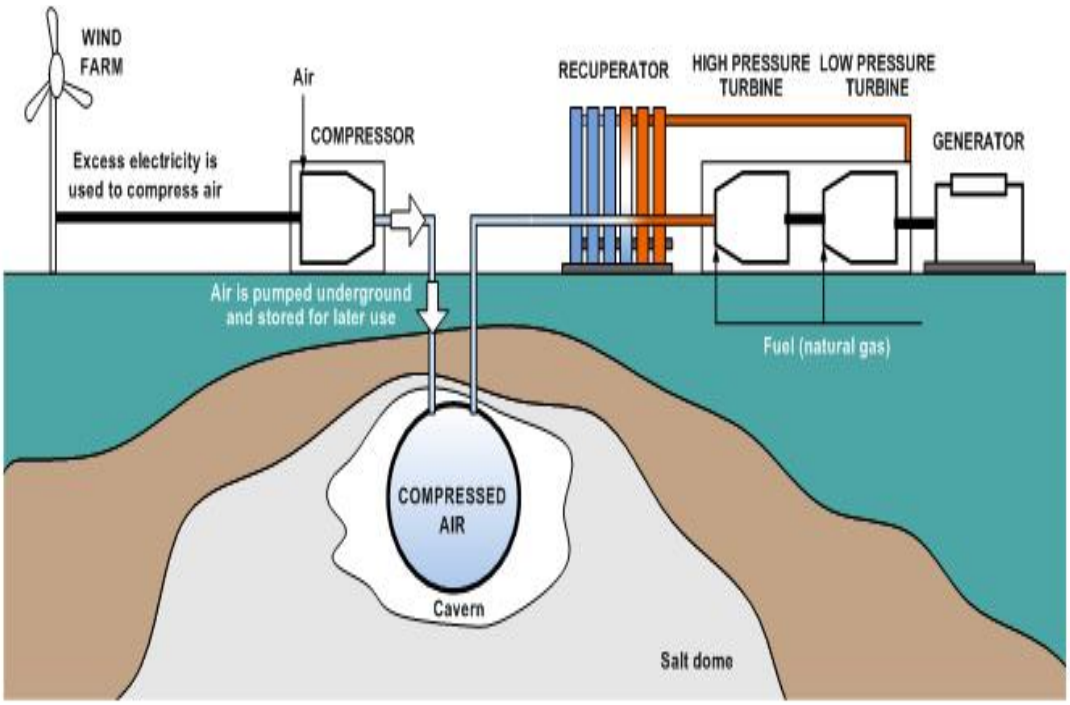

Fig. 3.4b: CAES operation. **(**Source: *SATL Inc.; Alberta-Saskatchewan Intertie Storage (ASISt) project*) [75]

It can be seen from Fig. 3.4a, that the generator and motor unit are located on a single shaft and acts as one unit. The CAES makes use of clutches for alternate engagement to the compressor or turbine train i.e. during compression, the "*clutch 10"* is engaged and "*clutch 11"* is disengaged while the CAES operates in the motor mode. On expansion/generation, "*clutch 10"* is disengaged and "*clutch 11"* is engaged while the CAES works in generation mode.

Fig. 3.4b shows in detail how the CAES operates. During off-peak period, excess electric power is used to run the air compressor and compresses air into the storage, during the peak period, when demand is high, the compressed air in storage is released, used to combust fuel for expansion and in turn used to run the turbine. The turbine is coupled to the generator which is in turn connected to the grid.

3.2.1 Electric Motor/Compressor unit

The electric motor is coupled to the compressor and uses excess power from the grid to drive the compressor. Some other configurations will allow for the wind farm connected directly to the motor and power from this wind-farm is used to drive the motor. The general idea is to use very low-cost power during the off peak to compress air in the storage. Compression occurs in more than one stage. Usually a 2-stage compression is used with aftercoolers after each compression stage to dissipate the heat produced from the compression process. The special thing about compressed air is that the air heats up considerably when being compressed from atmospheric pressure to a storage pressure of approx. 1,015psia (70 bar). Standard multistage air compressors use inter and after coolers to reduce discharge temperatures to about 149^0C-177^0C, and cavern injection air temperature to about 43^0C - 49^0C. When air is compressed, heat is generated and this heat has to be removed. The heat of compression therefore is extracted during the compression process or removed by the intermediate intercooler. [21]

3.2.2 Air Storage

The characteristics of the storage system of a CAES is very important in evaluating its performance. Underground CAES and under-water CAES are two basic types of air storage available. These two types can also be categorized as follows based on their thermodynamic conditions;

1. Constant Volume Storage
2. Constant Pressure Storage

The underground CAES as shown in Fig. 3.5a are constant volume type storage, and is also called sliding pressure storage. It is operated with a constant volume between two pressure levels i.e. minimum pressure and maximum pressure. A minimum pressure need to be maintained in the cavern which implies a minimum mass of air is needed in the storage to maintain this pressure. This minimum constraint cannot be violated while discharging. A chamber with non-collapsible boundaries i.e. rigid boundaries is used. Examples include solution mined caverns, above ground

vessels, aquifers. etc. [69]. With the constant volume configuration, the air pressure in the cavern changes during the charging and discharging process. During charging, the pressure builds up in storage as the mass of air in the storage increases until it gets to a predefined maximum pressure and charging is stopped. For the discharging process, if the turbine were driven with this sliding pressure, then its power would be reduced with discharging of the storage. Since this solution is not acceptable for the utility due to the load characteristics in its supply network, then the turbine is run with a constant inlet pressure to produce a constant power independent of the state of charge. For this purpose, the available pressure in the storage is throttled down to the turbine inlet pressure [76]. Most available CAES in the world are based on this storage configuration.

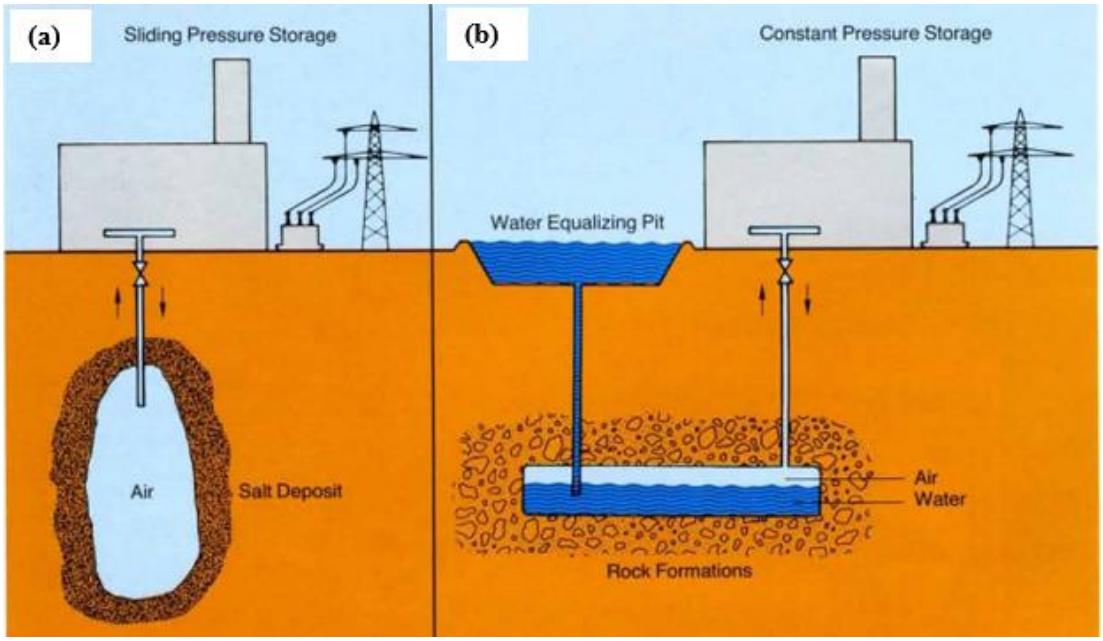

Fig. 3.5: An illustration of a) Constant volume CAES and b) Constant pressure CAES (Source: *BBC Brown Boveri Huntorf air storage gas turbine power plant*)

The constant pressure storage system includes under-water CAES or underground CAES as shown in Fig. 3.5b, it is suitable for sites where there is no possibility to construct a salt cavern. The vessel is kept at a constant pressure. A constant pressure storage can be constructed in underground rock formations where a hole is sunk into the ground from the top with a specific

diameter. The water equalising pit above the ground is used to maintain the pressure constant in the storage. As the air inside the storage reduces through the discharge process, it causes a corresponding drop in pressure, water is pumped into the storage to maintain the pressure at a constant in the storage, the volume changes accordingly. The required volume for a constant pressure is considerably smaller, since almost the entire air contained in the storage may be used to produce useful work [76]. Another type of constant pressure storage in an under-water balloon vessel where the storage vessel is positioned hundreds of meters underwater, the hydrostatic pressure of the water column above the storage vessel allows to keep the pressure to the desired level. This has found applications in [77, 78].

3.2.3 Turbine/Electric generator unit

The turbine/generator unit are the main components involved in the discharge process of the CAES. This discharge usually takes place during the peak load period. As stated in section 3.2.1, heat is generated during compression and has to be dissipated because the air has to be cooled before it can be stored, conversely, during expansion, the air needs to be heated up for it to be able to turn the turbine. The loss of this heat energy has to be made up in the expansion stage. The air is first heated up in combustion chamber using natural gas before expansion in the turbine. Just like the compression process, this expansion process is usually double stage. There is a high-pressure section and a low-pressure section as seen in Fig. 3.4b [75, 76]. The air is heated up for each of the stages of expansion, another configuration uses the heat from the turbine exhaust in a recuperator to heat the incoming air from the cavern before the expansion cycle, this process of recuperation will lead to increased efficiency of the system.

3.3 Existing and proposed CAES plant

CAES has been around for about 40 years now. Even though CAES is a mature and commercially available energy storage technology, there are only two CAES in operation today commercially. There are several CAES projects that have been planned, proposed or under

development today and an outline of some of them is shown below.

3.3.1 Existing/Operational CAES plants

There are only two operational CAES plants available today, the first is in Huntorf in Germany, while the other is in McIntosh, Alabama in the USA. The Huntorf CAES has been in operation for about 40 years since 1978 and is the oldest operating CAES system. It is a 290 MW, 50 Hz unit, owned and operated by Nordwestdeutche Krafiwerke, AG. The plant consists of two caverns which is located in a solution mined salt dome about 600 m underground, with each having a volume of 150,000 m^3, to give a total of 300,000 m^3. It runs on a daily cycle with eight hours of charging required to fill the cavern. The 60 MW compressor charges the air into the cavern at a mass flow rate of 108 kg/s operating for a maximum of 12 hours. At full load, the plant can generate 290 MW of electricity for 2 hours at a mass flow rate of 425 kg/s [74]. The operating pressure range for the Huntorf plan is between 46 bars to 66 bars. Its main use was for peak shaving and black starting [76]. Table 3.1 compares the technical specifications of the Huntorf plant to that of the McIntosh plant.

The commercial CAES plant, owned by the Alabama Energy Cooperative (AEC) in McIntosh, Alabama, has been in operation since 1991 for about 26 years now. The storage capacity is about 560,000m^3 with a generating capacity of 110 MW. The CAES system stores compressed air with a maximum pressure of 74 bar in an underground cavern located in a solution mined salt dome 450m below the surface. The compressor compresses air in the cavern using 53 MW compressors for 41 hours at a mass flow rate of 94 kg/s. At full load, it can provide 110 MW of power for 26 hours at a mass flow rate of 157 kg/s. The McIntosh CAES system utilises a recuperator to reuse heat energy from the gas turbine exhaust, which reduces fuel consumption by 25% compared with the Huntorf CAES [74, 79].

Table 3.1: Huntorf and McIntosh CAES technical specification [79]

Parameter	**Huntorf (Germany)**	**McIntosh AL (USA)**
Build Year	1978	1991
Power Capacity		
Turbine	290 MW (2 hours)	110 MW (26 hours)
Compressor	60 MW (12 hours)	53 MW (41 hours)
Cavern Volume	310,000 m^3	560,000 m^3
Mass Flow Rate Turbine Compressor	 417 kg/s 108 kg/s	 157 kg/s 94 kg/s
Cavern Air Pressures Discharged (Min) Charged (Max)	 50 bar 70 bar	 46 bar 74 bar
High Pressure Turbine Air Pressure Air Temperature	 43 bar 550 ºC	 44 bar 540 ºC
Low Pressure Turbine Air Pressure Air Temperature	 12 bar 830 ºC	 16 bar 870 ºC
Fuel	Gas	Gas/Oil
Recuperator	No	Yes
Heat Rate	5,800 kJ/kWh	4,300 kJ/kWh
Roundtrip Efficiency	42%	54%

Hydrostor, a company in Toronto, Canada developed a variant of the CAES solution that addresses intermittent renewable generation, load balancing, reserve capacity, and peak-shaving. Here, balloon like accumulators are placed in the ocean. The compressed air stream is pressurised to the same pressure found at the depth where the accumulators are located. The air displaces the water in the accumulators stored. The weight of the water forces the air back to surface under pressure during discharge. The stored heat is then added back to the air stream, and the heated air travels to the expander which drives the generator [77]

3.3.2 Proposed CAES Plants

Several CAES plants have been proposed in different parts of the world. Some are currently undergoing installation while some have been discontinued all together. Examples of these different CAES are highlighted below.

1. In Canada, an energy storage project was proposed by the Saskatchewan-Alberta tie line (SATL) Inc. called the Alberta Saskatchewan Intertie Storage Facility (ASISt"). It identified the Lloydminster region as an excellent location for a CAES project because of its salt formations, access to transmission and multiple markets such as Alberta and Saskatchewan grids. The ASISt project will use air compression and turbine technologies to build the first CAES plant in Canada. It will have a capacity to sustain between 135 MW and 160 MW of power for 60 hours with a maximum cavern pressure of 2500 psi or 172 bar. The ASISt plant is designed as a merchant facility that will receive revenue from the Alberta energy market, the Alberta ancillary services market and potentially from interregional arbitrage transactions [75].

2. Another Commercial CAES plant proposed is a 2700 MW CAES plant that is planned for construction in the United States at Norton, Ohio. It is to be developed by Haddington Ventures Inc. This plant will compress air to ~10 MPa or 100 bar in an existing limestone mine dome 670 m underground. The volume of the storage cavern is about 120,000,000 m^3 [74]

3. A Houston based company called Ridge Energy Storage recently began the development process for a 540 MW CAES plant in Matagorda, Texas. The plant will use an upgraded version of the Dresser-Rand design utilised at the McIntosh plant. The design calls for four independent 135 MW generators, each can reach full power in 14 minutes. The compressed air will be stored in a previously developed brine cavern and delivered to the expander at 700 psi or 48 bars and a mass flow rate of 181 kg/s – 185 kg/s [71].

4. The Iowa stored energy park project was planned by Iowa Association of Municipal Utilities. The project intention was to build a 270 MW CAES plant coupled with 75MW to 100MW of wind capacity, and planned to be operational by 2015. The plant was designed to take surplus

electrical energy generated by the wind farm at night and use it to compress air into a deep underground aquifer. However, the project had to be terminated in 2011. After years of study, the investors concluded that the porous sandstone aquifers in Iowa were not suitable for CAES [80].

5. Chubu Electric of Japan is surveying its service territory for appropriate CAES sites. Chubu is Japan's third largest electric utility with 14 thermal and two nuclear power plants that generate 21,380 MWh of electricity annually. Japanese utilities recognise the value of storing off-peak power in a nation where peak electricity costs can reach $0.53/kWh [74].

6. RWE Power, General Electric, Züblin and DLR are working together on the world first large-scale AA-CAES demonstration project, named ADELE in Germany. The feasibility study that the project partners have laid for the ADELE development program started in 2010. They have identified certain technical difficulties that must be overcome in implementing this AA-CAES system. For instance, without using intercooling, the air temperature inside the compressor can exceed 650 K with up to 100 bar pressure [27]. This aggressive environment may damage the compressor and other mechanisms. Thus, the AA-CAES requires the design of a high pressure and high temperature compressor with considerations of material selection, thermal expansion and thermo stresses, sealing concepts, and thermal limitations for bearings and lubrication [80].

3.4 Different Advancement in CAES Technology

Since the inception of the first CAES, a lot of research has been carried out to make the CAES even more efficient. In an ideal storage system, all the energy put in can be extracted later. When air is compressed, however the work that goes into compression produces heat as a side effect. This heat is lost to the environment making the CAES less efficient. *"CAES plant designs are categorized based on the method of managing heat from compression and expansion of the air."* [81] The various technologies available based on the way the heat generated from compression is treated are categorized in the following sub-sections.

3.4.1 Diabatic CAES Plants

The diabatic CAES plants are generally referred to as the “conventional” CAES [82]. The heat of compression is released into the atmosphere during the compression and heat is added from an external source to the air during expansion. This diabatic CAES is fully developed and operational. The first of such system has been in operation in Huntorf, Germany since 1979, while the second system has been in operation in McIntosh, Alabama after it was commissioned in 1991**.** A schematic Huntorf CAES system is shown in Fig 3.6. [82, 83]. When the atmospheric air is compressed in the ground, it generates heat. This heat of compression is released into the atmosphere as waste. The heat lost during compression has to be compensated for during expansion. This is done by heating the high-pressure air in combustors using natural gas fuel prior to expansion in the turbine, or as seen the in the McIntosh plant, as an addition, using the heat of a combustion gas turbine exhaust in a recuperator to heat the incoming air before the expansion cycle.

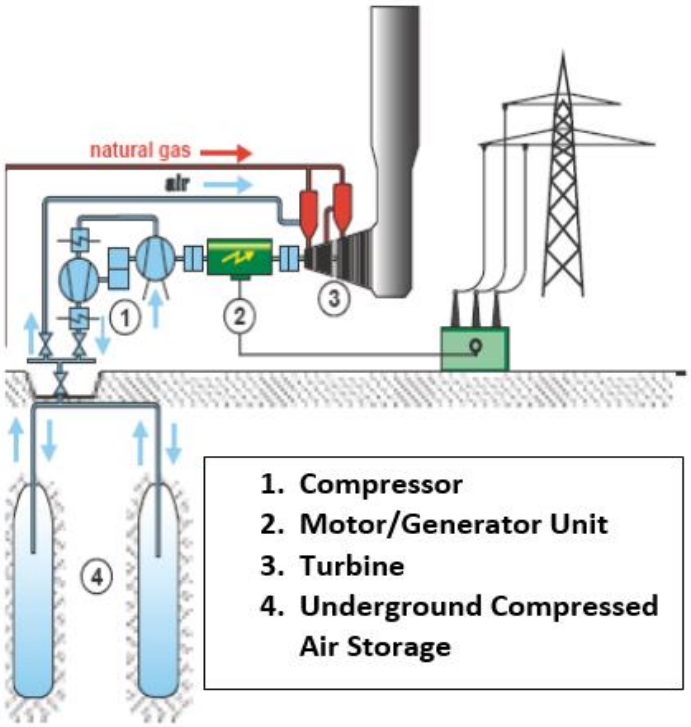

Fig. 3.6: Schematic diabatic CAES plant [83]

3.4.2 Advanced Adiabatic CAES Plants. (AA-CAES)

The adiabatic CAES concept came about in order to improve the efficiency of the CAES, and to eliminate the CAES dependency on the combustion of natural gas during the expansion stage leading to zero CO_2 emissions. The basic idea of the adiabatic CAES concept is to use a heat storage as a central element of the plant. This allows to supply heat needed for the expansion process from the otherwise rejected heat of compression and thus to avoid a gas combustor. During the charge period as seen in Fig. 3.7, the heat is extracted from the air stream and stored in thermal storage before the compressed air enters the cavern [84, 85]. When energy is required by the grid, the compressed air and heat energy is recombined and expanded through an air turbine

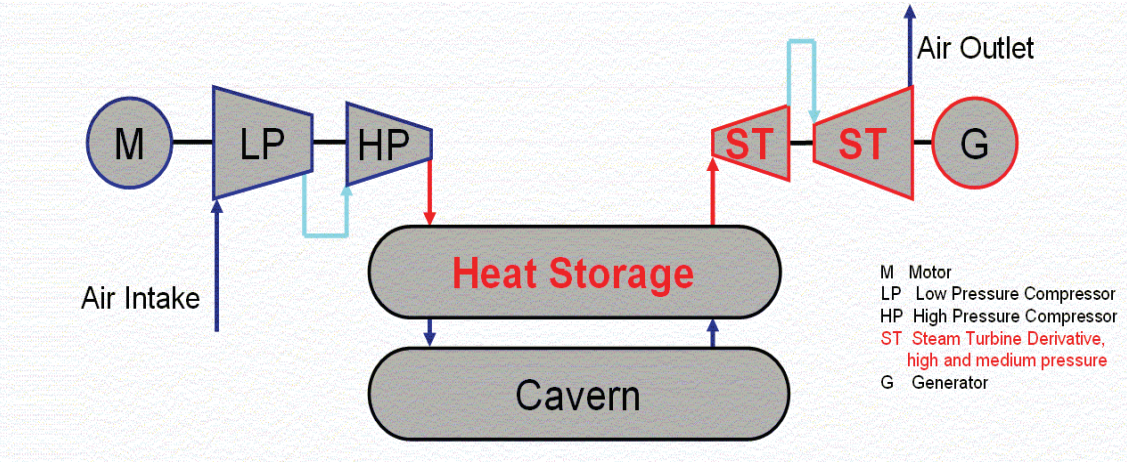

Fig. 3.7: Conceptual advanced adiabatic CAES plant [84]

The favourable characteristics of adiabatic CAES cycles compared to diabatic type have been known for the past 40 years which include zero CO_2 emission and higher storage efficiencies, and is being developed within the "AA-CAES" project (Advanced Adiabatic – Compressed Air Energy Storage), funded by the European Commission [85]. This project is investigating the technical potential of adiabatic technology, both for centralised and distributed storage [84].

3.4.3 Isothermal CAES Plants

Isothermal compression and expansion approaches attempt to maintain operating temperature by constant heat exchange to the environment [20, 81, 86]. They are only practical for low power levels, without very effective heat exchangers. The theoretical efficiency of isothermal energy storage approaches 100% for perfect heat transfer to the environment. In practice neither of these perfect thermodynamic cycles is obtainable, as some heat losses are unavoidable. [21, 81]. Controlling the pressure-volume (P-V) curve during compression and expansion is the key to efficient CAES. Roughly speaking, the closer the P-V curve resembles an isotherm, the less energy is wasted in the process. In principle, Isothermal CAES plant negates the need to store the heat of compression by some secondary means e.g. oil [21]. A slight variation of this is the near isothermal CAES where air is compressed in very close proximity to a large incompressible thermal mass such as a heat absorbing and releasing structure (HARS) or a water spray. A HARS is usually made up of a series of parallel fins. As the air is compressed the heat of compression is rapidly transferred to the thermal mass, so the gas temperature is stabilized. An external cooling circuit is then used to maintain the temperature of the thermal mass. Typically, with a near isothermal process an efficiency of 90-95% can be expected [21]. The isothermal CAES is still at the research and development stage and it could be sometime before large-scale deployment occurs [81].

3.5 Different Applications of CAES

CAES systems are designed to cycle on a daily basis and to operate efficiently during partial load conditions. This design approach allows CAES units to swing quickly from generation to compression modes. CAES plant can store large amount of energy for a long time and generate full power in relatively short time. As a result, CAES has the following applications in electric power systems [74].

- Peak Shaving: utility systems that benefit from the CAES include those with load varying significantly during daily cycle and with costs varying significantly with the generation

level or time of day. It is economically important for storing and moving low-cost power into higher markets and reducing peak power prices [74].

- Black Starting: The Huntorf CAES is being used for black starting the German grid. CAES plants can be used to build up a partial grid system, and for isolated operation, following a collapse of the power supply grid (blackout) [76].
- Load Leveling: CAES plants can respond to load changes to provide load following because they are designed to sustain frequent start-up/shut-down cycles. This application is seen in the McIntosh CAES plant [74].
- Renewable Energy Utilisation: The use of CAES can increase renewable energy penetration in the electric power grid. Linking CAES to intermittent renewable resources such as wind power can lead to an increase in the capacity credit of wind and improve environmental characteristics [74].
- Energy Management: CAES systems can allow customers to shift energy from a period when demand is low to a period when demand is very high. This can be done on a seasonal basis or on an annual basis.
- Load Management: CAES plants provide an effective load management means to lower the capacity and installed cost of distributed generators since storage plants could take care of the peak demand thus allowing the distributed generator to operate, in general, as a base loaded device [87].
- Delayed Facility Expansion: In an uncertain future for how the electric infrastructure will evolve in the near to long term, CAES plants in many cases provide lower cost alternatives to building new transmission, distribution, and generation equipment [87].

3.6 Mathematical Models for Power Flow

Several mathematical models have been developed over time for converting the flow of air into useful power. In [88, 89], Vongmanee and Monyakul described a model that used the volumetric flow rate of air instead of using the mass flow rate of air which is commonly used, it

also doesn't address the states of CAES completely. The state of storage pressure which is critical for placing constraint on the CAES vessel is omitted. A model that captures the essential dynamics related to air mass flow rates in and out of the reservoir and the reservoir internal pressure will be appropriate. The state of the internal energy is not needed for CAES analysis in terms of energy storage and power generation on hourly basis [89]. For this thesis, the model described in [89] is used and is explained below. The model is developed in terms of the three main storage operations namely; charging (compression), discharging (expansion) and storage.

(a) Charging Operation

An expression that relates the power to the compressor to the mass flow rate of air from the compressor which is fed into the storage is shown in Equation (3.1). This equation describes the adiabatic compression process which relates the compressor power input, $P_{C,}$ to the mass flow rate of air, $\dot{m}_{in,}$ into the reservoir [90]. This is valid for single stage compression.

$$\dot{m}_{in} = \frac{P_c}{c_{p1} T_{in} \left[\left(\frac{P_2}{P_1} \right)^{\frac{\gamma-1}{\gamma}} - 1 \right]} \eta_c \tag{3.1}$$

Where:

η_c=overall efficiency of compressor

P_2=pressure at outlet of compressor

P_1=pressure at inlet of compressor

γ=specific heat ratio of air (C_p/C_v)

C_{P1}=specific heat at pressure P_1

C_v=specific heat at constant volume

In Equation (3.1), all the parameters to the right hand of the equation are known and constant, except for P_1 and P_2 that change continuously with time as the mass of air in the cavern

$\dot{m}_{in}$ is changed. These values are calculated iteratively as $\dot{m}_{in}$ changes with time. It is assumed that pressure at the outlet of the compressor equals pressure inside the reservoir in the next iteration. For a constant volume configuration, a pressure constraint is imposed. There will be a minimum pressure and a maximum pressure allowed in the cavern or reservoir. This limit has to be maintained.

For a two-stage compression. The equation is given below;

$$\dot{m}_{in} = \frac{P_c}{c_p T_{in}\left[\left(\frac{P_2}{P_1}\right)^{\frac{\gamma-1}{\gamma}} - 1\right] + c_p T_2\left[\left(\frac{P_{out}}{P_2}\right)^{\frac{\gamma-1}{\gamma}} - 1\right]} \eta_c \tag{3.2}$$

Where:

P_1=pressure of injected air at inlet of first stage

P_2=pressure of air at inlet of second stage

P_{out}=pressure of air at outlet of final stage which equals to the pressure in the reservoir

T_{in}=temperature of air at inlet of first stage which is typically taken as ambient temperature

T_2=temperature of air at inlet of final stage

C_p= the specific heat of air at constant pressure

The input temperature of air to the first and second stage is assumed to be constant. P_{out} is the output pressure of the compressor which is also assumed to be the pressure of the storage as well and varies between P_{min} and $P_{max.}$ P_{min} and P_{max} are the minimum and *maximum pressure respectively the cavern can accommodate. The specific heat ratio (γ) for* air is taken to be 1.4. C_p is the specific heat of air at constant pressure is known to be 1.005 kJ/kgK.

(b) Discharging Operation

The turbine is modelled as a double stage air turbine. The air from the reservoir compressed

at a high pressure is released and subsequently expanded in combination with heat at a low pressure. The total mass flow into the turbine $\dot{m}_{Total}$ is the summation of the mass flow of air from the reservoir, $\dot{m}_{out}$, and the mass flow rate of fuel, $\dot{m}_{fuel}$, and is shown in (3.3).

$$\dot{m}_{Total}=\dot{m}_{out}+\dot{m}_{fuel} \tag{3.3}$$

The operational values of $\dot{m}_{fuel}$ and $\dot{m}_{out}$ for the Huntorf CAES plant are 11 kg/s and 425 kg/s respectively at rated power [76]. The ratio of these two quantities is called the air-fuel ratio, $\dot{m}_{ratio}$. The $\dot{m}_{ratio}$ for the Huntorf plant is calculated as 0.0259 [76].

The mass of air discharged from the reservoir is calculated using the equation in (3.4) utilising fuel input at the expansion stage.

$$\dot{m}_{out} = \frac{P_{GEN}}{\eta_m \eta_G [1+m_{ratio}] \left[c_p T_1 \left[1- \left(\frac{P_2}{P_1}\right)^{\frac{\gamma-1}{\gamma}} \right] + c_p T_2 \left[1- \left(\frac{P_{out}}{P_2}\right)^{\frac{\gamma-1}{\gamma}} \right] \right]} \tag{3.4}$$

Where:

η_m=mechanical efficiency

η_G=electrical efficiency

P_1=pressure of air at inlet of first stage

P_2=pressure of air at inlet of second stage

P_{out}=pressure of air at outlet of second stage which equals to the atmospheric pressure

T_1=temperature at inlet of first stage

T_2=temperature at inlet of second stage

C_p = the specific heat of air at constant pressure

P_{GEN}=power delivered by turbine

An increase in the $\dot{m}_{ratio}$ will result in a reduction in the mass flow rate of air. The ratio is zero for adiabatic expansion since there is no fuel input. Equation (3.4) is modified to (3.6) for

adiabatic expansion.

$$\dot{m}_{out} = \frac{P_{GEN}}{\eta_m \eta_G \left[c_p T_1 \left[1 - \left(\frac{P_2}{P_1} \right)^{\frac{\gamma-1}{\gamma}} \right] + c_p T_2 \left[1 - \left(\frac{P_b}{P_2} \right)^{\frac{\gamma-1}{\gamma}} \right] \right]} \tag{3.6}$$

Equation (3.6) relates the mass flow rate out of the storage which equals the mass flow rate input to the turbine which is proportional to the electric power produced by the generator.

(c) Storage

This study considers underground storage with constant volume configuration. The energy level of an ESS is generally expressed by its state of charge (SOC) at any instant of time. The SOC of a CAES is directly related to the mass of air stored, m_{stored}, which can be calculated at each instant of time by (3.7) assuming no leakage from the storage.

$$m_{stored} = \int_0^t \dot{m}_{in} dt \tag{3.7}$$

The net pressure inside the reservoir can be calculated using (3.8).

$$P = \frac{RT}{V} \int_0^t \dot{m}_{in} dt \tag{3.8}$$

For constant volume, a minimum mass m_{min} of air needs to be in storage to maintain the minimum pressure limit, P_{min}. P_{min} is known and m_{min} is calculated using (3.9). The mass of air available for power generation, or the usable mass of air m_{usable} is given by (3.10)

$$m_{min} = \frac{P_{min} * V_{st}}{R * T_{st}} \tag{3.9}$$

Where

V_{st}= volume of the storage

T_{st}= temperature of the storage

P_{min}= minimum pressure limit to be maintained in storage

R = gas constant

$$m_{usable} = m_{stored} - m_{min} \tag{3.10}$$

Therefore, for constant volume configuration of CAES, the $\dot{m}_{out}$ is derived from (3.11) for a known m_{usable} and duration of discharge denoted as D_{disc} assuming a constant discharge.

$$\dot{m}_{out} = \frac{m_{usable}}{D_{disc}} \tag{3.11}$$

3.7 Conclusion

The different energy storage types are introduced and outlined in this chapter. The relative advantage of one storage type over another is discussed with the aid of different figures. The operation of the CAES is explained by describing its major sections and components. Existing and proposed CAES plants around the world are discussed, and their differentiating characteristics are explained in detail. A general review of the two earliest installed CAES plants are provided. Their technical specifications and the differences in design and applications are outlined. The research explained in this thesis makes use of the Huntorf CAES plant characteristics. The different applications of the CAES and its application to the research outlined in the thesis are also discussed. The different ways the CAES technology has evolved over the years are shown. The features of the CAES at the various stages of evolution are outlined as well. Mathematical models for representing the CAES power flow is explained and outlined in detail in this chapter. These

mathematical models are utilised in developing the SOC model for the charging period and the generation model for the discharge period for the research work described in this thesis.

4. CAES MODELLING FOR WIND INTEGRATED POWER SYSTEMS

4.1 Introduction

Power system reliability evaluation is routinely done in electric power systems using established reliability models to represent the system components. The CAES differs from other conventional components as it can be operated both as a load and as a generation at different operating periods. The dependence of its capacity on different system variables and on its time sequence of operation creates considerable challenges in accurately modelling its behaviour. A technique that can accurately capture the time chronology of the charging and discharging behaviour of the CAES will be required to model the SOC of a CAES. A period analysis is proposed to separate the charging, discharging and idle operating periods within a day in order to incorporate the correlation of generation and load with the SOC of the CAES. Also, many situations can occur in which the generation and load models vary depending on diurnal and seasonal effects within the year. Factors such as seasonal de-ratings of the generating units, scheduled maintenance, seasonal variation of wind speed and system load, also the correlation between the wind speed and system load contribute to seasonal variability of the models within the year [1]. A period analysis can incorporate the inter relation of these numerous factors for reliability evaluation.

The operation of the CAES in a wind integrated power system is highly dependent on the wind and load characteristics for that particular area. The load model for the different season is developed for the province of Saskatchewan. The concept of representing load in period analysis using a daily model having a peak period and an off-peak period as described in [9, 69] is adopted in this research. The technique is extended further in this research to determine the operation of the CAES. The standard operational procedure of the CAES is to charge during the off-peak period and discharge during the peak period. A hybrid of both analytical and Monte Carlo simulation techniques is used for developing the SOC model of the CAES and performing its reliability evaluation. The developed technique is applied to the IEEE-RTS generation model connected to a

wind farm.

4.2 Incorporation of Correlation between Wind speed and Load

The modelling concept for a wind integrated power system (WIPS) is shown previously in Fig 2.9. The annual wind power capacity model is developed separately and is added to the annual conventional generation model which is then convolved with the annual load model to obtain the annual risk model. The annual models are simple to use, but inadequate to capture the correlation between the wind speed, the load and the performance of the CAES. Hence, a period analysis is proposed and is explained in detail in the sub-sections below.

4.2.1 Period Analysis

The variation in Saskatchewan daily average load and wind speed at the Swift Current site in the province of Saskatchewan are shown in Fig. 4.1. The daily peak system load and the maximum wind speed are 2889 MW and 65 km/hr respectively, and the data in Fig. 1 are shown in per unit of the peak values.

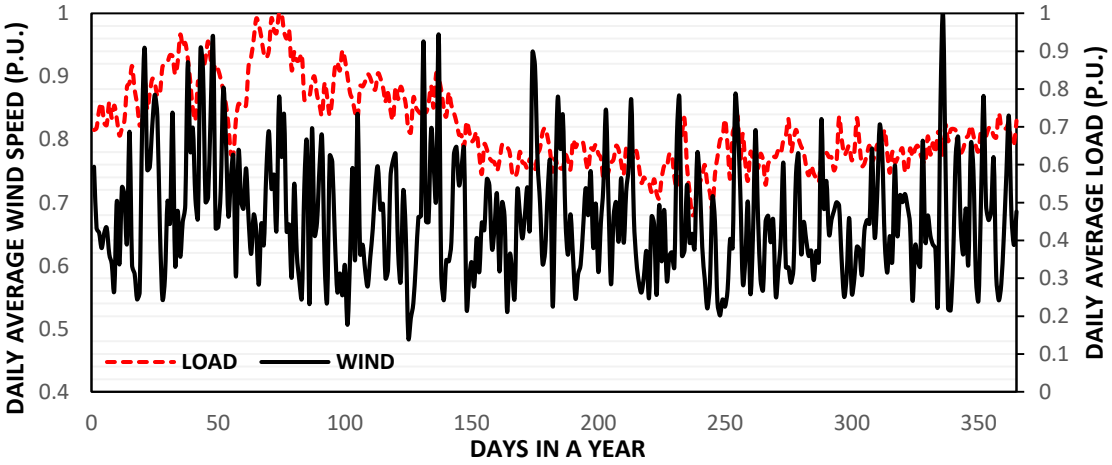

Fig 4.1: Daily average load and wind speed for a sample year

The load following pattern of the wind is very important in the incorporation of CAES in this research. A period analysis is done to incorporate the correlation between the load and the

wind speed, and to determine the operating state of the CAES. Period analysis as described previously in Chapter 2 is the process of dividing the annual period into smaller sub-periods and evaluating the reliability indices for each sub-period. The indices for each sub-period are then combined to obtain the annual indices [9]. A seasonal period analysis for the conventional generation without considering wind power is shown in Table 4.1. For this analysis, the entire year is broken up into four periods represented by the four different seasons in Canada. The generation model used is the IEEE-RTS generation model which has 32 generators with an installed capacity of 3405 MW [91], while the load model used is the Saskatchewan load model for a representative year with a peak load of 2700 MW. The annual LOLE obtained without period analysis is 8.4152 hrs/yr. This value is very close to the LOLE obtained using the period analysis.

Table 4.1: Seasonal sub-periods LOLE

PERIODS	**MONTHS**	**LOLE(hr/pd)**	**%LOLE**
WINTER	November-February	7.0749 (hr/2880hrs)	84.52%
SPRING	March-May	0.5747 (hr/2208hrs)	6.87%
SUMMER	June-August	0.4526 (hr/2208hrs)	5.41%
FALL	September-October	0.2677 (hr/1464hrs)	3.20%
TOTAL		8.3699 hr/yr	100%

It can also be seen that the winter sub-period contributes about 85% to the total annual LOLE pointing to the fact that the province of Saskatchewan has a winter peaking load model. The objective will be to reduce the winter LOLE as much as possible. The methodology and operating principle of the CAES in combination with the wind will have a considerable effect on the LOLE and a major objective of this research is to determine the optimal operation of the CAES in combination with wind to reduce the LOLE and improve the reliability of the system. The diurnal load following capability of the wind power is however not addressed by the seasonal analysis. Refs [9, 69] present a technique to incorporate the correlation between load and wind during the peak and off-peak periods for a diurnal analysis and the technique is used in this research.

4.2.2 Diurnal Evaluations

The strategy of operating the CAES will be highly dependent on the load profile for the particular site in most cases. The wind profile for the site will also be a major determinant on how the CAES is operated especially when the wind farm is coupled to the CAES or when renewable energy benefits are to be fully utilized. Both the system load and the wind at a particular site have a specific diurnal pattern. Fig. 4.2 shows the Saskatchewan load and the Swift Current wind pattern for a typical day for all four seasons.

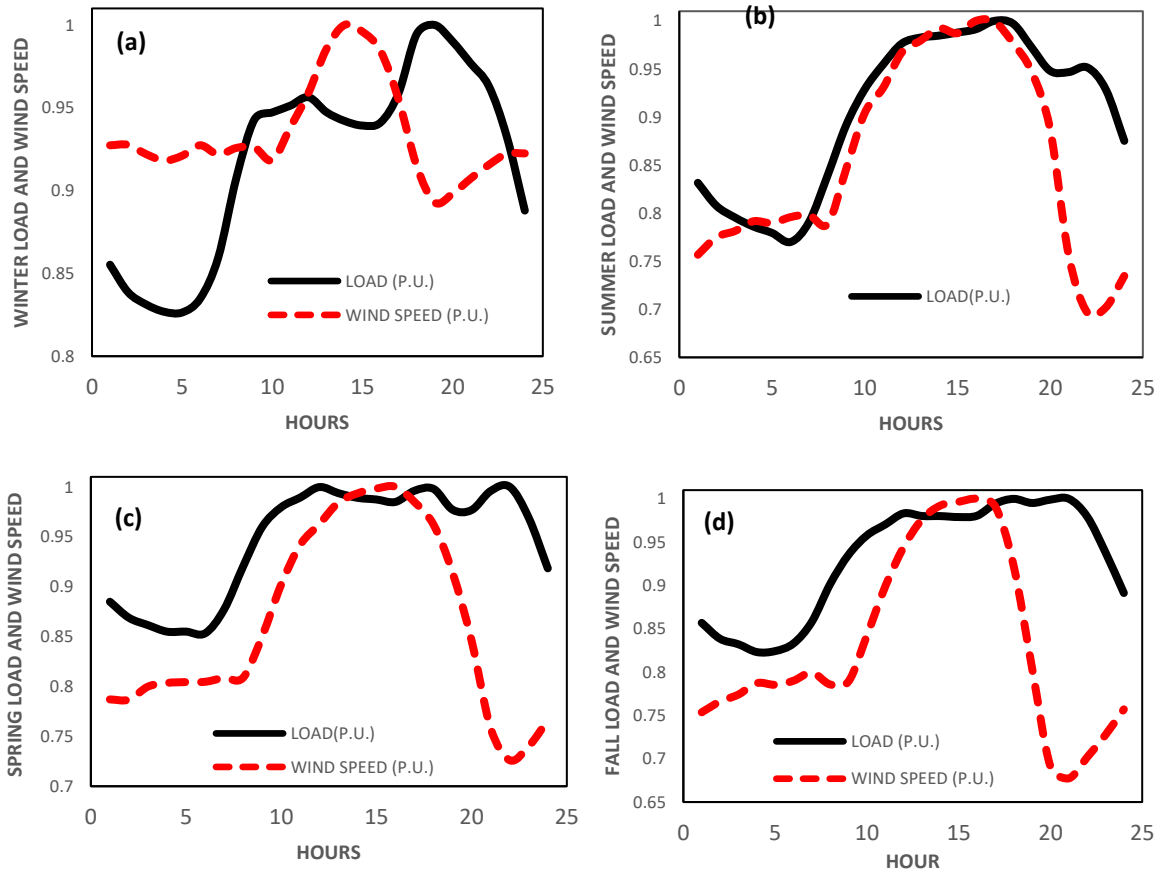

Fig. 4.2: Load and wind speed profile of a typical day during (a) winter (b) summer (c) spring and (d) fall.

Fig. 4.2 shows that on a typical winter day, the load following capability of the wind is greatly reduced since the speed of the wind drops when the load peaks while for the typical summer day, the load following capability of the wind is very strong. For the fall and spring season, the load following capability of the wind isn't as good as that of the summer season but is better than the winter season. This load following capability has implications for the incorporation of CAES since one major objective is to store as much wind as possible during periods of low demand and discharge during periods of high demand. A 2 diurnal sub-periods for a season is proposed in [9] to capture the load following capability of wind. For this study, a day is divided into two sub-periods; peak and off-peak hours. The peak hours generally will make the greater contribution to the overall reliability indices i.e. LOLE. The correlation between the load and the wind during the different sub-periods will be incorporated to obtain accurate results.

The determination of the contribution of wind power to avoiding load curtailments during the peak hours of the year is important in assessing the capacity value of wind sources [9]. A detailed description is given in [9]. From [9], the capacity credit of wind in the Pennsylvania-New Jersey-Maryland (PJM) interconnected system is calculated based on the wind generation during the peak 5 hours from 3 PM to 7 PM of the peak season from June 1 through August 31 [13, 14]. The New York Independent System Operator determines wind capacity credit using the wind generation between 2-6 PM from June through August and 4-8 PM from December through February [92, 93]. The peak 5 hours of the day in the winter season was, therefore, considered in this study to determine the peak load period for the diurnal evaluation as used in [9]. The duration for which the system load exceeds 98% of the daily peak was therefore considered as the diurnal peak load period for each season. Fig. 4.3 shows average load data for a day normalized by the daily peak load for each season. The peak periods for each season are presented in Table 4.2. The remaining hours of day are off-peak hours.

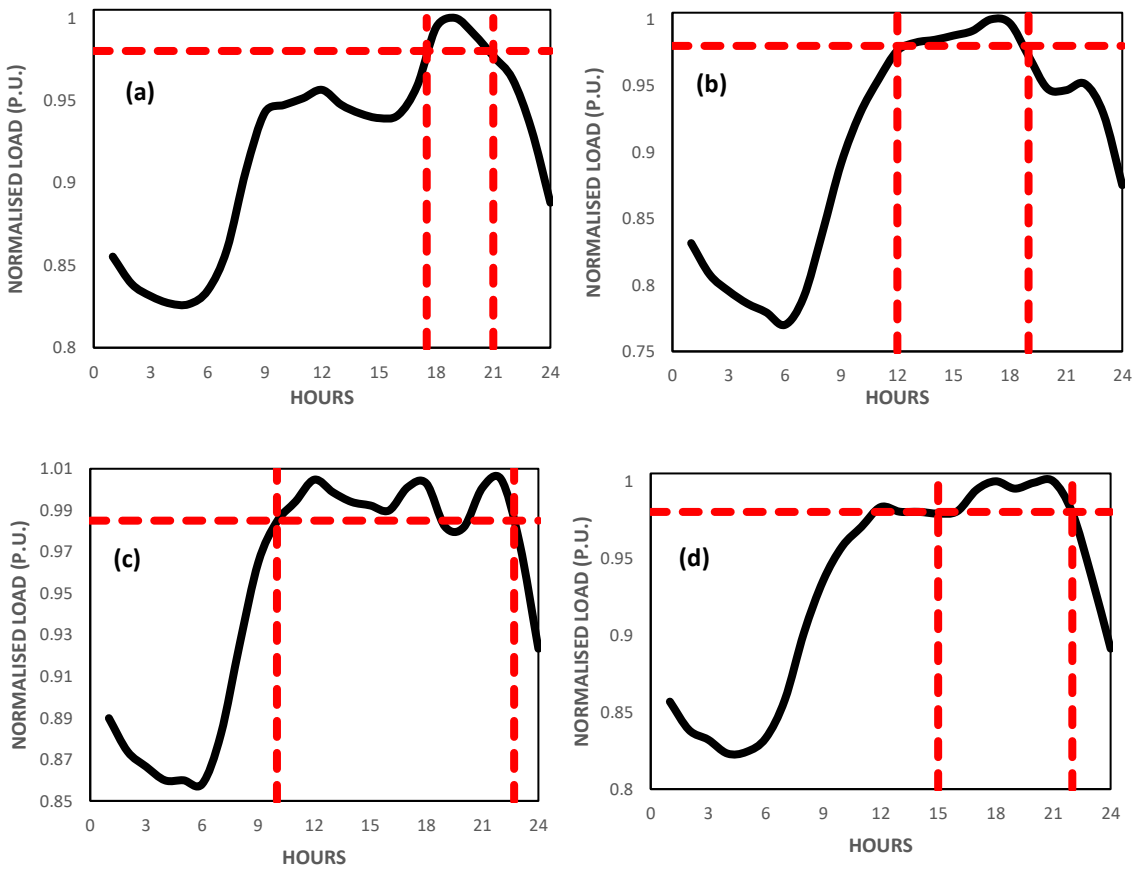

Fig. 4.3: Normalised daily load peak period hours for (a) winter (b) summer (c) spring (d) fall

Table 4.2: Peak load duration for each season

Season	Peak Hours
Winter	17th-21st hour
Spring	9th-22nd hour
Summer	12th-19th hour
Fall	15th-22nd hour

4.3. Development of Reliability Model for CAES

The winter peaking characteristics of the Saskatchewan load profile has the resultant effect of the winter season contributing the largest percentage to the LOLE compared to the other three

seasons as seen in Table 4.1. The focus here will be on developing a reliability model for the operation of the CAES in the winter period. An extension of this can be made for the other seasons but their effect may be practically insignificant since their contribution to the annual LOLE is very small. In developing the reliability model for the CAES, the load model will be used to determine the strategy for operating the CAES. Fig. 4.4 shows the charging and discharging operation of the CAES for a typical day in the winter. The standard operation of the CAES in order to improve the reliability of the power system and lower the LOLE will be to charge during the off-peak load period (hours 1-16 and 22-23) and discharge during the peak load period (hours 17-21) as can be seen in Fig. 4.4.

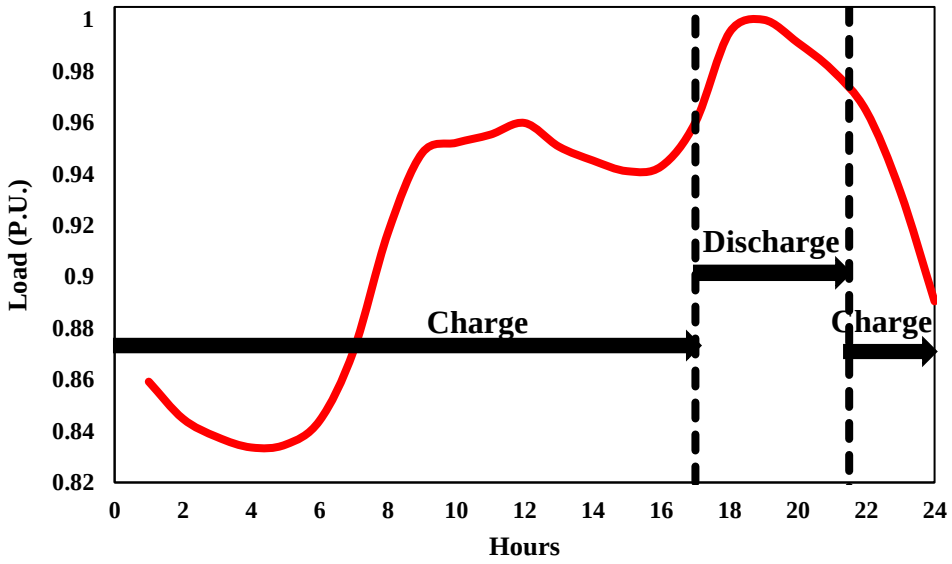

Fig. 4.4: Winter diurnal charge/discharge operation for a 2-period analysis

When a wind farm is coupled to the CAES, the state of charge at the end of the charging cycle will be different for each day because of the intermittency and the variable nature of the wind speed. To accurately model the CAES and capture this intermittency, and to incorporate the failure events, a hybrid approach is used which combines both sequential Monte Carlo Simulation (MCS) and analytical approach to determine the generation adequacy assessment of the system.

Both the Monte Carlo Simulation (MCS) and analytical approaches have been used for reliability evaluation of different cases of power systems. When dealing with energy storage, it

requires modelling the chronology of the SOC of the storage system as well as the variability of the wind level, the MCS methods becomes the more suitable option in incorporating all the dependencies and correlations between these various factors. It is however difficult to develop a generalized tool for different configuration and scenarios using this approach. The analytical method generates the multistate probability distribution which can be easily convolved with the generation capacity probability distribution of conventional units to get the combined generation model. The research work presented in this thesis proposes a hybrid approach of both analytical and MCS in developing a simplified SOC model of CAES for reliability evaluation. The overall reliability analysis is done using a period analysis in order to incorporate the seasonal variability and correlation of the different factors such as wind, conventional generation, load etc. Also, since the charging and discharging operation of the CAES occurs within a diurnal cycle, the method also proposes a sub-period approach within a diurnal cycle. The developed approach integrates wind energy and conventional generation and is applied to the IEEE-RTS.

4.3.1 Proposed Diurnal Hybrid Approach

The proposed period analysis approach divides a year into seasons, and assumes that each season consists of days with similar diurnal profile or characteristics**.** The seasonal analysis can also be extended to monthly assessment to improve the accuracy of the evaluated reliability indices. Each day consists of a diurnal cycle of 24-hours and this diurnal cycle is further divided into two sub-periods of off-peak and peak period as shown in Fig. 4.4. The charging operation of the CAES usually occurs during the off-peak period when load demand and electricity prices are relatively low, and the discharge operation occurs during the peak period when load demand and electricity prices are high. Discharge can also occur at other times during a loss of load scenario. This approach can be further extended to 3 periods namely; charging, idle and discharge period. In the idle period, the CAES neither charges nor discharges. A hybrid method is proposed consisting of the Monte Carlo simulation and an analytical technique. The MCS approach is used to determine the SOC of the CAES during the charging period recognizing the time chronology

and the correlation between the variation in the wind, the load and the SOC of the storage. The analytical approach is used to convolve the generation model in the form of discrete probability distribution with the load model to obtain the adequacy indices in each sub-period.

The SOC of the storage, which is related to the quantity of the mass of air in storage at a given time, is influenced mainly by two factors namely; 1) the amount of power available to compress air in the cavern, and 2) the failure and repair characteristics of the components of the CAES. The MCS approach sequentially simulates the wind power generation and load to determine the power available to compress the air into the cavern and to determine the chronological change in SOC to create the CAES SOC model during the charging period. The simulation process also incorporates the failure characteristics of the motor/compressor set of the CAES. Failure is a random event and can occur anytime, and this influences the amount of mass of air that can be stored during CAES charging. The SOC at a given point in time depends on its previous condition. A sequential MCS approach can easily incorporate the sequence of events in time chronology, and therefore, is a useful technique for systems that contain many time dependent random variables [1]. Analytical method is used to evaluate the adequacy indices using the generation model obtained for the period by including the SOC model created using MCS. This method therefore uses both the analytical and MCS approach for reliability modelling of electric power system considering CAES.

4.3.1.1 Modelling of the Charging Period

The charging and discharging process of the CAES is decoupled as shown in the schematic diagram of the CAES in Fig. 3.4a. The charging process takes place distinctly from the discharge and occurs at separate times as well. The SOC of the CAES is proportional to the mass of air in cavern, and the mass of air is dependent on the mass flow rate of air into the cavern. This mass flow rate of air into the cavern is mainly influenced by the power available to run the motor/compressor unit denoted as P_c as seen in (3.2).

For a time (t) during charging, the power available to charge the CAES, P_a depends upon

the committed conventional generation P_{com} , the power available from the wind P_w and the load demand L_d at that instant. This is obtained using (4.1).

$$P_{a(t)} = P_{com(t)} + P_{w(t)} - L_{d(t)} \tag{4.1}$$

The input power to the CAES compressor, P_c, is given by (4.2)

$$P_c = \begin{cases} P_{a(h)}, & P_{a(h)} < P_{r(h)} \\ P_{r(h)}, & P_{a(h)} \geq P_{r(h)} \end{cases} \tag{4.2}$$

Where, $P_{r(h)}$ is the rated capacity of the CAES compressor motor. The turbine is modelled as a double stage air turbine.

The SOC of the CAES for each day is modelled using the MCS method for repeated samples. Finally, a probability distribution of the SOC is created using Sturges' rule [24]. The major components of the CAES with failure probability of concern is the motor/compressor set during the charging period and the turbine/generator set during the discharging period. These components are represented by a 2-state Markov model as shown in Fig. 4.5. The model can also be modified to include additional components if necessary.

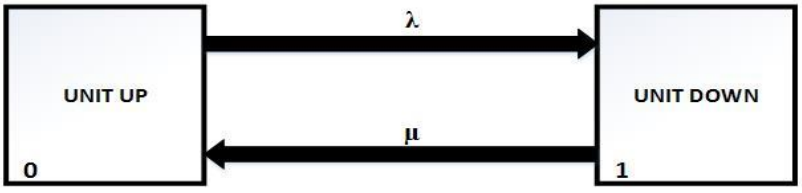

Fig. 4.5: Two-state Markov model for CAES SOC modelling

The motor/generator is a single unit for the Huntorf CAES and shares one single shaft and changes mode depending on whether it is working as a load (charging) or working as a generator (discharging). The operating history of CAES components is obtained from the state transitions and are expressed in (4.3) and (4.4).

$$Up\ time = -\frac{1}{\lambda} \ln (X_1) \tag{4.3}$$

$$Down\ time = -\frac{1}{\mu} \ln (X_2) \tag{4.4}$$

Where λ = expected failure rate and μ =expected repair rate and X_1 and X_2 are uniformly distributed random numbers [1].

The SOC for each hour (SOC_h) is sequentially calculated during the charging period. The SOC at the end of the charging cycle, SOC_d is obtained by (4.5). As noted earlier, the SOC is related to the mass of air in storage.

$$SOC_d = \sum_{h \in x} SOC_h \tag{4.5}$$

Where, $h \in x$ excludes all hourly intervals associated with the outage of the motor/compressor set during the charging period. The charging cycle within the seasonal period is repeatedly simulated for N samples. The set of the simulated SOC samples is converted into a discrete probability density function; $F(SOC) = P(SOC_{k=1\ to\ s})$, where s is number of SOC states determined by Sturges' Rule [68] in (4.6), and $P(SOC_k)$ is the probability that the CAES will have a state of charge equal to SOC_k at the end of a charging cycle.

$$s = 1 + 3.322 \log_{10}(N) \tag{4.6}$$

The class size (CS) of each of the class interval is calculated using (4.7). SOC_{max} is the maximum SOC assuming rated power is available for compression during all the charging hours.

$$CS = SOC_{max}/s \tag{4.7}$$

The simulation process to obtain the CAES SOC during a charging cycle is shown in Fig. 4.6.

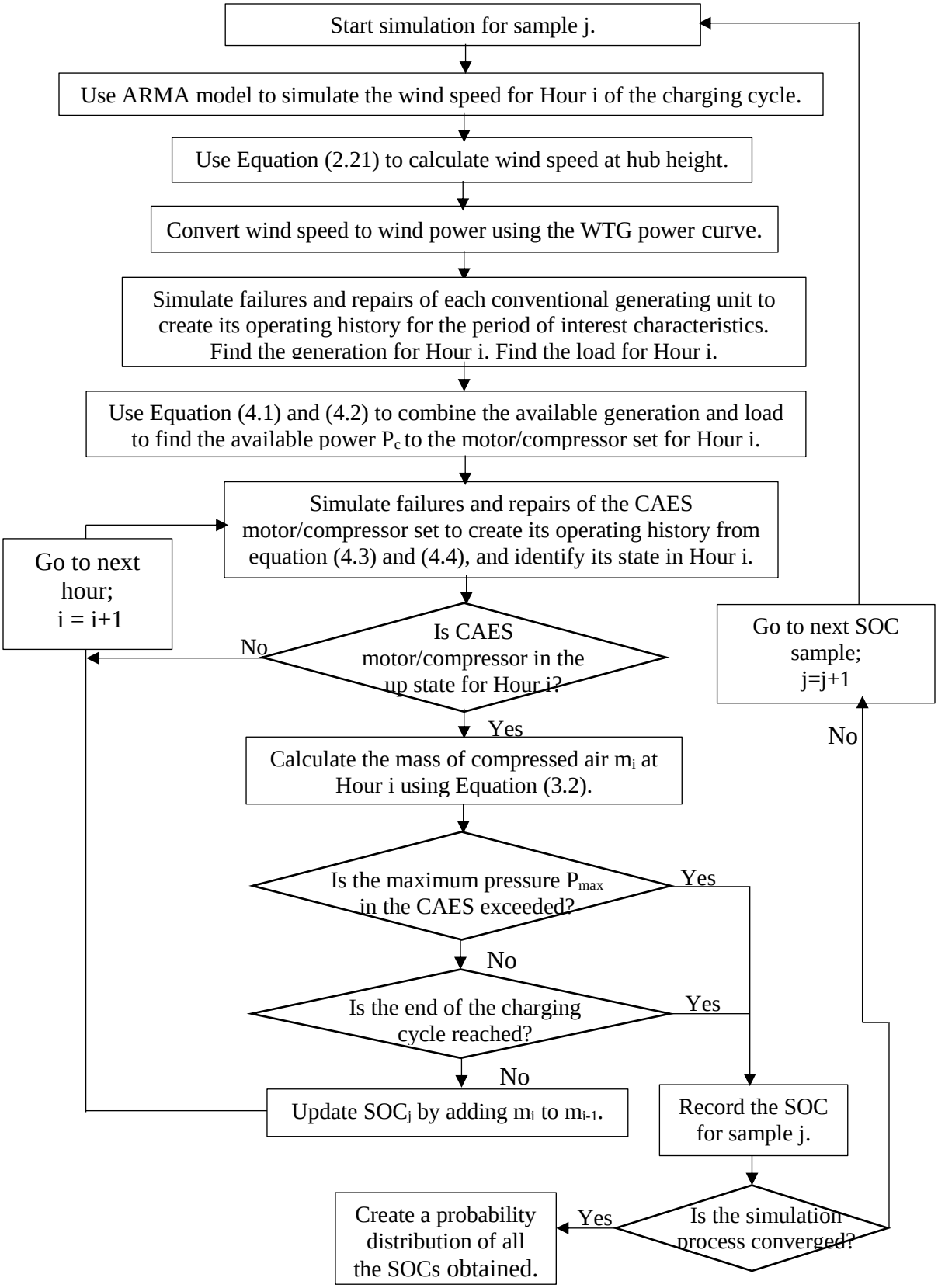

Fig. 4.6: Simulation process for the CAES SOC modelling

The system model for a wind integrated power system including CAES during the charging period is shown in Fig. 4.7.

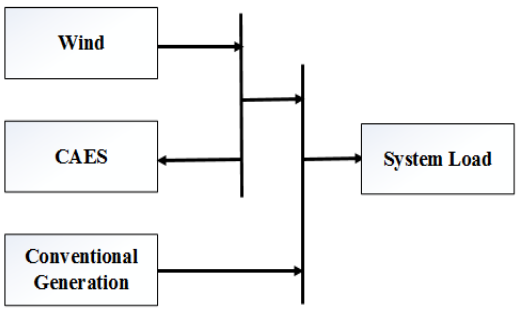

Fig. 4.7a: System model for a WIPS including CAES coordinated with wind resources

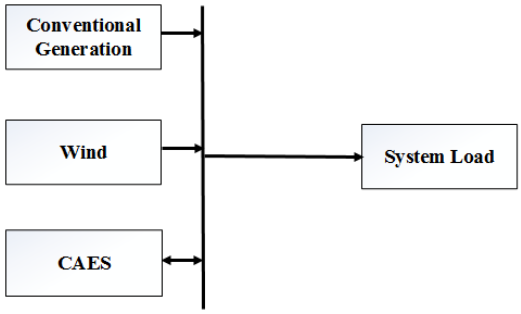

Fig. 4.7b: System model for a WIPS including CAES connected to the grid

Four models are considered in the adequacy evaluation of a WIPS incorporating CAES during charging as shown in Fig. 4.7; the CAES SOC model, the wind generation model, the load model and the conventional generation model. In the system model depicted in Fig. 4.7a, the CAES is operated in coordination with the wind resources to absorb the variability of wind power to promote renewable energy utilization in the system. The CAES is served by the wind resource only, and therefore, the original system load is not affected by the operation of the CAES as can be seen in Fig. 4.8a. In the model shown in Fig. 4.7b, the CAES is connected to the grid and behaves as a load during the charging period by taking power from the grid and using it to compress air. The original system load is therefore changed due to CAES charging as shown in Fig 4.8b. The figure shows that the charging profile of the CAES is superimposed with the original load profile to obtain a modified load. The modified load is used as the system load model for risk evaluation in this case.

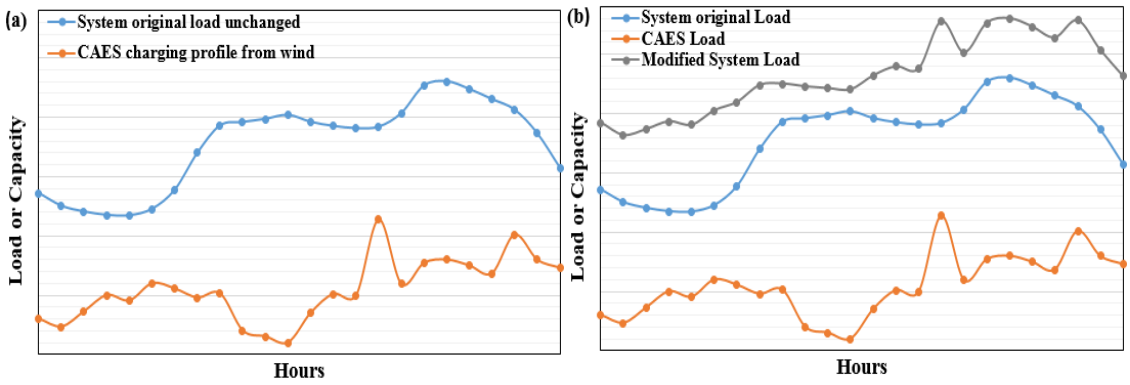

Figure 4.8: System load depiction when the CAES is (a) served by only the wind resources and (b) is connected to the grid

4.3.1.2 Modelling of the Discharging Period

The discharge generally occurs during the peak period of the day. The CAES shifts the excess generation from the off-peak period to the peak period to serve the peak load.

During discharge, the compressed air from the reservoir is fed to the turbine which is coupled to the generator. The power produced by the generator is dependent on the mass flow rate of air out of the storage into the turbine as calculated in (3.4).

As described in Section 4.3.1.1, the CAES SOC model obtained at the end of the charging period is represented by a discrete probability distribution. The mass flow rate of compressed air out of the cavern, $\dot{m}_{out}$ is calculated for each state of the SOC model using (4.8), and a probability distribution of $\dot{m}_{out}$ is created.

$$\dot{m}_{out(k)} = \frac{m_{stored(k)} - m_{min}}{D_{disc}} \tag{4.8}$$

Where, the expression for m_{stored} and m_{min} are obtained from (3.7) and (3.9) respectively.

The power output of the CAES generator $P_{GEN(k)}$ is calculated using (3.4) from the $\dot{m}_{out(k)}$ obtained from (4.8) for all the k states of the discrete distribution. A probability distribution of the output power P_{GEN} is thus created. In this way the multistate SOC model obtained during the

charging period is converted to a multistate generation model that serves as additional generation during the peak period. This multi-state generation model is then modified with the forced outage rate of the turbine/generator as shown in Table 4.3 to obtain the generation model incorporating the failure and repair of component during discharge. State "1" means that the generator is fully up with a probability of P_{in} while state "0" means that the generator is full down with a probability P_{out} represented by the FOR.

Table 4.3: CAES generation availability table

State	Probability
1	$P_{in}=(1-FOR)$
0	$P_{out}=(FOR)$

The reliability system modelling for the discharge period is shown in Fig. 4.9. The probability distribution of the total generation F_{gen} available during the discharge period is seen in (4.9). F_{gen} is the convolution of all the generation sources in the system.

$$F_{gen}=F_{conv} * F_{wind} * F_{caes} \tag{4.9}$$

Where F_{conv} is the conventional generation model available for that period in form of discrete probability distribution, F_{wind} is the wind generation available for the peak period in the form of multi-state capacity model. F_{caes} is the multi-state generation model obtained from the CAES in the form of discrete probability distribution. The total generation model F_{gen} is convolved with the load model for that period and the peak period reliability indices are obtained.

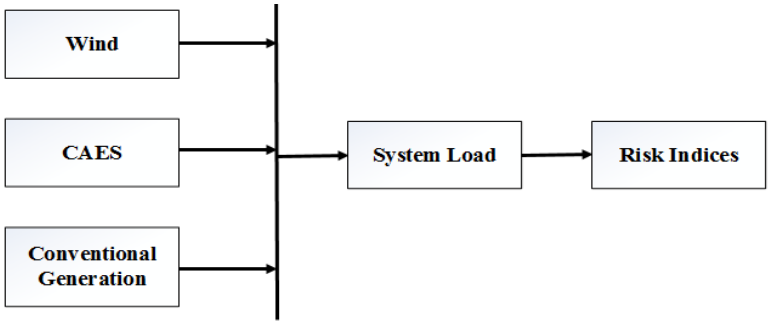

Fig. 4.9: System model for a WIPS including CAES for discharge period

4.3.1.3 Modelling of the Idle Period

The idle period is the time during which the CAES neither charges nor discharges. This period usually occurs during intermediate load levels, neither peak nor off-peak. During this period, the CAES can discharge to avoid a loss of load event. The probability of a loss of load event occurring during this intermediate load level is very small.

The CAES will maintain its original SOC during this idle period if LOLE events do not occur. The SOC level will drop if or when such events occur, but since the probability of the loss of load event occurring during this period is very small, it is assumed in the reliability modelling process that the change in the SOC level during this period can be ignored. Therefore, the generation model obtained at the end of the charging cycle is also considered the same for this period.

The reliability system modelling for this period is shown in Fig. 4.10. It will include a total generation model which is a combination of the wind generation model and the conventional generation for that period and this is convolved with load model for that period to obtain the period reliability risk indices. The CAES generation model can also be included in the case of a loss of load event.

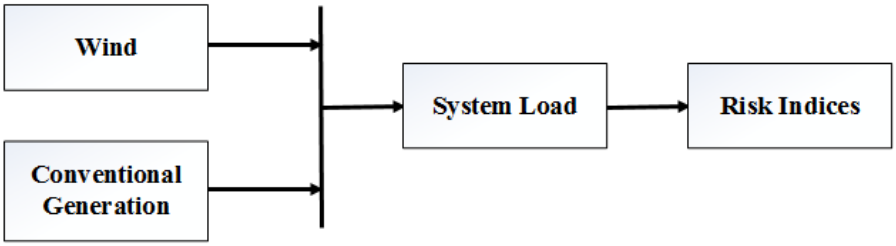

Fig. 4.10: System model for a WIPS including CAES for the idle period

The total reliability risk indices are obtained by the addition of the sub-period risk indices. The risk indices for the charging and discharging sub-periods within a day are added together in the case of the two-period analysis while the risk indices for the idle period is also added to that of the charging and discharging period in the case of the three-period analysis. The diurnal risk indices are multiplied by the number of days in a season to obtain the results for a particular season for the year. This method also is extended to derive the annual reliability indices as well.

4.3.2 Application to a test system

The strategy of operating the CAES is highly dependent on the load model for a site. The peak five hours of the day in the winter season was used to determine the discharge period while the remaining hours of the day were considered off-peak hours as seen in Fig. 4.4. Fig. 4.4 shows the charge and the discharge duration based on the load model for a typical Saskatchewan winter day. The conventional generation model used is the IEEE-RTS generation model which has 32 generators with a total installed capacity of 3405 MW [1]. The load model used is the Saskatchewan load model for a sample year with a peak load of 2700 MW. A 100 MW motor/compressor is used for the CAES connected to a 100 MW wind site assuming that the CAES is directly coordinated with the wind resource and that all the wind enters the storage. The rating of the motor constrains the amount of wind generation that can be allowed. The SOC model at the end of a charging cycle is shown in Fig. 4.11 with maximum SOC of $1.3*10^7$ kg of air in cavern.

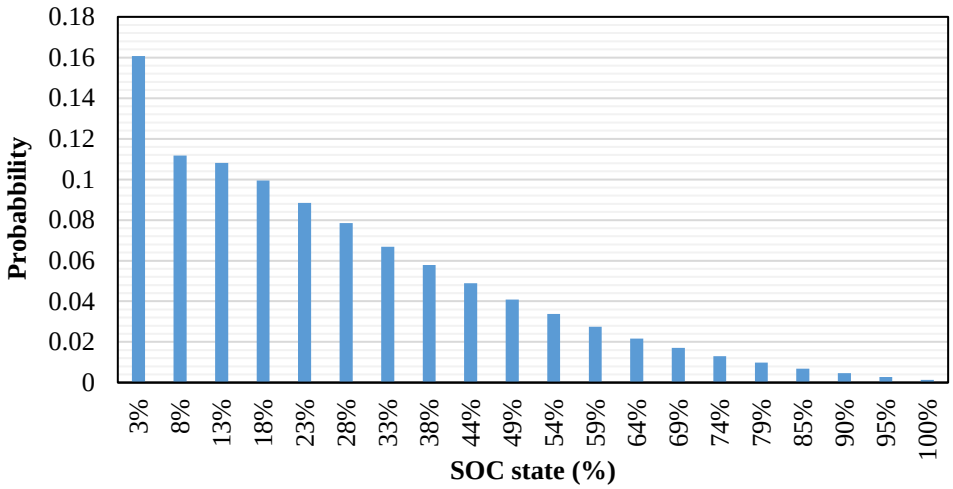

Fig. 4.11: Multistate CAES SOC model

The multistate generation model for the CAES considering a 100 MW generator with a FOR of 6.38% is shown in Table 4.4a. The model considers a 5-hour discharge period. Table 4.4b shows the model if the generator size is doubled.

Table 4.4a: Multistate CAES generation model for a 100 MW generator size

MW	PROB
0	0.0638
12.51	0.150496
37.54	0.104579
62.57	0.101170
87.6	0.093047
100	0.486907

Table 4.4b: Multistate CAES generation model for a 200 MW generator size

MW	PROB
0	0.0638
12.51	0.150496
37.54	0.104579
62.57	0.101170
87.6	0.093047
112.63	0.082836
137.66	0.073569
162.69	0.062585
187.72	0.054177
200	0.213740

4.3.3 CAES Period Analysis

The loss of load expectation (LOLE) is the most widely used reliability index, and is

therefore, used in this study. As described in chapter 2 of this thesis, a loss of load event occurs when the capability of the generating capacity remaining in service is exceeded by the system load level. The lower the LOLE index, the more reliable the system. The LOLE expression is shown in (4.10).

$$\text{LOLE} = \sum_{i=1}^{n} P_i(C_i - L_i) \text{ hour/period (hr/pd)} \quad (4.10)$$

Where,

C_i=available capacity in hour i

L_i=forecast peak load in hour i

$P_i\ (C_i\text{-}L_i)$ = probability of loss of load on day i [1].

The model described in section 4.3.1 is applied to a test system and 3 different scenarios are considered. The scenarios are described below.

1. **SCENARIO 1**: Only wind energy is used to charge the CAES which is constrained by the rating of the motor/compressor performing the compression of air. The excess wind energy that the motor cannot utilise is spilled.
2. **SCENARIO 2**: Only wind energy is used to charge the CAES which is constrained by the rating of the motor/compressor performing the compression of air. The excess wind energy that the motor cannot utilise is used to serve the load during the charging period.
3. **SCENARIO 3**: The total generation is obtained by summing the committed conventional generation with the wind generation for each hour. The load demand for each hour is then subtracted from the total generation, the remainder of which is used to compress air in the CAES.

For all the scenarios explained above, 2 cases are considered. Case 1 considers a 19-hour charging and 5-hour discharge period while Case 2 considers a 10-hour charging and 14-hour discharge period. The analysis is done for increasing wind penetration relative to the conventional generation. The study includes wind penetration level of 5% (179 MW) up to 30% (1459 MW). The peak load of the test system is assumed to be 2700 MW. The LOLE was calculated for the charging period and the discharging period respectively and summed up to get the total winter

LOLE.

1. SCENARIO-1 CASE 1:

This case considers a charging period of 19-hours and a discharging period of 5 peak hours (17^{th}-21^{st} hour). The results obtained are shown in Fig. 4.12. Fig. 4.12a shows the LOLE with increasing wind penetration for the charging period considering a 100 MW compressor motor. The solid line without any marker shows the base case LOLE of the IEEE-RTS for the 19-hour period without considering wind power or CAES in the system. The solid line with the triangular marker shows the LOLE during the charging period when the system includes wind power and CAES. The dash line shows the LOLE for the same period considering wind power without CAES in the system. Fig. 4.12b shows the LOLE with increasing wind penetration for the discharging period considering two different generator capacities of 100 MW and 200 MW. The solid line without any marker shows the base case LOLE of the IEEE-RTS for the peak 5-hour period without considering wind power or CAES in the system. The solid line with the triangular and square marker shows the LOLE when the CAES generator of 100 MW and 200 MW respectively is used in combination with the wind and conventional sources for that period. The broken line shows the LOLE for the same period considering wind power without CAES in the system. The LOLE obtained in the two sub-periods of 19 hours and 5 hours are aggregated to obtain the LOLE of the entire period, and the results are shown in Fig. 4.12c.

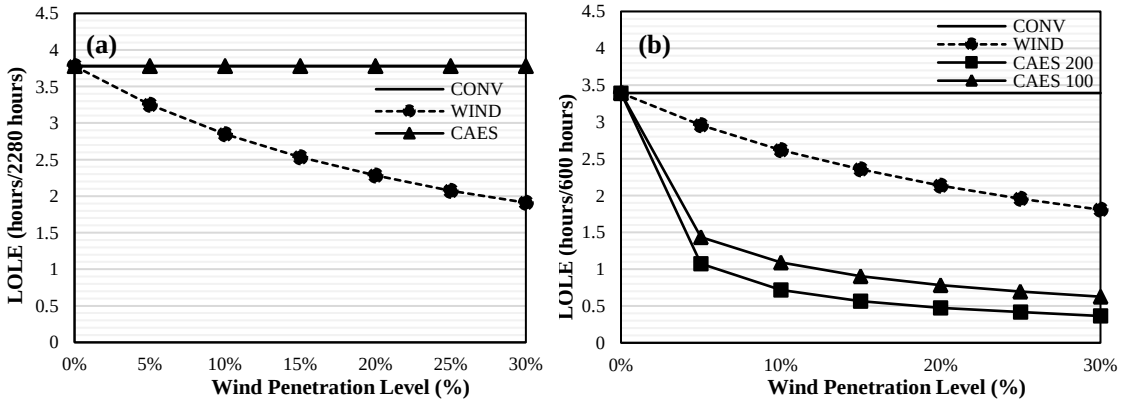

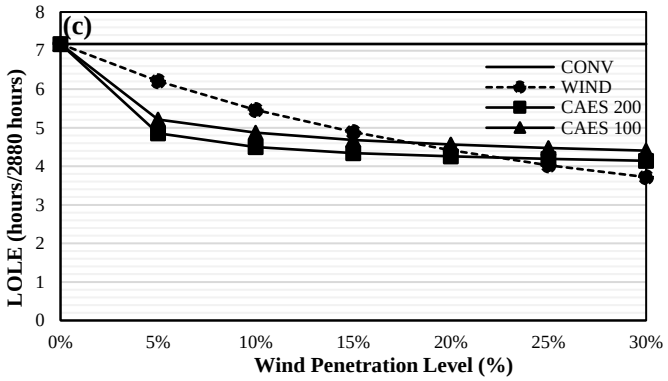

Figure 4.12: Scenario 1, Case 1 LOLE analysis for increasing wind penetration for (a) Charging, (b) Discharging and (c) Total winter period.

Fig. 4.12 shows that the system LOLE decreases with increase in wind penetration even without adding CAES to the system. The incremental benefit in reliability however decreases with increasing wind penetration. With the addition of CAES and wind, Fig. 4.12a shows that the LOLE is equal to that of the base case during the charging period for Scenario 1 when all the wind power is used for charging the CAES. The wind power does not contribute to the load in this case, and the LOLE is therefore the same as that of the base case. The contribution of the CAES to the reduction of LOLE during the discharge period is quite significant as seen in Fig 4.12b. The improvement in system reliability quantified by the reduction in LOLE due to CAES during discharge is shown in Table 4.5 for the different wind penetration levels.

Table 4.5: Reliability improvement due to CAES operation with the wind during discharge for Scenario1 Case 1

A	B	C	D
Wind Penetration Level	**LOLE (hr/pd), with no CAES**	**Change in LOLE due to CAES with a 100 MW generator**	**Change in LOLE due to CAES with a 200 MW generator**
0%	3.3917	-	-
5%	2.9572	-52%	-64%
10%	2.6176	-58%	-73%
15%	2.3559	-62%	-76%
20%	2.1350	-63%	-78%
25%	1.9544	-64%	79%
30%	1.8075	-65%	-80%

It can be seen in Table 4.5 that the % reduction in the LOLE in column C and D increased as the wind penetration level in the system increased. The reliability contribution of adding CAES to the system is significant when wind penetration is increased from low levels, such as 5% to 10%, but the benefits tends to saturate at higher penetration levels. The reason for this has to do with the capacity of the CAES generation for increasing wind penetration level. The increase in expected output of the CAES multi-state generation initially increases for the 5% wind penetration level, this increase becomes marginal and drops further as the wind penetration increases. A comparison of the results in the last two columns of Table 4.5 shows that increasing the generator capacity from 100 MW to 200 MW can contribute between 12-15% further reductions in the system LOLE during the discharge period. System LOLE studies done to assess the generation adequacy do not normally consider the operational details. The operating constraints related to the ramping and wind following capability of the generating units are not considered in this study.

The effect of using the CAES isn't as significant for the total winter period as seen in Fig. 4.12c when compared to the discharging period as seen in Fig 4.12b. The improvement in system reliability quantified by the reduction in LOLE due to CAES during the total winter season is shown Table 4.6. The results show that the reliability benefits due to CAES in fact decreases with increase in wind penetration.

Table 4.6: Reliability Improvement due to CAES operation with the wind for the winter period for Scenario 1 Case1

A	**B**	**C**	**D**
Wind Penetration Level	**LOLE (hr/pd), when the wind was used with the base case**	**Change in LOLE relative to column B using a 100 MW generator**	**Change in LOLE relative to column B using a 200 MW generator**
0%	7.1701	-	-
5%	6.2086	-16%	-22%
10%	5.4650	-11%	-18%
15%	4.8901	- 4%	-11%
20%	4.4180	+3%	- 4%
25%	4.0282	+11%	+4%
30%	3.7183	+18%	+11%

Columns C and D in Table 4.6 shows a decreasing % reduction in the LOLE as the wind penetration increased in the system. This shows a complete opposite to the trend of an increase in Table 4.5. As the wind penetration increases, the reduction in LOLE decreases up to a certain point and then with further increase in the wind penetration, the CAES increased the system LOLE relative to when the wind was used as seen in Table 4.6. The adverse impact of the CAES on system reliability can be seen at the 20% wind penetration level and above for the 100 MW generator and at the 25% wind penetration level and above for the 200 MW generator. At the 20% wind penetration level and above when the 100 MW generator was used, Table 4.6 shows a positive value indicating that instead of a decrease in LOLE relative to column B, there was an increase in the LOLE which is not desirable. This was also the case for the 25% and 30% wind penetration level when the generator size was doubled. This phenomenon is clearly seen in Fig 4.12c, when the dash lines fall below the curves for the CAES resources. The reason for this is due to the LOLE contribution from the off-peak period. The LOLE contribution during the 19 hours off-peak period has a dominance effect on the overall system LOLE as seen in Fig 4.12a and 4.12b and therefore causes the system LOLE when the CAES was used to increase above that when the wind was used after a certain wind penetration level.

2. SCENARIO 1 CASE 2: This case considers a charging period of 10-hours (1^{st}-8^{th}, 23^{rd}-24^{th}), and a discharging period of 14 peak hours (9^{th}-22^{nd} hour). The result obtained is shown in Fig. 4.13. Fig 4.13a shows the LOLE results for the charging period, Fig 4.13b shows the LOLE results for the discharging period while Fig 4.13c shows the LOLE results for the total winter period.

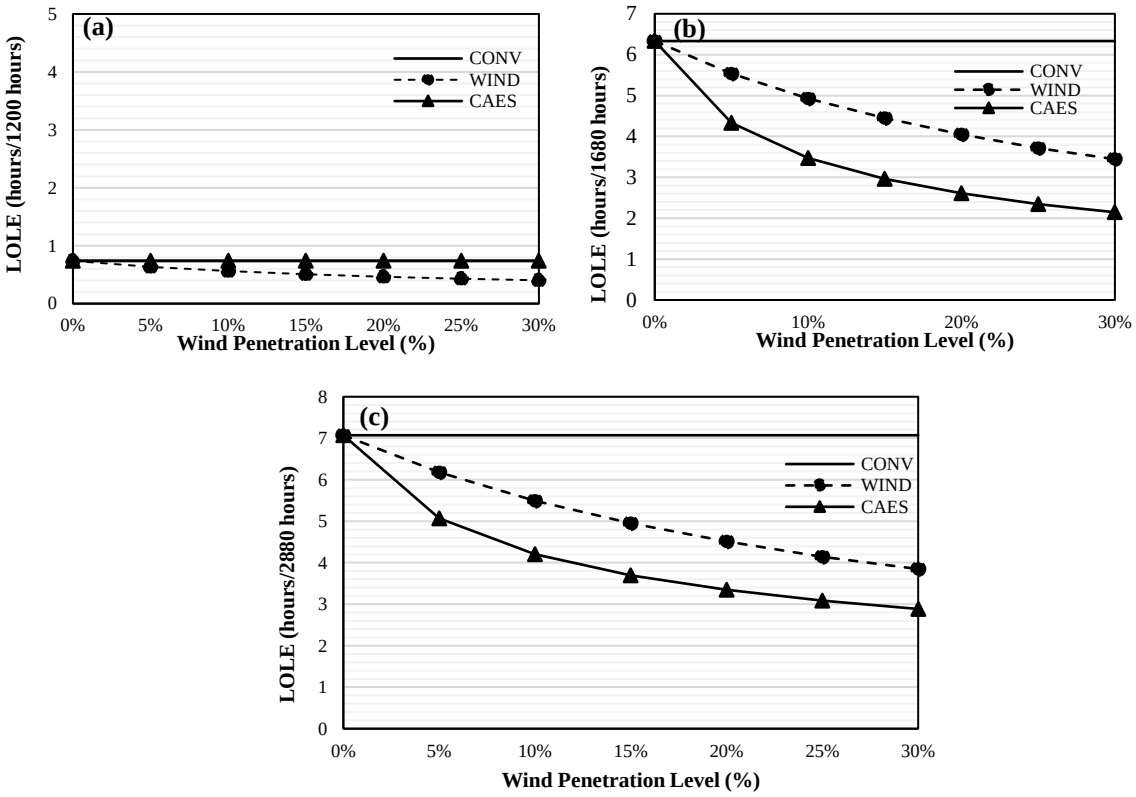

Figure 4.13: Scenario 1, Case 2 LOLE for increasing wind penetration for (a) Charging (b) Discharging and (c) Total winter period.

The base case LOLE for the charging period of Case 2 is 0.7386 hrs/pd as shown in Fig 4.13a. It should be noted that the base case LOLE for Case 1 is 3.7784 hrs/pd. The reason for the reduction in the LOLE for the charging period in Case 2 is due to some loss of load events being transferred from the charging period to the discharging period. This transfer, results in an increase in LOLE for Case 2 during the discharge period. As discussed in Case 1 of this scenario for the charging period, the wind does not contribute to the load since all the wind is used in charging the CAES, the LOLE remains the same as that of the base case when the CAES is charging.

The contribution of the CAES to the reduction of LOLE during the discharge period in this case as seen in Fig 4.13b isn't quite as significant as that of Case 1 as seen in Fig 4.12b. This is due to the loss of load events that has been transferred to the discharge period from the charging period. Also, a reduction in the charging hours leads to a reduction in the SOC available at the end of the charging period that can be used during the discharge. The improvement in system reliability

quantified by the reduction in LOLE due to CAES during discharge is shown in Table 4.7 for the different wind penetration levels.

Table 4.7: Reliability improvement due to CAES operation with the wind during discharge for Scenario 1 Case 2

A	B	C
Wind Penetration Level	**LOLE (hr/pd), when the wind was used with the base case**	**Change in LOLE relative to column B using a 100 MW generator**
0%	6.3329	-
5%	5.5395	-22%
10%	4.9276	-30%
15%	4.4478	-33%
20%	4.0491	-36%
25%	3.7138	-37%
30%	3.4444	-38%

From Table 4.7, the % reduction in the LOLE in column C increased as the wind penetration level in the system increased as well. The % reduction in Column C increased as the wind penetration increased but the incremental increase in % reduction in Column C reduced as the wind penetration increased. A comparison of Table 4.7 and 4.5 shows that CAES in Case 1 provides a higher level of reliability improvement than in Case 2. A combination of longer charging hours and lower LOLE scenarios in the discharge period for Case 1 accounts for this. Fig 4.13c shows the LOLE results for the entire winter period for Case 2. The improvement in system reliability quantified by the reduction in LOLE due to CAES for the total winter season is shown Table 4.8.

Table 4.8: Reliability improvement due to CAES operation with the wind for the winter period for Scenario 1 Case 2

A	B	C
Wind Penetration Level	**LOLE (hr/pd), when the wind was used with the base case**	**Change in LOLE relative to column B using a 100 MW generator**
0%	7.1701	-
5%	6.2086	-18%
10%	5.4650	-23%
15%	4.8901	-25%

20%	4.4180	-26%
25%	4.0282	-26%
30%	3.7183	-26%

The % reduction in the LOLE generally increased as the wind penetration level increased in the system up to a certain level as seen in Table 4.8. It then stayed constant after the 15% level. The reason for this has to do with the capacity of the CAES generation for increasing wind penetration level. The increase in expected output of the CAES multi-state generation increases as the wind penetration increases. The incremental increase in the expected power output however becomes smaller as the wind penetration increases. From Table 4.6 and 4.8, it is seen that Case 2 gave better reliability benefits than Case 1. Table 4.8 shows that for every level of wind penetration, the CAES in combination with the wind gave better reliability improvement than when the wind was used. The operation of the CAES in this manner gives more improvement in the system reliability than that of Case 1.

3. SCENARIO-2 CASE 1: The excess wind power above the rating of the CAES motor is used to meet the load during the charging period in this scenario. The legends in the plots used to describe the different LOLE results for increasing wind penetration level used for all the cases in scenario 1 also applies for the two cases in this scenario and for the cases in the third scenario as well. The **s**ame period is used as that of Case 1 of Scenario 1, i.e. a charging period of 19 hours and a discharge period of 5 hours. The result obtained is shown in Fig. 4.14. Fig 4.14a shows the LOLE results for the charging period, Fig 4.14b shows the LOLE results for the discharging period while Fig 4.14c shows the LOLE results for the total winter period. The discharge period analysis is unaffected and remains the same as that of the Case 1 of Scenario 1. Fig 4.14b is the same as Fig 4.12b. Only the charging period analysis changes, since there is now additional generation from the excess wind not used by the motor/compressor. This is used to meet the off-peak load and which contributes to lowering the total winter period LOLE.

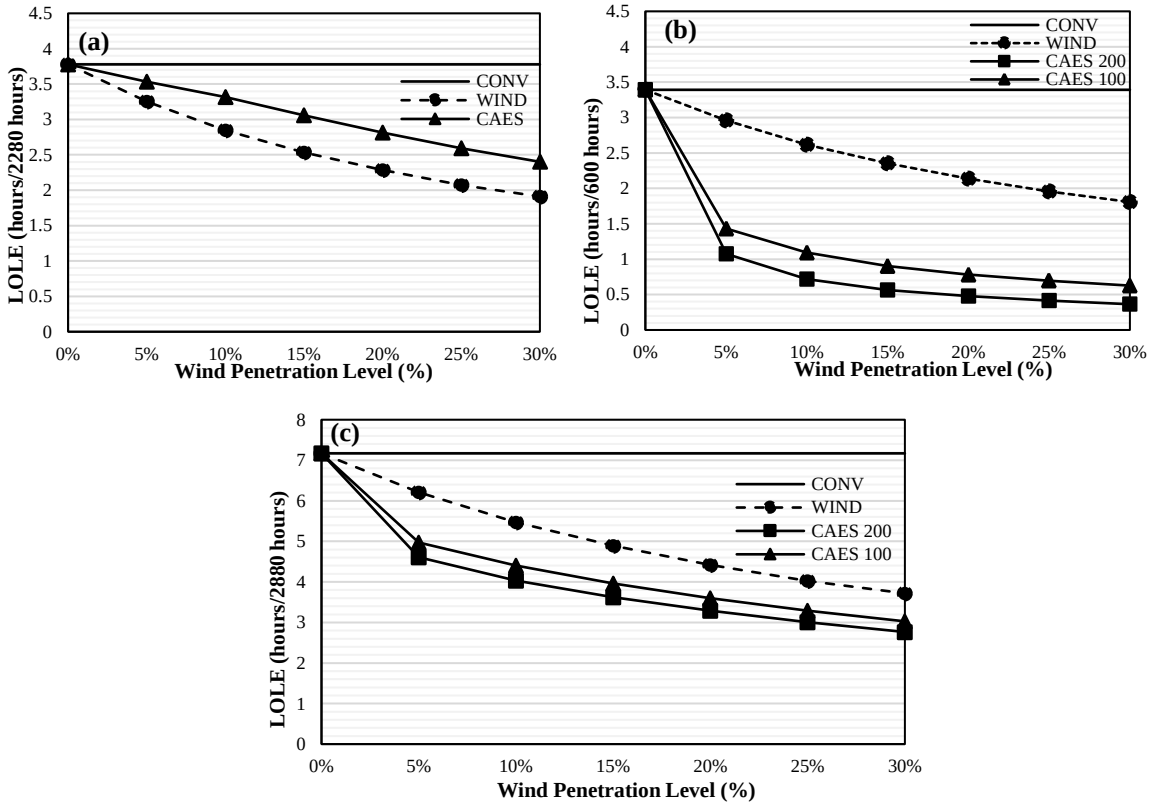

Figure 4.14: Scenario 2, Case 1 LOLE for increasing wind penetration for (a) Charging (b) Discharging and (c) Total winter period.

Fig. 4.14a shows that the LOLE during the charging period for Scenario 2 when the wind power is used for charging the CAES is different from that of the base case for the different wind penetration level. The excess wind power that the CAES cannot utilise in charging contributes to the load in this case, and the LOLE is therefore reduced from that of the base case. Fig 4.14a shows that the excess generation available that is used to meet the off-peak load increases as the wind penetration increases. Fig. 4.14c shows the aggregation of the LOLE results from the charging and the discharging period. The improvement in system reliability quantified by the reduction in LOLE due to CAES during total winter period is shown in Table 4.9 for the different wind penetration levels.

Table 4.9: Reliability improvement due to CAES operation with the wind during winter period for Scenario 2 Case 1

A	B	C	D
Wind Penetration Level	**LOLE (hr/pd), when the wind was used with the base case**	**Change in LOLE relative to column B using a 100 MW generator**	**Change in LOLE relative to column B using a 200 MW generator**
0%	7.1701	-	-
5%	6.2086	-20%	-26%
10%	5.4650	-19%	-26%
15%	4.8901	-19%	-26%
20%	4.4180	-19%	-26%
25%	4.0282	-18%	-25%
30%	3.7183	-18%	-25%

Table 4.9 shows a significant reduction in LOLE when the CAES was used in coordination with the wind. But the percent reduction in LOLE due to CAES remained approximately constant at around 19% with the 100 MW generator and around 26% with the 200 MW generator. Table 4.9 shows that doubling the generator size added about 7% more reduction in the LOLE. Comparing the total winter period LOLE result of Scenario 1 Case 1 to Scenario 2 Case 1. It is seen that Scenario 2 Case 1 generally provided better reliability improvement, which is due to the extra generation obtained from the excess wind during the charging period.

4. SCENARIO-2 CASE 2: This case considers 10 hours charge and 14 hours discharge periods similar to that in Scenario 1**.** The result obtained is shown in Fig. 4.15. Fig 4.15a shows the LOLE results for the charging period, Fig 4.15b shows the LOLE results for the discharging period while Fig 4.15c shows the LOLE results for the total winter period. The discharge period LOLE results are unaffected by the difference in the two scenarios, and remains the same as that of the Case 2 of Scenario 1. Fig 4.15b is therefore the same as Fig 4.13b. Only the off-peak period LOLE and the total winter period LOLE are changed. The excess wind generation available to serve the load increases as the wind penetration level increases. The effect of this increase on the LOLE is seen in Fig 4.15a.

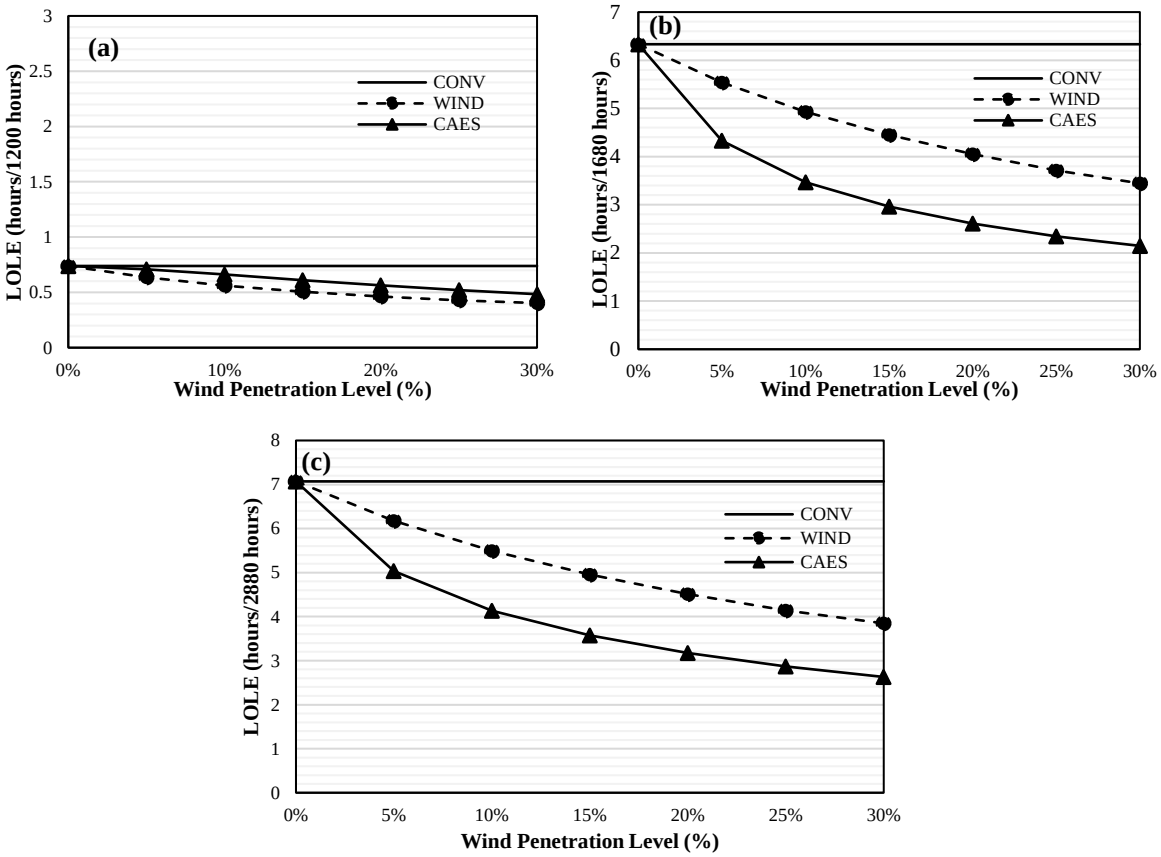

Figure 4.15: Scenario 2, Case 2 LOLE for increasing wind penetration for (a) Charging (b) Discharging and (c) Total winter period.

Fig. 4.15a shows that the LOLE during the charging period for Scenario 2 when the wind power is used for charging the CAES differs from that of the base case for the different wind penetration level. The excess wind power that the CAES cannot use in charging contributes to the load in this case, and the LOLE is therefore different from that of the base case. As the wind penetration increases, the excess wind energy available also increases. Fig. 4.15c shows the aggregation of the LOLE results from the charging and the discharging period. The improvement in system reliability quantified by the reduction in LOLE due to CAES during total winter period is shown in Table 4.10 for the different wind penetration levels.

Table 4.10: Reliability improvement due to CAES operation with the wind during winter period for Scenario 2 Case 2

A	B	C
Wind Penetration Level	**LOLE (hr/pd), when the wind was used with the base case**	**Change in LOLE relative to column B using a 100 MW generator**
0%	7.1701	-
5%	6.2086	-18%
10%	5.4650	-25%
15%	4.8901	-28%
20%	4.4180	-30%
25%	4.0282	-31%
30%	3.7183	-32%

Table 4.10 shows that the % reduction in LOLE due to CAES has an increasing trend for increasing wind penetration. It can be seen from Table 4.10 that the % reduction in the LOLE in Column C increased as the wind penetration level in the system increased. It can also be seen that the reliability contribution of adding CAES to the system is significant when wind penetration is increased from low levels, such as 5% to 10%, but the benefits tends to saturate at higher penetration levels. The Column C of Table 4.10 showed higher level of percentage reduction when compared to Columns C and D of Table 4.9 as wind penetration increased. Generally, the two cases in this scenario had better reliability performance when compared to the two cases in the first scenario.

5. SCENARIO-3 CASE 1: For Scenario 3, it is assumed that all the generation capacity available in the system is first used to meet the system load. Any excess is used in charging the CAES. The major difference between this scenario and the previous two scenarios is that the CAES facility has access to both the excess off-peak conventional generation and the off-peak wind power during charging while for the other two scenarios, the CAES only has access to the off-peak wind power. The same period is used here as that of Case 1 of Scenarios 1 and 2 i.e. 19 hours charge and 5 hours discharge period. The CAES 100, CAES 200 and CAES MAX represents when a 100 MW, 200

MW generator and maximum generator rating that can capture all the SOC available (about 500 MW in this case) are used respectively. The peak and off-peak period analysis is done and the result obtained is shown in Fig. 4.16 below. Fig 4.16a shows the LOLE results for the charging period, Fig 4.16b shows the LOLE results for the discharging period and Fig 4.16c shows the LOLE results for the total winter period.

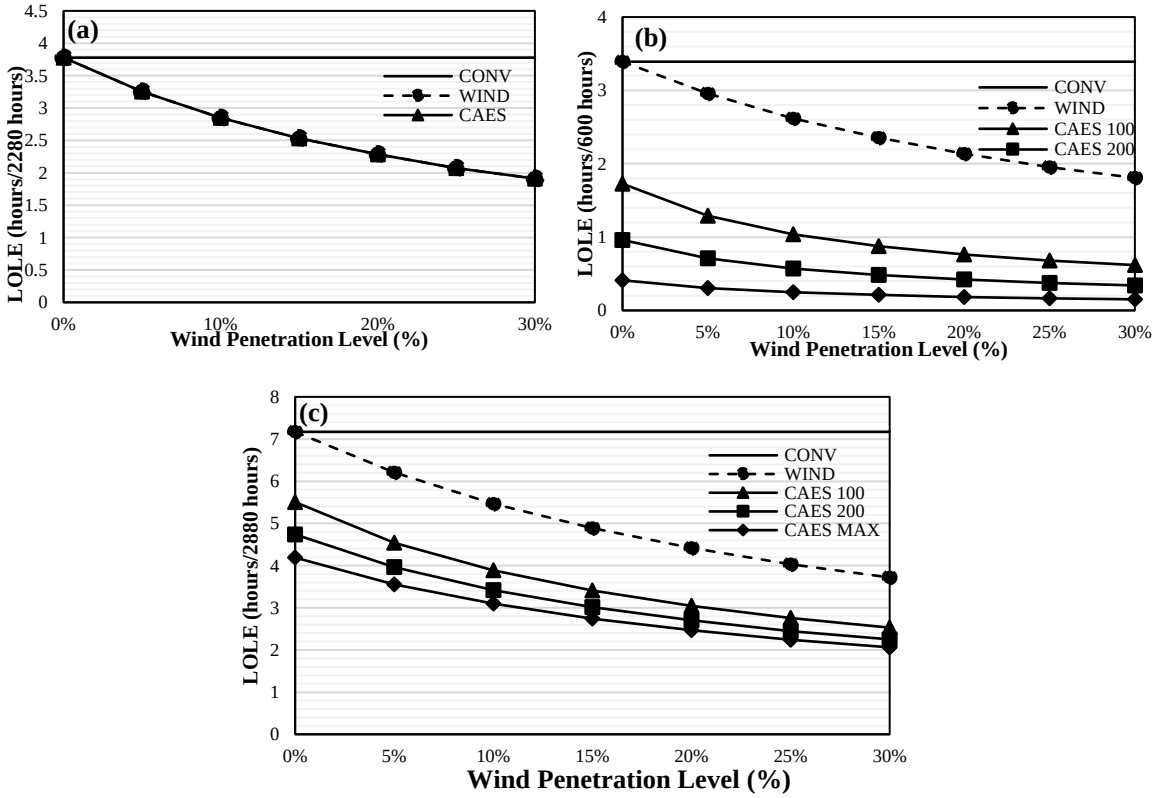

Figure 4.16: Scenario 3, Case 1 LOLE for increasing wind penetration for (a) Charging (b) Discharging and (c) Total winter period.

Fig. 4.16 shows that the system LOLE decreases with increase in wind penetration when wind is added even without CAES in the system. The incremental benefit in reliability however decreases with increasing wind penetration. With the addition of CAES, Fig. 4.16a shows that the LOLE is equal to that when the wind resource was used during the charging period for varying wind penetration level. This is so, since the combination of the wind energy and the conventional generation is first used to meet the load before charging the CAES, the system LOLE when the CAES and wind is added becomes the same as when only the wind is added to the base case. For

Fig 4.16b, the difference between Scenario 3 and the previous two scenarios are the availability of charge at the 0% wind penetration; i.e. when there is no wind energy in the system. This SOC is obtained from the off-peak conventional generation after the load has been met. The improvement in system reliability quantified by the reduction in LOLE due to CAES during discharge period is shown in Table 4.11 for the different wind penetration levels. There is a significant % reduction in the LOLE at the 0% wind penetration when the CAES was used as seen in columns C, D and E.

Table 4.11: Reliability improvement due to CAES operation with the wind during discharge for Scenario 3 Case 1

A	**B**	**C**	**D**	**E**
		Change in LOLE relative to column B using the CAES generator size below		
Wind Penetration Level	**LOLE (hr/pd), when the wind was used with the base case**	**100 MW**	**200 MW**	**500 MW**
0%	3.3917	-49%	-72%	-88%
5%	2.9572	-56%	-76%	-90%
10%	2.6176	-60%	-78%	-90%
15%	2.3559	-63%	-80%	-91%
20%	2.1350	-64%	-80%	-91%
25%	1.9544	-65%	-81%	-92%
30%	1.8075	-66%	-81%	-92%

The general trend observed in Table 4.11 in columns C, D and E is an increasing % reduction in the LOLE with movement down the columns when the CAES is used compared to when there was no CAES. An increasing % reduction trend is also noticed with movement from left to right of Table 4.11 from column C to E. Varying the generator size gives varying level of % reduction in the LOLE with respect to when the wind resource was used. Generally, the bigger the generator rating, the higher the % reduction in the system LOLE for the discharge period for varying wind penetration level. For the 0% wind penetration, there was a 49% reduction when the 100 MW generator was used, a 72% and 88% reduction when the 200 MW and 500 MW generator were used respectively. At the 30% wind penetration level, the % reduction increased to 66% for the 100 MW generator, and increased to 81% and 92% for the 200 MW and 500 MW generator

respectively.

Fig. 4.16c shows the aggregation of the LOLE results from the charging and the discharging period. The improvement in system reliability quantified by the reduction in LOLE due to CAES during total winter period is shown in Table 4.12 for the different wind penetration levels.

Table 4.12: Reliability improvement due to CAES operation with the wind during winter period for Scenario 3 Case 1

A	**B**	**C**	**D**	**E**
		Change in LOLE relative to column B using the CAES generator size below		
Wind Penetration Level	**LOLE (hr/pd), when the wind was used with the base case**	**100 MW**	**200 MW**	**500 MW**
0%	7.1701	-23%	-34%	-42%
5%	6.2086	-27%	-36%	-43%
10%	5.4650	-29%	-37%	-43%
15%	4.8901	-30%	-38%	-44%
20%	4.4180	-31%	-39%	-44%
25%	4.0282	-32%	-39%	-44%
30%	3.7183	-32%	-39%	-45%

The trend observed in Table 4.12 in columns C, D and E is an increasing % reduction in the LOLE with movement down the columns when the CAES is used with increasing wind penetration level. An increasing % reduction trend is also noticed with movement from left to right of Table 4.12 moving from column C to E. A comparison of the results in the last three columns of Table 4.12 shows that doubling the generator size can contribute between 7-11% additional reductions in the system LOLE while an increase in generation capacity to 500 MW can contribute between 12-19% additional reductions in the system LOLE for the entire winter period. Varying the generator size as seen in Table 4.12, gives varying levels of % reduction in the LOLE with respect to when the wind resource was used. At the 20% wind penetration level, the 100 MW generator gave 31% reduction in the LOLE when the CAES was used. Doubling the generator size added a further 8% reduction in the LOLE while an increase to the 500 MW generator added a

further 5% reduction in the LOLE. The increase in the reliability contribution to the system reduces as the generator size increases. This is due to the incremental increase in the expected power output, which becomes smaller as the generator size increases. This result can inform the sizing of the generator factoring the LOLE level to be achieved and the wind penetration level available. This case gave better reliability result than that of Case 1 of Scenario 1 and 2.

6. SCENARIO-3 CASE 2: The same period is used here as that of Case 2 of Scenario 1 and 2. A 10-hour charging and a 14 hours discharge period is used. The result obtained is shown in Fig. 4.17. Fig 4.17a shows the LOLE results for the charging period, Fig 4.17b shows the LOLE results for the discharging period while Fig 4.17c shows the LOLE results for the total winter period.

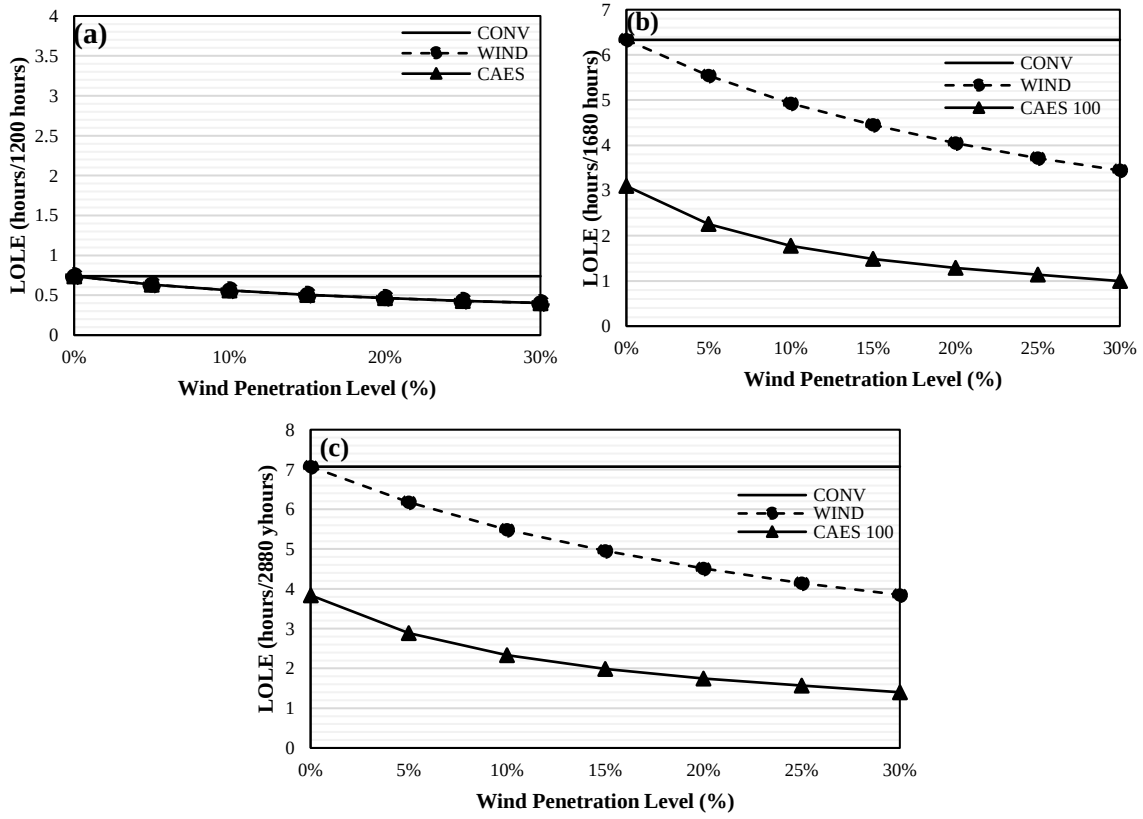

Figure 4.17: Scenario 3, Case 2 LOLE for increasing wind penetration for (a) Charging (b) Discharging and (c) Total winter period.

As discussed in Case 1 of this scenario for the charging period, the LOLE when the CAES was used is the same as when the wind alone was used during the charging period for different wind penetration. This is seen in Fig. 4.17a. For Fig 4.17b, SOC is available at the 0% wind penetration; i.e. when there is no wind energy in the system. This SOC is obtained from the off-peak conventional generation after the load has been met without considering wind in the system. The improvement in system reliability quantified by the reduction in LOLE due to CAES during discharge period is shown in Table 4.13 for the different wind penetration levels.

Table 4.13: Reliability improvement due to CAES operation with the wind during discharge for Scenario 3 Case 2

A	B	C
Wind Penetration Level	**LOLE (hr/pd), when the wind was used with the base case**	**Change in LOLE relative to column B using a 100 MW generator**
0%	6.3329	-51%
5%	5.5395	-59%
10%	4.9276	-64%
15%	4.4478	-67%
20%	4.0491	-68%
25%	3.7138	-69%
30%	3.4444	-71%

The trend observed in Table 4.13 in Column C is an increasing % reduction in the LOLE with movement down the columns when the CAES is used compared to when there was no CAES in the system with increasing wind penetration level. For the 0% wind penetration, there was a 51% reduction in the LOLE. At the 30% wind penetration level, the % reduction increased to 71%.

Fig. 4.17c shows the aggregation of the LOLE results from the charging and the discharging period. The improvement in system reliability quantified by the reduction in LOLE due to CAES during total winter period is shown in Table 4.14 for the different wind penetration levels.

Table 4.14: Reliability improvement due to CAES operation with the wind during winter period for Scenario 3 Case 2

A	B	C
Wind Penetration Level	**LOLE (hr/pd), when the wind was used with the base case**	**Change in LOLE relative to column B using a 100 MW generator**
0%	7.1701	-46%
5%	6.2086	-53%
10%	5.465	-57%
15%	4.8901	-60%
20%	4.418	-61%
25%	4.0282	-62%
30%	3.7183	-64%

The % reduction in the LOLE when the CAES was used generally increased as the wind penetration level increased in the system. The incremental increase however becomes smaller as the wind penetration increased. The % reduction in the LOLE for the total winter period when the CAES was used relative to when there was no CAES in the system for this scenario generally gave better reliability improvement compared to Scenario 1 and 2. A comparison of the % LOLE reduction for the total winter period for the Case 2 of this scenario and the Case 2 of Scenario 2 as seen in Table 4.14 and Table 4.10 respectively shows that for all the level of wind penetration, Scenario 3 Case 2 gives better reliability improvement in the system than Scenario 2 Case 2.

The summary of the results obtained for the analysis when the 100 MW CAES generator is used for the total winter period at the 30% wind penetration level is shown below in Table. 4.15.

Table 4.15: Summary of results of LOLE analysis

Total Winter LOLE (hrs/2880 hrs) for 30% Wind Penetration						
Diurnal Charge Duration	**Scenario 1**		**Scenario 2**		**Scenario 3**	
	LOLE	% Reduction	LOLE	% Reduction	LOLE	% Reduction
Case 1: 19 hrs	4.405	+18%	3.0279	-19%	2.5294	-45%
Case 2: 10 hrs	2.8846	-26%	2.6269	-32%	1.4001	-64%

From Table 4.15, it is seen that Case 2 gives better result compared to Case 1 for all three scenarios. This shows that the choice of a suitable charging and discharging period is very important and can play a big role in how reliable the system is. A comparison of the total winter LOLE for the Case 2 of all the three scenarios for the 30% wind penetration shows that Scenario 1 gives 2.8846 hrs/pd, Scenario 2 gives 2.6269 hrs/pd while Scenario 3 gives the best result of 1.4001 hrs/pd. These three different scenarios can have varied applications in power system operation and planning. A combination of energy management strategy by determining the appropriate peak and off-peak period and the connection of the CAES (to the wind farm directly or to the grid) will determine the extent of the benefit that can be derived from the CAES in the reduction of the system LOLE.

4.4 Conclusion

This chapter presents details on the incorporation of correlation between the wind speed and the load in the development of the reliability modelling for the CAES. A period analysis is employed in the development of the CAES reliability model using diurnal evaluations. The diurnal hybrid approach in developing the reliability model for the CAES is proposed and explained. The diurnal approach involves dividing the day into two or three periods depending on the type of analysis to be carried out. For the two-period analysis, charging of the CAES takes place during the off-peak period, while discharging occurred during the peak period where demand is very high. For the three-period analysis, a third period is included called the idle period where no activity is carried out; no charging or discharging of the CAES. The hybrid portion implies that a combination of two techniques are used to evaluate the system reliability indices. The MCS technique is used to develop the SOC model during the charging period while the analytical technique is used to convolve the different models to obtain the system reliability indices. Three scenarios are used to study the effect of incorporating the CAES in an electric power system. Two different operating strategies based on the variation of the charging and the discharging period are studied for the three scenarios. It was observed that, for the scenario and case that gave the best reliability result, the

CAES had access to the conventional generation off-peak power because of its connection to the grid. Also, the charging and discharging period was chosen in such a way that the LOLE of the charging period was very low while the LOLE of the discharge period was high before the CAES was used because some loss of load events had been transferred to the discharging period being considered. A combination of how the CAES is connected, either connected directly to maximise wind resources or connected to the grid, and the choice of the charging and discharging period will determine the extent of the benefit that can be derived from the CAES for electric power system reliability improvement. The three scenarios can have varied applications in the electric power system. The ownership of the CAES is not just enough, the right strategy in operating the CAES is very important. The different strategies adopted for the operation the CAES will determine the extent of the benefit that can be derived for power system reliability improvement.

5. APPLICATION OF CAES IN WIND INTEGRATED POWER SYSTEMS

5.1 Introduction

The operation of the CAES can be carried out in various ways in the electric power system based on the objective to be met. This objective drives the operation strategy of the CAES. Electric utilities have traditionally operated as vertically-integrated systems operating under a monopoly franchise. A vertically integrated system performs all the functions involved to produce, transmit, distribute and sell electric power for an area under its jurisdiction. Many jurisdictions around the world have deviated from the vertically integrated structure to operate as deregulated electricity markets. In a deregulated structure, the major functions of a power system are unbundled, and different parts of the electric power generation and delivery process are owned by multiple entities. At the generation level, different companies generate electricity and compete to sell at the energy market. The transmission facility can be owned by different entities with control and regulation provided by an independent system operator, and the distribution systems are owned by different entities [94]. In an energy market scenario, the CAES could be owned by one of the power system entity, or by an independent owner that participates in the electricity market. In Canada, both the vertically integrated and the deregulated electricity markets exist. The province of Saskatchewan operates as a vertically integrated entity while the provinces of Alberta and Ontario operate within deregulated electricity markets.

Competition is one of the major results of the deregulation process of the electric power system. In order for the de-regulated power industry to work efficiently, some additional functions and entities have to be created. The two major ones are the power market and the system operator, and both require objectivity and some form of fairness in operation. In the power market, independent power producers can offer their generation in a very competitive manner and transact sales while the system operator is an independent body that receives bid to buy and sell electricity by different entities [94].

5.2 Objectives of CAES Operation

The objectives to be achieved will determine how the CAES is operated in a power system. The primary objective that has driven the need for energy storage in a power system is to integrate as much renewable energy as possible at affordable cost, while maintaining an acceptable level of system reliability. System studies to meet this objective is presented in Chapter 4 by assuming the CAES is owned by the wind farm owner. Here, the CAES is operated in coordination with the wind resources to absorb the variability of wind power to promote renewable energy utilization in the system. This objective has been explored in detail in Chapter 4 of this thesis. The system model depiction for this objective is seen in Fig 4.7a. A CAES owned by a merchant participating in an energy market is however operated with an objective to maximize profits from energy arbitrage opportunities that exist in a deregulated electricity market. This operating strategy may not result in perceived reliability benefits to the power system. In order to meet the objectives of maximizing reliability benefits, the CAES should be operated to provide proper power and energy management. This is done by operating the CAES in such a way as to appropriately move the energy from off-peak period to peak period considering the diurnal and seasonal variations. The major question that will be attempted to be answered is this, "how does the behavior of the merchant-owned CAES affect the system reliability?" Fig. 4.7b shows the evaluation model for a system in which the CAES is independently operated.

For a merchant that owns and operates an energy storage system, energy arbitrage opportunities exist in a deregulated electricity market that were not available previously in a vertically integrated market. The major objective of the merchant is to make profit. This is done by exploiting short-term differences in electricity prices by buying low and selling high [95]. Electricity prices demonstrate significant short-term variations for several reasons. Load varies considerably over short time periods (hours and days). At times of low load, only inexpensive plants are running, while at high load, plants with high variable cost must also generate. In general, electricity prices are at the highest when demand peaks. Thus, the marginal cost of producing power can vary considerably over short time frames [95]. This chapter will seek to access how the

operation of the merchant owned CAES can affect the reliability of the power system. Fig. 5.1 shows the hourly pool price data obtained from the Alberta Electric System Operator (AESO) for the 2013/2014 winter season [96].

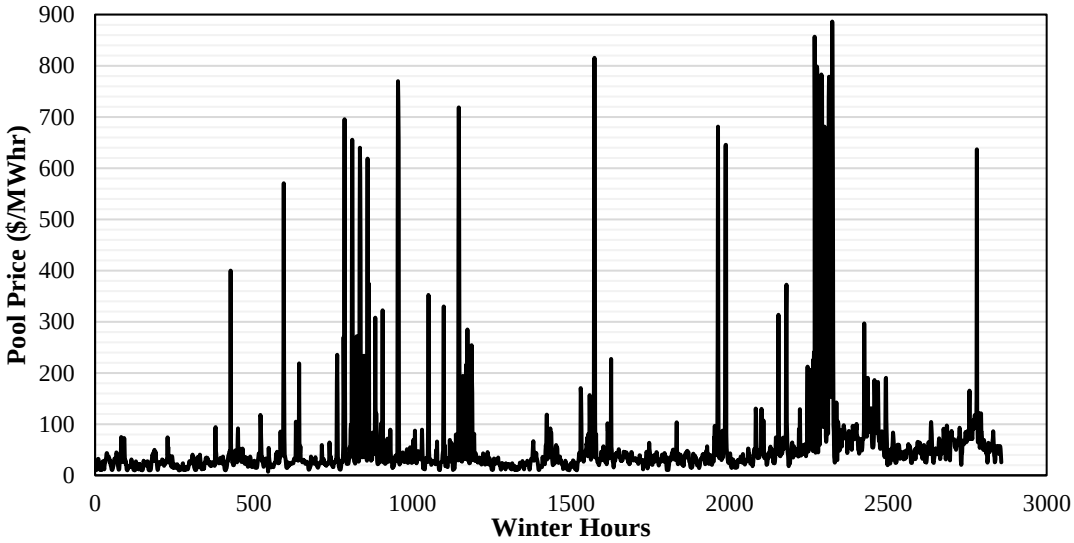

Fig 5.1: Electricity hourly pool price for the winter season. (Source: Alberta Electric System Operator (AESO))

5.3 Correlation between System Load Level and Electricity Price

The operation of the CAES by the merchant in a WIPS is highly dependent on the price of electricity, which depends on the load profile. These factors are related and are taken into consideration in determining the charging and discharging hours. The relationship between the load level and the price is shown in Fig. 5.2 as an example. The hourly price data is obtained from the AESO database. The average diurnal peak system load and the maximum pool price for the winter season are 10,496 MW and 68 $/MWhr respectively, and the data in Fig. 5.2 are shown in per unit of these peak values.

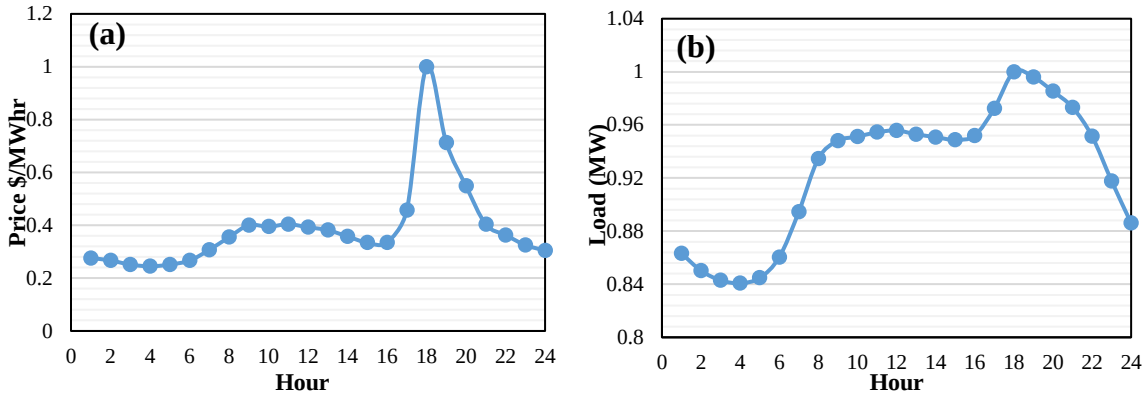

Fig. 5.2: AESO averge diurnal winter (a) pool price (b) load model

Fig. 5.2 shows that when the load peaks, the electricity pool price also peaks. This shows that the electricity price is highly dependent on the load level. The Alberta load profile as seen in Fig. 5.2 (b) has similar shape with the Saskatchewan load profile shown in Fig. 4.4. The correlation between average winter diurnal wind profile for the Swift current site and the pool price is shown in Fig. 5.3. Fig. 5.3 shows that when the wind is high, the price is low but when the wind is low, the price of electricity is high.

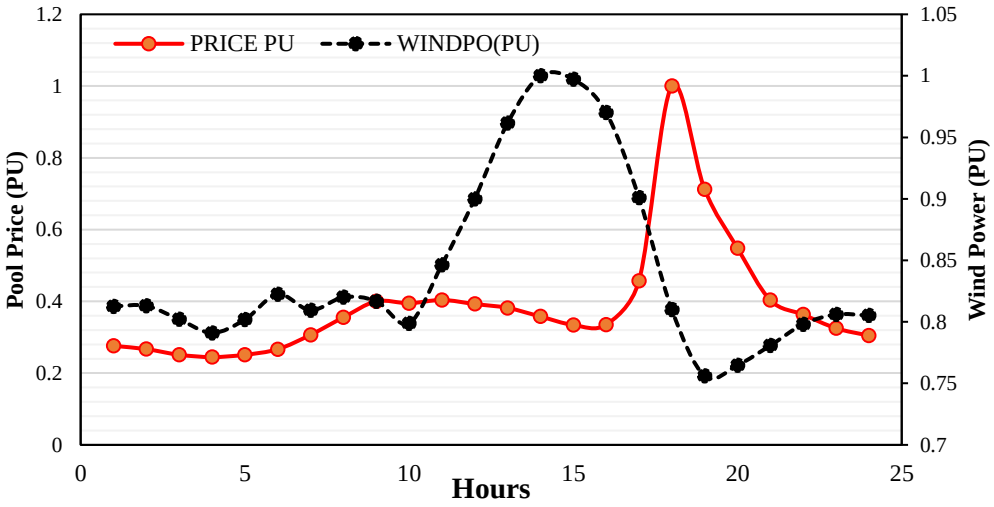

Fig. 5.3: Average diurnal winter wind power and pool price

5.4 Analysis of the Operation of the CAES in the Energy Market

The operation of a CAES usually consists of three stages; charge, idle or hold, and discharge. A 3-period analysis is therefore carried out by dividing a day into three periods namely; charging period, discharging period and the idle period. The charging of the storage occurs in the off-peak period when the price of electricity is very low, the discharge occurs during the peak period when the price of electricity is high, and an idle period when no charging or discharging activity is carried out by the merchant. The merchant will not sell at this period because it will be too cheap to sell and will not buy because it will be too expensive to buy. Fig 5.4 shows the Saskatchewan average daily winter load model depicting the three periods.

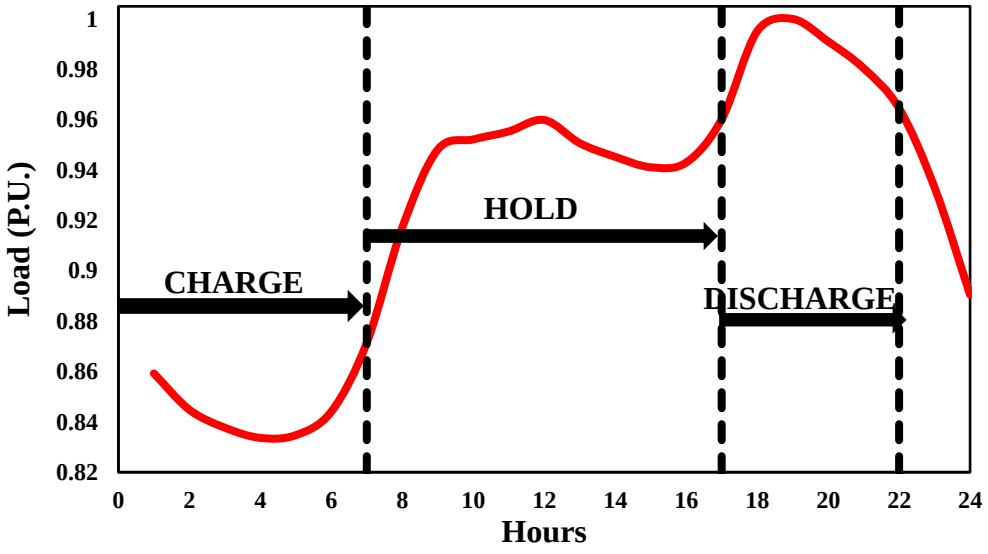

Fig. 5.4 shows that the CAES is charged for eight hours off-peak period between 11:00 pm -7:00am and discharged during the 6 hours peak period between 5:00pm and 10:00pm, and the cycle continues again. For the idle period which occurs for 10 hours between 8:00 am and 4:00 pm, the CAES is on standby and will only be operated to avoid a loss of load event. The probability of this loss of load occurring is very small. As explained in Section 4.3.1.3, the CAES will maintain its original SOC during this idle period if loss of load events does not occur. The SOC level will drop if or when such events occur, but since the probability of the loss of load event

occurring during this period is very small, it is assumed in the reliability modelling process that the change in the SOC level during this period can be ignored. Therefore, the generation model obtained at the end of the charging cycle is also considered the same for this period.

5.5 Application of the CAES to the IEEE-RTS

The impacts of operating a CAES in a wind-integrated system on the system reliability and the associated profits from energy arbitrage is investigated by application to the IEEE-RTS [1]. It is assumed that a wind farm characterized by the Swift Current wind data is connected to the IEEE-RTS. The Saskatchewan load profile is considered with a peak system load of 2700 MW. It is assumed that a CAES is connected to the system and has the parameters similar to the Huntorf CAES [79], with a 100 MW motor/compressor and a 100 MW turbine/generator.

For the operation of the merchant owned CAES, a constant charging level is assumed, this level is determined by the size of the motor running the compressor. The wind has priority to charge the storage and any instance the wind power level drops below the motor capacity, the deficiency is taken from the conventional generation. The motor is run at its rated capacity all the time during the charging period. Wind capacity in excess of the motor rating is directly supplied to the system load.

The study is carried out for an increasing level of wind penetration. The AESO electricity price data shown in Fig. 5.1 is used in the cost evaluation. The profit from energy arbitrage for the entire winter season is calculated at $3.09M. The LOLE obtained considering a range of wind penetration in the IEEE-RTS is shown in Fig. 5.5. The solid line without any marker shows the base case LOLE of the IEEE-RTS without considering wind power or CAES in the system. The solid line with the triangular marker shows the LOLE during the charging period when the system includes wind power and CAES. The dash line shows the LOLE for the same period considering wind power without CAES in the system. The legends in the plots used to describe the different LOLE results for increasing wind penetration is used consistently throughout this chapter.

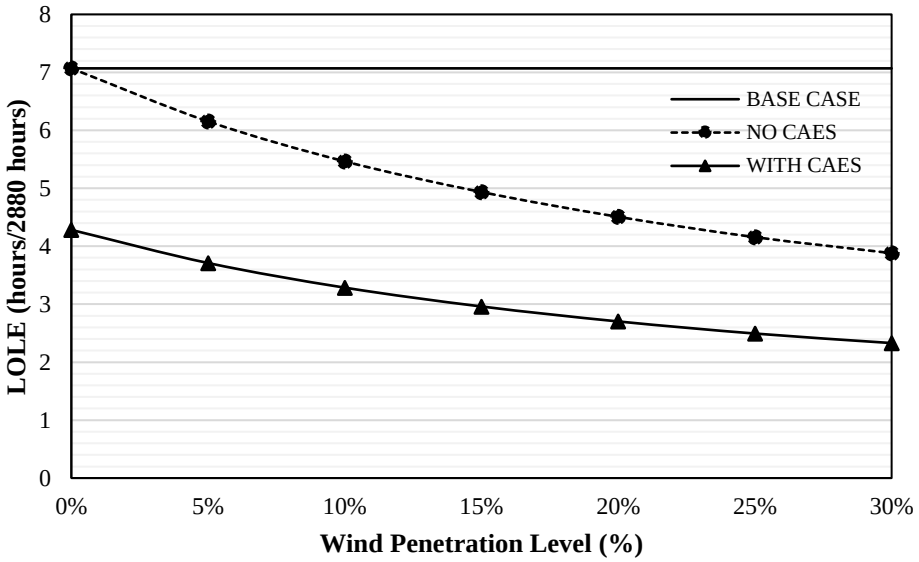

Fig. 5.5: 3-Period LOLE analysis for increasing wind penetration with and without CAES

The dashed line in Fig. 5.5 shows that the system LOLE decreases with increase in wind penetration even without adding CAES to the system. The incremental benefit in reliability however decreases with increasing wind penetration. With the addition of CAES, Fig. 5.5 shows that the LOLE is improved considerably. The contribution of the CAES to the reduction of LOLE is quite significant as seen in Fig 5.5. The improvement in system reliability quantified by the reduction in LOLE due to CAES is shown in Table 5.1 for the different wind penetration levels.

Table 5.1: Reliability improvement due to addition of CAES

A	B	C
Wind Penetration Level	**LOLE (hr/pd) without CAES**	**Reduction in LOLE due to CAES**
0%	7.0689	-39%
5%	6.1538	-40%
10%	5.4641	-40%
15%	4.9353	-40%
20%	4.5074	-40%
25%	4.1571	-40%
30%	3.8807	-40%

Table 5.1 shows that a significant reduction in LOLE occurs when the CAES is added to the wind-integrated power system, but the percent reduction in LOLE due to CAES remained approximately constant at around 40% for the different wind penetration levels. It should be noted that there is a 39% reduction in LOLE due to CAES even for the case when wind is not integrated in the system, i.e. for the 0% penetration case.

The result is based on the CAES operated to make profit for energy arbitrage opportunity. The charging and discharging periods in this case was selected in coordination with the electricity prices with the objective to make profit. If the charging and discharging periods were different, there will be changes in the profit the merchant can make and on the system reliability as well. The next section investigates these concerns.

5.5.1 Impact of Operating Strategy on Profit and System Reliability

A sensitivity study was done by varying the charging, idle and discharge periods. The study investigates how the variation in the operating cycle affects the system reliability and the profit the merchant can make. Data for the hourly pool price ($/MWh) obtained from the AESO historical data for the winter season for the year 2013/2014 is used in this study. An hour by hour analysis is done using the actual pool price data. The study carried out in this chapter consists of profit due to energy arbitrage and does not consider other costs that may occur in other types of market participation. It is assumed that the IEEE-RTS has a 20% wind penetration and a CAES with 100 MW motor and 100 MW generator. The Saskatchewan winter load profile with a peak load of 2700 MW is used in this study.

The merchant exploits the short-term differences in the price by buying during the off-peak period and selling this power during the peak period. Different operating strategies are explored by varying of the charging, discharging and idle periods. Four different scenarios as described in Table 5.2 are considered in this sensitivity study.

Table 5.2: The different periods of the 4 operating scenarios

Operating Scenario	Charging Period	Idle Period	Discharge Period
Scenario 1	12 am-7 am (8 hrs)	8 am-4 pm, 11 pm (10 hrs)	5 pm-10 pm (6 hrs)
Scenario 2	11 pm-7 am (9 hrs)	8 am-3 pm (8 hrs)	4 pm-10 pm (7 hrs)
Scenario 3	11 pm-7 am (9 hrs)	8 am-4 pm (9 hrs)	5 pm-10 pm (6 hrs)
Scenario 4	12 am-7 am (8 hrs)	8 am-3pm, 11pm (9 hrs)	4 pm-10 pm (7 hrs)

The reliability contribution in terms of LOLE reduction and the profit for the winter season are computed and compared for the four scenarios. The results are shown in Table 5.3.

Table 5.3: Reliability improvement and profit for the four scenarios using 100 MW generator and 100 MW motor

CAES Operating Scenarios	Diurnal charge hours	Diurnal discharge hours	LOLE without CAES	LOLE with CAES	Reliability Improvement	Profit ($M)
1	8	6	4.5074	2.7026	40%	3.096
2	9	7	4.4913	2.9583	34%	3.113
3	9	6	4.5040	2.9650	34%	2.641
4	8	7	4.4951	2.6960	40%	3.568

Table 5.3 shows that Scenarios 1 and 4 gave the best reliability improvement among the four scenarios, while Scenario 2 and 3 gave the least. In terms of the profit the merchant can obtain, Scenario 4 gave the best result while Scenario 3 gave the worst result. In Scenario 4, the price is highly correlated with the load, so that when the load is high, the price is high as well and when the load is at its lowest, the price is at its lowest as well which leads to the maximum profit. In terms of the maximum reliability improvement, the merchant sells at these high periods which leads to extra capacity available to meet the system peak load. Fig. 5.3 also shows that when the wind is high, the price is low but when the wind is low, the price of electricity is high providing opportunity to store wind energy and mitigate its variability, and therefore, contribute to both reliability improvement and profit. The CAES is charged at 11 pm in Scenarios 2 and 3, while

Scenarios 1 and 4 considered the 11 pm as an idle hour. Charging at 11 pm added to the loss of load in Scenarios 2 and 3 thereby reducing the reliability when compared to Scenarios 1 and 4. Scenarios 2 and 4 have more discharge hours than in Scenario 1 and 3 by including the 4 pm hour to discharge instead of making it idle. The pool price at this hour is high enough for the merchant to sell in order to make profit. This conclusion is drawn for this load profile and the pool price data, but if other load profiles and pool price data are considered, the conclusion will be different. If the price is not strictly correlated with the load because of the wind profile and other generation restrictions, operating for maximum profit may result in limited or adverse reliability improvement to the system. In this case, it is important that market policies be restructured to ensure that the system reliability is not adversely affected by the merchant objective of profit making.

In order to maximise the profit and the reliability contribution to the power system, optimisation techniques can be utilized to find the best charging, discharging and idle periods. This study only consists of profit due to energy arbitrage and does not consider other costs that may occur from other types of market participation.

5.5.2 Sensitivity Study on the Motor and Generator Ratings of the CAES

In this section, different sensitivity analysis is carried out to observe how the different CAES parameters affect the reliability of the system and the profit from market arbitrage.

5.5.2.1 Impact of the CAES Compressor/Motor Rating

The motor for compressing the air is varied in this analysis. A 50 MW, 100 MW and 150 MW motor and the periods for Scenario 1 are used in this study. The other CAES parameters including the generating rating remains the same as that used in Section 5.5.

Table 5.4 shows the reliability improvement due to CAES using the different motor ratings on the test system with 20% wind penetration. The table also shows the profit due to energy arbitrage for the three motor ratings.

Table 5.4: Reliability Improvement and profit for different CAES motor size

Motor Size	**50 MW**	**100 MW**	**150 MW**
Selling ($M)	6.078	6.305	6.305
Buying ($M)	1.604	3.209	4.813
Profit ($M)	4.471	3.096	1.492
Reliability Improvement	37%	40%	34%

Table 5.4 shows that there is an increase in the reliability improvement as the motor rating is increased from 50 MW to 100 MW, but the reliability improvement decreases with further increase in the motor rating. It shows that the improvement is reduced to 34% for a 150 MW motor, which is even lower than that of the 50 MW motor. The increased off-peak LOLE when using the 150 MW constitute a significant portion of the total LOLE and this added to the LOLE thereby causing a reduction in the system reliability. The increased off-peak LOLE isn't as dominant for the other two motors. This shows that reliability increases with an increase in the motor size, but up to a certain point, after which it begins to decrease. The profit made, generally reduced with an increase in the motor size. This is due to the lower amount spent in buying energy for the low rated motor relative to the bigger rated ones.

The analysis above is done for only Scenario 1. When other operating scenarios are used, this can affect the level of reliability and profit that can be achieved. An extension of the analysis is done for all the four scenarios. The profit and the reliability improvement obtained are computed and compared to when there was no CAES in the system. The results for the reliability improvement and the profit obtained from all four scenarios are shown in Table 5.5.

Table 5.5: Reliability improvement and profit for the four scenarios using different motor size

A	**B**	**C**	**D**	**E**	**F**	**G**
	Reliability Improvement			**Profit ($M)**		
Scenarios	**50 MW Motor**	**100 MW Motor**	**150 MW Motor**	**50 MW Motor**	**100 MW Motor**	**150 MW Motor**
1	37%	40%	34%	4.471	3.096	1.492
2	37%	34%	24%	4.440	3.113	1.281
3	37%	34%	24%	4.473	2.641	0.810
4	36%	40%	34%	3.993	3.568	1.963

Table 5.5 shows that the reliability improvement stayed constant for the 50 MW motor for all four scenarios except for Scenario 4 that had a 1% reduction. Scenario 1 had the most improvement in reliability when the motor rating was increased from 50 MW to 100 MW, while Scenario 2 and 3 resulted in reduced reliability. Scenario 2 and 3 gave the most reduction in the reliability when moving from the 100 MW motor to the 150 MW compared to Scenario 1 and 4. This shows that the operating scenario can have a big impact on the reliability level for different motor size. In terms of the profit, a decreasing trend is observed as the motor size increases for all four scenarios. Scenario 3 gave the best profit for the 50 MW motor but gave the worst profit for the 100 MW and 150 MW motors. Conversely, Scenario 4 gave the worst profit for the 50 MW motor but gave the best profit for the 100 MW and 150 MW motors. This shows that one operating scenario may give a great profit for a particular motor size and may give less profit for another motor size.

A study was also carried out to analyze the effect of motor size at different wind penetrations. Fig 5.6 shows the effect of varying the motor size at different wind penetration level using Scenario 1.

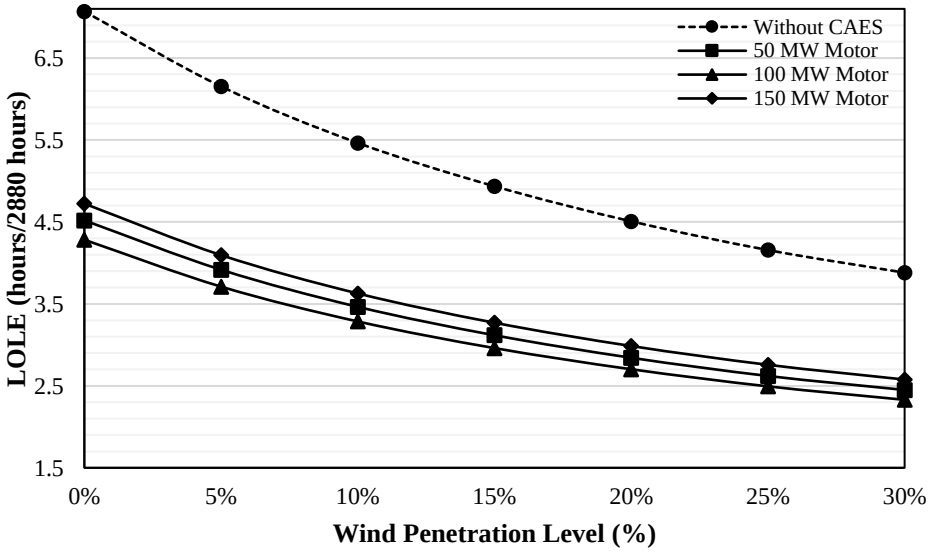

Fig. 5.6: Varying the motor size for the winter period using 100 MW generator

Fig 5.6 shows that the 100 MW motor gave the most reliability contribution for all the wind penetration level while the 150 MW gave the least reliability contribution for all the wind penetration level. Fig 5.6 also shows that the reliability contribution from the three motors relative to one another remains relatively constant for the different wind penetration.

5.5.2.2 Impact of CAES Generator Rating

A study was carried out to investigate the impact of generator size of a CAES on the profit from energy arbitrage and on the system reliability. The analysis is carried out on the IEEE-RTS with 20% wind penetration using the Scenario 1 operating strategy. The CAES motor is rated at 100 MW. Four different CAES generator ratings were considered in the study: 100 MW, 150 MW, 300 MW and the maximum generator size to exploit the stored energy, which was calculated to be 187.7 MW. The results for the reliability improvement and the profit obtained for the different generator ratings of the CAES are shown in Table 5.6.

Table 5.6: Reliability improvement and profit for different generator size

Generator Size	**100 MW**	**150 MW**	**187.7 MW**	**300 MW**
Selling ($M)	6.305	9.457	11.834	12.485
Buying ($M)	3.209	3.209	3.209	3.209
Profit ($M)	3.096	6.248	8.625	9.276
Reliability Improvement	40%	49%	53%	44%

Table 5.6 shows that an increase in generator size leads to an increase in the reliability benefits. There is increased capacity available to meet the loss of load events and the higher the generator rating, the more the capacity available. The results show that the reliability contribution of the CAES increases as the generator size is increased until it reaches the maximum capacity that exploits all stored energy, which in this case is 187.7 MW. Further increases in generator size results in reduction in system reliability. Table 5.6 shows that the reliability benefit increased as the generator sized increased from 100 MW to 150 MW and further to 187.7 MW. But this benefit reduced when the generator size was further increased from 187.7 MW to 300 MW. When the

generator size is increased to 300 MW which is beyond the maximum rating it can deliver for the entire duration of the discharge period, the reliability improvement was lower than that of the 150 MW and 187.7 MW generator but slightly higher than the 100 MW generator. This is due to using most of the stored energy at the early hours of the discharge period and not having enough capacity to meet the later hours of the discharge period.

The results in Table 5.6 shows that the profit due to arbitrage increases with an increase in generator size. There is more capacity available to sell during the discharge period. The profit was the highest for the 300 MW generator case as the merchant was able to sell everything within the first four hours of the discharge period. The high rating of the generator size relative to the other generators is the reason the profit was the most in this case even though the discharge wasn't available for the entire duration of the discharge period. The very large profit obtained by using the 300 MW generator does not result in an equivalent reliability improvement.

The above analysis was extended to the four different operating scenarios to investigate the level of reliability and profit that can be achieved for different operating scenarios. The profit and the reliability improvement obtained are computed and compared with when there was no CAES in the system. The maximum generator size to exploit all the stored energy will be different for different operating scenarios because of the different charging, idle and discharging periods. These values were calculated for the 4 scenarios and are shown in Table 5.7.

Table 5.7: Maximum generation size for the four scenarios

Scenarios	**Maximum Generator Rating (MW)**
1	187.7
2	179.8
3	209.7
4	160.9

The result obtained for reliability improvement and profit when the 100 MW, 150 MW, 300 MW and maximum generator rating was used is shown in Table 5.8.

Table 5.8: Reliability improvement and profit for the four scenarios using different generator size

A	B	C	D	E	F	G	H	I
	Reliability Improvement				**Profit ($M)**			
Scenarios	**100 MW Gen.**	**150 MW Gen.**	**Max Gen. size**	**300 MW Gen.**	**100 MW Gen.**	**150 MW Gen.**	**Max Gen. size**	**300 MW Gen.**
1	40%	49%	53%	44%	3.096	6.248	8.625	9.276
2	34%	47%	50%	37%	3.113	6.501	8.521	10.029
3	34%	46%	51%	45%	2.641	5.794	9.577	11.458
4	40%	51%	52%	37%	3.568	6.956	7.633	6.932

Table 5.8 shows that the reliability improvement increased with an increase in generator size until the maximum size was reached, and further increase in generator size results in a decrease in reliability improvement for all four scenarios. Table 5.8 shows that when the generator size is increased to 300 MW which is beyond the maximum rating it can deliver for the entire duration of the discharge period; the reliability improvement was lower than that of the 150 MW and 187.7 MW generator but higher than the reliability contribution from the 100 MW generator for all four scenarios. This is due to using most of the stored energy at the early hours of the discharge period and not having enough capacity to meet the demand for the later hours of the discharge period. This also shows that the choice of when to charge, discharge or stay idle can have a significant impact on the reliability improvement the system can achieve. The results in Table 5.8 also show that the profit due to energy arbitrage increases with increase in the generator size for all four scenarios, except for Scenario 4, in which case the profit decreased when the generator size was increased from the maximum generator rating of 160.9 MW to 300 MW. This is due to Scenario 4 having the lowest maximum generator rating out of all the four scenarios. This low maximum generator rating is a function of the low number of charging hours and high number of discharging hours. Scenario 4 was able to discharge the stored energy quickly using the early hours of the discharge period but unable to utilise the later discharge hours. The later discharge hours have a bigger price gap between the off-peak pool price and the peak pool price compared to the early discharge hours. The use of the 300 MW generator is not beneficial in terms of the reliability and

the profit for Scenario 4. The last hours in the peak period that the generator didn't contribute to cause the very low reliability improvement and the low profit. Conversely, Scenario 3 gave the largest reliability improvement and profit out of all the other scenario when using the 300 MW generator. This is due to Scenario 4 having the largest maximum generator rating of 209.7 MW.

A study was also carried out to analyze the effect of generator size at different wind penetrations. Fig 5.7 shows the effect of varying the generator size at different wind penetration level using Scenario 1.

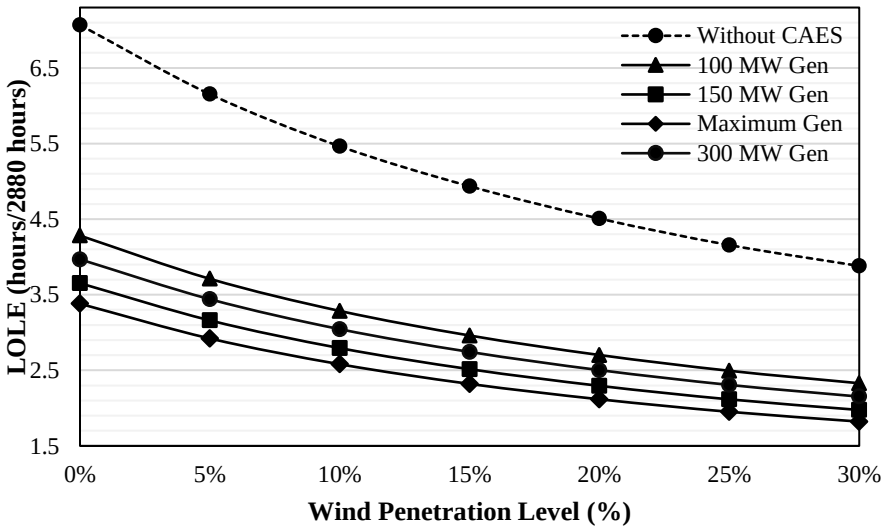

Fig. 5.7: Variation of different CAES generator at different wind penetration

Fig 5.7 shows that the maximum generator gave the most reliability contribution for all the wind penetration level while the 100 MW gave the least reliability contribution for all the wind penetration level. The 300 MW generator, which is rated above the maximum generator only gave better reliability improvement than the 100 MW generator for every wind penetration level. Also, the incremental benefits gotten from an increase in generator size reduced. Fig 5.7 also shows that the reliability contribution from the three generators relative to one another remains relatively constant for the different wind penetration level.

5.5.2.3 Impact of Different Generator Rating and Different Motor Rating

The previous analysis that have been carried have been done by varying the motor size at a constant generator rating, and varying the generator size at a constant motor rating. In this section, both motor and generator are varied and some conclusions are made based on the effect on the system reliability and profit.

Three cases are considered namely; 50 MW motor and 100 MW generator; 100 MW motor and 150 MW generator, 150 MW motor and 200 MW generator. The analysis is done at the 20% wind penetration level using Scenario 1. Table 5.9 shows the reliability improvement and profit obtained from the three cases.

Table 5.9: Reliability Improvement and profit for different CAES motor and generator size

A	**B**	**C**	**D**
Component Size	**50 MW Motor 100 MW Gen**	**100 MW Motor 150 MW Gen**	**150 MW Motor 200 MW Gen**
Selling ($M)	6.305	9.457	12.609
Buying ($M)	1.604	3.209	4.813
Profit ($M)	4.701	6.248	7.796
Reliability Improvement	37%	49%	53%

Table 5.9 shows that there is reliability improvement when the motor size and generator size are increased as seen from Columns B and C but the reliability incremental benefits reduced with further increase in both motor and generator as seen in Columns C and D. The decision on the size of components to use will be informed by the reliability level to be achieved and the cost of those components. The profit also increased from Column B to C but there was a decrease in the incremental profit from Column C to D.

The analysis performed above is extended to the other three scenarios and the results are compared. The result obtained for reliability improvement and profit is shown in Table 5.10.

Table 5.10: Reliability improvement and profit for the four scenarios using different generator and motor size

A	B	C	D	E	F	G
	Reliability Improvement			Profit ($M)		
Scenarios	50 MW Motor, 100 MW Gen	100 MW Motor, 150 MW Gen	150 MW Motor, 200 MW Gen	50 MW Motor, 100 MW Gen	100 MW Motor, 150 MW Gen	150 MW Motor, 200 MW Gen
1	37%	49%	53%	4.701	6.248	7.796
2	37%	47%	46%	4.440	6.501	8.057
3	37%	46%	45%	4.473	5.794	7.114
4	36%	51%	54%	3.993	6.956	8.739

Table 5.10 shows that reliability improvement increased from Column B to C for all the scenarios but that is not the case when moving from Column C to D. Scenario 2 and 3 show a reduction in reliability improvement while Scenario 1 and 4 show an increase in the reliability improvement. This is due to the 11pm hour being made idle for Scenario 1 and 4 while charging took place for Scenario 2 and 3. Charging at 11 pm added to the loss of load in Scenario 2 and 3 thereby reducing the reliability when compared to Scenario 1 and 4. The profit generally increased with an increase in both generator size and motor size. Scenario 4 gave the least profit when the lowest generator and motor size are used but with an increase in the rating of both the generator and the motor, the profit was the most out of all scenarios as seen in Column F and G. These different scenarios gave different results in terms of the reliability improvement and the profit when the motor and generator size are varied. The best scenario can be obtained by optimisation to give the best reliability and profit combination.

The analysis is performed at different wind penetration and the results are shown in Fig 5.8.

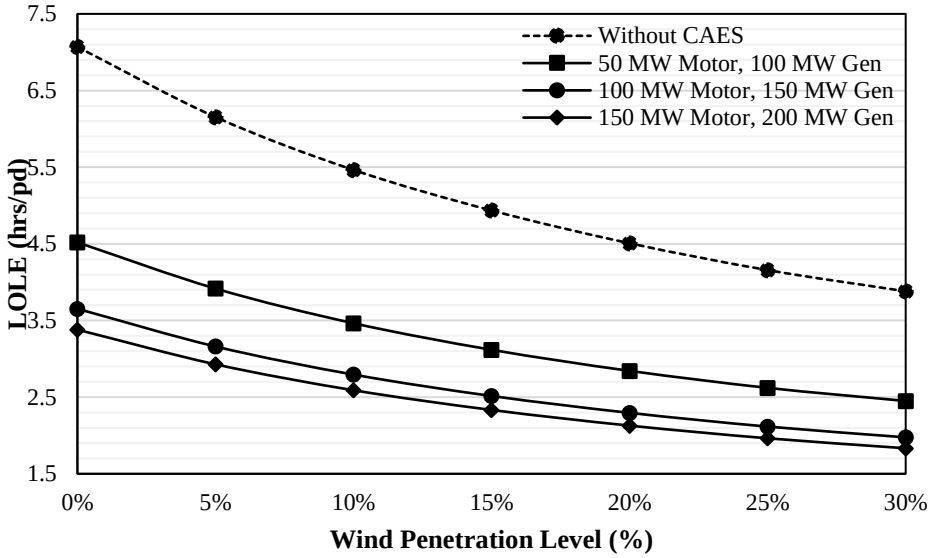

Fig. 5.8: Variation of different CAES generator and motor size at different wind penetration

Fig 5.8 shows that the maximum generator and motor size gave the most reliability contribution for all the wind penetration level while the 50 MW motor and 100 MW generator gave the least reliability contribution for all the wind penetration level. Also, the incremental benefits gotten from an increase in generator and motor size reduced. Fig 5.8 also shows that the reliability contribution from the three generators relative to one another remains relatively constant for the different wind penetration level.

5.6 Energy Management of the CAES for an Annual Reliability Evaluation

The reliability of the electric power system can be improved with appropriate energy management strategy. The proposed diurnal period analysis in Chapter 4 assumes that each season consists of days with similar diurnal profile or characteristics. Each day consists of a diurnal cycle of 24-hours and this diurnal cycle is further divided into sub-periods. The period analysis is extended to an annual assessment in this section. In the annual period analysis, the entire year is divided into four seasons namely; spring, summer, fall and winter season.

Table 5.11 shows the duration of the four seasons in the year and their contributions to the

annual LOLE. It shows that the winter season contributes about 85% to the annual LOLE while the spring, summer and fall combined to contribute about 15% to the annual LOLE. This study uses the Saskatchewan load profile where the system load peaks during the winter season, while the system load during the other three seasons, i.e. March 1st to October 31st is relatively low.

Table 5.11: Seasonal period LOLE in a year

Periods	**Duration**	**LOLE(hr/pd)**	**%LOLE**
Winter	November-February	7.0749	84.52%
Spring	March-May	0.5747	6.87%
Summer	June-August	0.4526	5.41%
Fall	September-October	0.2677	3.20%
Total		8.3699 hr/yr	100%

The high LOLE for the winter season in Table 5.11 shows that it has very high demand and deficient capacity while the low LOLE for the other three seasons shows that the load is relatively low and there is surplus capacity. There is a potential to move the surplus energy from spring, summer and fall season to the winter season in a way that the reliability of the system is improved. This potential is explored in this section utilizing the CAES. In addition to daily arbitrage as considered in Section 5.5, the operation of the CAES should also consider the seasonal effect on merchant profit when energy is moved from one season to another.

5.6.2 Application to a Test System

The transfer of energy from the off-peak season to the peak season can create loss of load event in the off-peak season thereby increasing the LOLE. To mitigate this, it is assumed that half of the SOC obtained from the off-peak season is used in the peak period of the off-peak season while the remaining half is transferred to the peak winter season. The effect of the energy transfer on the different seasons in the off-peak season is also considered in this study. It is assumed in the presented analysis that the motor running the compressor is operated at its rated capacity of 100 MW for all the charging hours in the off-season. With the CAES used in the study, the power

available to the load at every hour of the peak period of each day in the peak season is 273.2 MW. It is assumed that the generator is sized appropriately at this rating to accommodate the maximum power available. The three seasons constituting the off-season are represented with three different diurnal load models as shown in Fig. 4.3, the winter season is considered as the peak season in this study assuming an annual peak load of 2700 MW.

The four seasons contained in a year are represented by different load and wind profiles in a seasonal period analysis. The day in each season is further divided into sub-periods as shown in 5.12.

Table 5.12: Annual peak and off-peak hours for the four seasons

Season	**Peak hours**	**Days**	**Total peak hours**	**Total off-peak hours**	**Total idle hours**	**Total hours**
Spring	9^{th}-22^{nd}	March 1^{st} - May 31st	1288	920	-	2208
Summer	12^{th}-19^{th}	June 1^{st} – Aug 31^{st}	736	1472	-	2208
Fall	15^{th}-22^{nd}	Sept 1^{st}-Oct 31^{st}	488	976	-	1464
Winter	17^{th} -22^{nd}	Nov 1^{st}-Feb 28^{th}	720	960	1200	2880
Total			3232	4328	1200	8760

Table 5.12 shows the off-peak hours for each season where charging is done and the peak hours where discharge is carried out. The total hours available for charging the storage during the off-peak season is 3368 hours. These total off-peak seasons charging hour is an aggregation of the off-peak hours for the spring, summer and fall season.

Fig. 5.9 shows the energy transfer profile from one season to another.

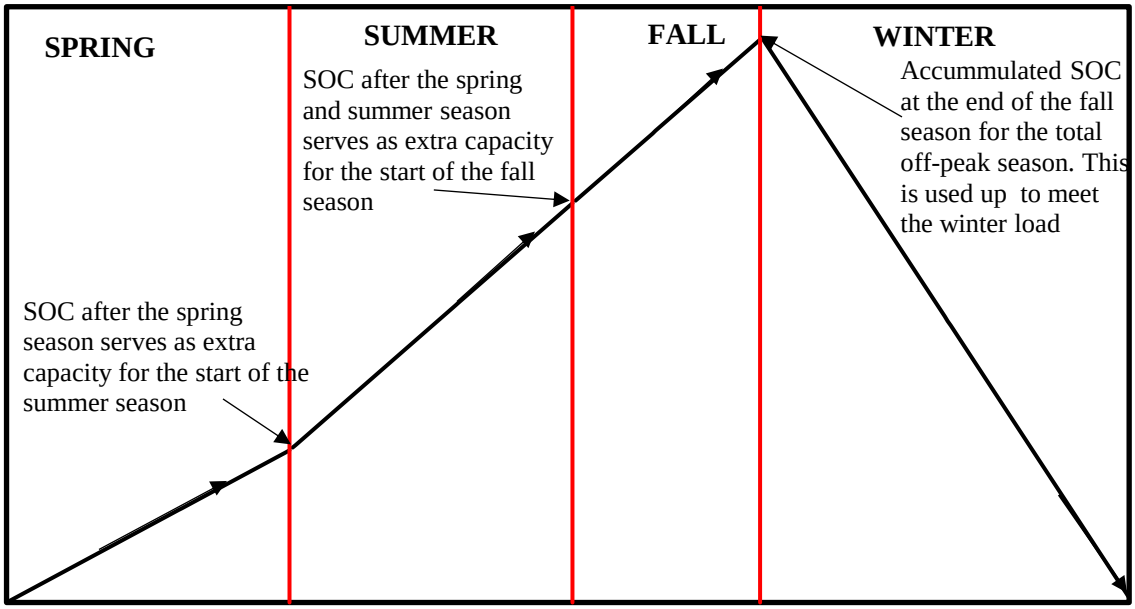

Fig. 5.9: Energy transfer from one season to another

The improvement in system reliability of the IEEE-RTS quantified by the reduction in LOLE due to CAES for the different seasons before and after energy transfer is shown in Table 5.13 for the 20% wind penetration level. The % reduction is calculated relative to when there was no CAES in the system.

Table 5.13: Reliability improvement before and after energy transfer for the 20% wind penetration

Season	**% LOLE Reduction before Energy Transfer**	**% LOLE Reduction after Energy Transfer**
Spring	-30%	-9%
Summer	-29%	-26%
Fall	11%	6%
Winter	-53%	-83%
Total	**-48%**	**-72%**

Table 5.13 shows that there is reduction in the reliability of the system for the spring and

summer season after energy was transferred. The reduction in reliability was large for the spring season and just a small reduction for the summer season. There was however, an increase in the reliability of the system for the fall and winter season. The increase is small for the fall season but very large in the winter season.

The reliability comparison and the ratio of the four seasons before and after energy transfer at the 20% wind penetration is shown in Table 5.14.

Table 5.14: Annual/seasonal LOLE comparison after energy transfer

A	B	C	D	E	F
SEASONS	**LOLE before energy transfer**	**%LOLE before energy transfer**	**LOLE after energy transfer**	**% LOLE after energy transfer**	**% change in LOLE after energy transfer**
Spring	0.2333	8%	0.3012	20%	29%
Summer	0.2108	8%	0.222	15%	5%
Fall	0.1945	7%	0.1851	12%	-5%
Winter	2.1168	77%	0.7845	53%	-63%
TOTAL	**2.7554**	**100%**	**1.4928**	**100%**	**-46%**

The contribution of the winter LOLE to the annual LOLE has been reduced from 77% to 53% as seen in Table 5.14. The spring season experienced the biggest increase from 8% to 20%. The result obtained in this evaluation can help utilities in the planning of the electric power system. It can also help in realising a more efficient maintenance procedure of the electric power system. This can be done by choosing the right period or season to carry out the maintenance of the system so that it has little or no effect on the overall system annual reliability.

Table 5.15 shows the result for the profit from energy arbitrage before and after energy is transferred.

Table 5.15: Profit comparison before and after the energy transfer

Season	Profit before Energy Transfer **($M)**	Profit after Energy Transfer **($M)**
Spring	4.633	1.104
Summer	23.432	9.109
Fall	1.777	-0.251
Winter	8.417	13.669
Total	**38.259**	**23.63**

Table 5.15 shows that the profit reduced for the spring, summer and fall season after energy transfer. The profit for the winter season increased after energy transfer because of the extra energy transferred from the off-peak season. The summer season shows a huge profit before energy transfer compared to the other seasons, this is due to the big gap between the off-peak pool price and the peak price and the complete capacity available for arbitrage. The profit for the fall season is relatively low before energy transfer which is due to the small gap between peak pool price and off-peak pool price. After energy transfer, there was a loss instead of a profit for the fall season. The relatively small gap between the peak pool price and the off-peak pool price in combination with the reduced capacity accounts for the loss in the fall season. Storing the charge from the off-peak season for use during the peak season improves the overall system reliability but can have adverse impact on the profit. The major objective of the merchant is to make profit without any consideration for the system reliability. An optimisation technique can be applied to determine the best way to transfer energy maximizing both the profit for the merchant and the system reliability. Also, appropriate incentive can be introduced to make the merchant act in a way that the system reliability is improved. The analysis above is done considering 20% wind penetration in the IEEE-RTS. Fig. 5.10 shows the analysis for wind penetration ranging from 5% to 30%. The results before and after energy is transferred for all the seasons are shown in Fig. 5.10 for the four seasons.

Fig. 5.11 shows the annual LOLE before energy transfer and after energy transfer.

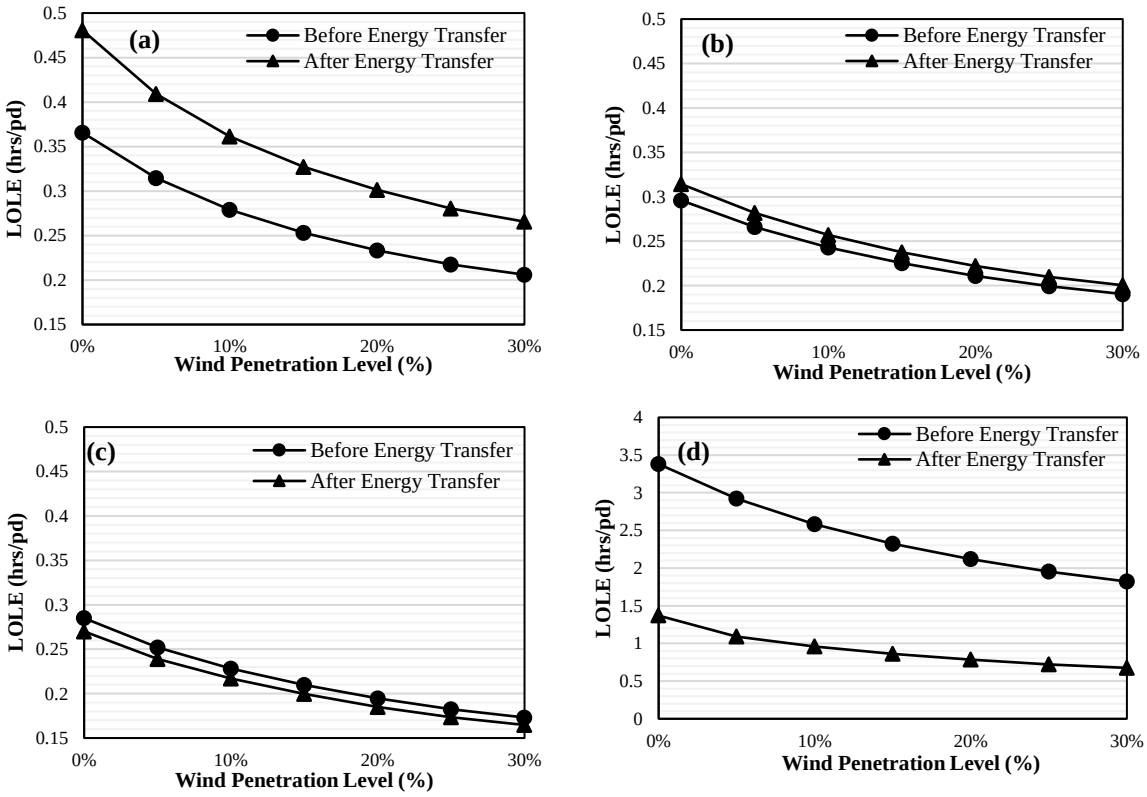

Fig. 5.10: Effect of energy transfer on LOLE for (a) spring (b) summer (c) fall and (d) winter

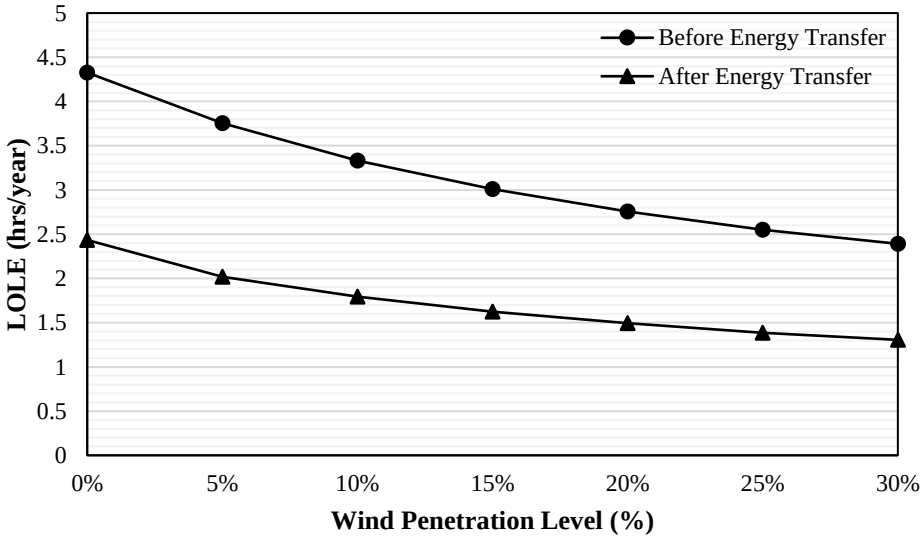

Fig. 5.11: Annual LOLE after energy transfer

Fig. 5.10 shows that the reliability of the spring and summer season reduced after energy was transferred, it shows a greater reduction for the spring season than the summer season. There was however, an increase in reliability for the fall and winter season after energy transfer, the increase is slight for the fall season while for the winter season, the increase in significant. This increase is due to the extra capacity available from the energy transferred. Fig 5.10 also shows that the effect of the energy transfer on the three seasons constituting the off-peak season is very minimal. This is due to their low LOLE which is negligible when compared to the winter LOLE. The effect of the energy transfer on the winter season is very substantial as seen in Fig 5.10d. Fig 5.11 shows a significant improvement in system reliability for the entire year after energy was transferred to the winter season. The improvement in system reliability quantified by the reduction in LOLE due to CAES for the entire year before and after energy transfer is shown in Table 5.16 for the different wind penetration levels.

Table 5.16: Reliability improvement due to CAES operation for the annual energy management

A	B	C	D	E	F
	LOLE (hrs/yr)			% Reduction in LOLE due to CAES	
Wind Penetration Level	Without CAES	CAES before energy transfer	CAES after energy transfer	Before energy transfer	After energy transfer
0%	8.3418	4.327	2.4344	-48%	-71%
5%	7.2461	3.7539	2.0191	-48%	-72%
10%	6.4315	3.3308	1.7938	-48%	-72%
15%	5.8108	3.0085	1.6248	-48%	-72%
20%	5.3127	2.7554	1.4928	-48%	-72%
25%	4.9065	2.5499	1.3865	-48%	-72%
30%	4.5897	2.3914	1.3059	-48%	-72%

Table 5.16 shows the reliability improvement remained relatively constant at 48% before energy was transferred for the different wind penetration level. It remained at 72% after energy was transferred. The annual LOLE reduced by about 24% after the energy is transferred from the off-peak seasons to the winter season for varying wind penetration levels. The relatively low LOLE

values for the three seasons constituting the off-peak season is the reason why energy transfer can be done from the off-peak season to the peak season without adversely affecting the overall system reliability.

5.7 Conclusion.

This chapter presents studies to analyze how the operation of a CAES affects the profit from energy arbitrage and the overall reliability of the electric power system. In a market structure where the CAES is owned by a merchant, the major objective of the merchant is to make profit by exploiting short-term differences in electricity prices by buying low and selling high. Based on this objective, an assumption is made that the CAES motor/compressor is operated at its rated capacity for all the hours of the charging period with priority given to the wind farm to charge the storage. A period analysis is used in this chapter which makes use of a charging period, discharging period and an idle period where the merchant neither charges or discharges. Analysis is done based on this method using an analytical technique. The charging, discharging and idle period were varied and four different scenarios were considered. It was observed that the scenario that gave the best reliability improvement was not the same as the one that gave the highest profit. This shows that one operating principle of the CAES may achieve a high reliability improvement to the system but may adversely affect the profit from energy arbitrage, while another operating practice may provide maximum profit as desired by the CAES merchant but with adverse impact to the overall system reliability. Sensitivity studies were carried out by varying the motor size and generator size. It was observed that the choice of the motor/compressor and generator size significantly influences the reliability level and the profit to be achieved. Energy management of the CAES for an annual reliability evaluation was done. The method used was to divide the entire year into four seasons. The spring, summer and fall seasons were considered as off-peak season while the winter season was considered as peak season based on their LOLE contribution to the annual LOLE. Energy transfer was done by transferring excess energy from the off-peak season to the peak season. There was a significant reduction in the winter season LOLE after the energy

was transferred. This significant reduction in the winter LOLE led to a corresponding significant reduction in the annual LOLE. The profit the merchant could make for the year however, was reduced after energy was transferred to the winter season. An optimisation technique can be used to determine the best way to transfer energy, maximizing both the profit for the merchant and the system reliability. The studies indicate the need to develop policies and incentives which should be structured in such a way that merchant operating practices do not adversely affect the system reliability. The results obtained can serve as a good reference for utilities for long term planning purposes. This study does not include the maintenance schedule of generating system. If maintenance is to be included in the analysis, the operation of the CAES will be affected based on the units available for generation. The excess capacity available for transfer to the peak season will also be affected by the amount of generating unit available when maintenance is scheduled.

6. SUMMARY AND CONCLUSIONS

Renewable energy as a source of electrical power in the electrical power system has seen substantial growth in recent times and is expected to keep growing. The adoption of Renewable Portfolio Standard (RPS) by different countries and jurisdictions, the modernisation of the grid and the increased interest of utilities in micro grid and smart grid have aided in the upward trend of renewable energy utilisation. Wind energy is one form of renewable energy that has gained widespread acceptance due to its huge potential for large scale power production and its minimal environmental pollution. An increase in wind energy in the system however introduce challenges in maintaining the system reliability. Wind is intermittent and variable in nature and is unable to accurately follow demand. This behavior of wind has placed a limitation on the amount of wind energy the power system can absorb while maintaining system stability and reliability. Energy storage can be incorporated to increase wind energy utilisation in the power system. Energy storage can reduce the risk with increasing wind penetration in the system by absorbing the variability of wind. It also has the potential of shifting energy from periods of low demand to periods where demand is high. This thesis is focussed on the CAES which has high potential to be used on a grid scale level. The potentials of the CAES and its contribution to the reliability studies in this thesis is assessed using quantitative tools. The thesis presents a hybrid technique comprising of the MCS technique and the analytical technique to assess the reliability improvement on the system when the CAES is used. The MCS technique is used in modelling the state of charge (SOC) of the CAES during the charging period while the analytical technique is used in the adequacy assessment of the different periods. The purpose of this research was to quantitatively assess the reliability contribution of the CAES when it is incorporated into the system. The effect of the merchant operation of the CAES on system reliability and profit was studied. The potential of the CAES to shift energy from the off-peak season to the peak season was investigated and the effect of the energy shifting on system reliability and profit was discussed.

Chapter 1 presents an introduction of the basic concept regarding power system reliability. The chapter also includes description of electric power systems with wind and energy storage, the

researches done on electric power system with CAES and the research gap this thesis planned to address. The research problem statement and thesis outline were presented.

Chapter 2 describes the basic techniques in carrying out the generating system adequacy evaluation of power system. The deterministic techniques and the probabilistic techniques used in reliability evaluation were described. The MCS and analytical technique comprising the probabilistic techniques were explained in detail. The sequential MCS and analytical techniques were used in this thesis. The reliability evaluation of a wind integrated system was explained. The chapter describes the process of modelling the different component of the power system; the load, the conventional generation, wind power and the overall system risk model. A detailed method for generating artificial wind speed using ARMA model was explained and its modelling described extensively. The concept of modelling the wind power as a negative was explained. The concept of the period analysis, the reason for employing the period analysis in incorporating the CAES into the electric power system were highlighted in Chapter 2.

Chapter 3 describes the importance and the need of energy storage in a wind integrated power system. It further described the different energy storage types available. The relative advantage of one storage type over another was discussed with the aid of different figures. The way the CAES works was explained by describing its major section and components and how these components interact with one another. Existing and proposed CAES plants around the world were highlighted, and their differentiating characteristics were explained in detail. The two earliest installed CAES plants were reviewed. Their technical specifications and the differences in design and applications were outlined. The CAES model used in this research made use of the Huntorf plant characteristics. The different applications of the CAES and its application to the research outlined in this thesis were discussed. The different ways the CAES technology had evolved over the years were shown. The features of the CAES at the various stages of evolution were outlined as well. Mathematical models for representing the CAES power flow were explained in detail in this chapter. These mathematical models were applied in developing the SOC model for the charging period and the generation model for the discharge period for the research work described in this thesis.

Chapter 4 proposes a diurnal hybrid approach in developing the reliability model for the CAES. The chapter also presents details on the incorporation of correlation between the wind speed and the load in the development of the reliability modelling for the CAES. The proposed diurnal hybrid approach divides a year into seasons, and assumes that each season consists of days with similar diurnal profile or characteristics. Each day consists of a diurnal cycle of 24-hours and this diurnal cycle is further divided into two sub-periods of off-peak and peak period. Charging of the CAES takes place during the off-peak period, while discharging occurred during the peak period where demand is very high. Discharge was also done at other times during a loss of load scenario. A combination of two techniques of MCS and analytical are used to evaluate the system reliability indices. The MCS technique is used to develop the SOC model during the charging period recognizing the time chronology and the correlation between the variation in the wind, the load and the SOC of the storage, while the analytical technique is used to obtain the system reliability indices in each sub-period by convolving the generation model in the form of discrete probability distribution with the load model.

Three different operating scenarios are used to study the effect of incorporating the CAES in an electric power system in Chapter 4. Two different operating periods are studied for the three scenarios by varying the charging and discharging period. The studies conducted on the different scenarios and cases show that, for the scenario and case that gave the best reliability improvement to the system, the CAES was connected to the grid giving it access to the off -peak conventional power. The charging and discharging period was also chosen in such a way that the major portion of the loss of load event was located at the discharge period when the CAES was not used and when there was no wind in the system; about 89% in this case. With an increase in wind penetration, the reliability improvement the CAES provides to the system also increased. A combination of how the CAES is connected, either connected directly to maximize wind resources or connected to the grid, and the choice of the charging and discharging period will determine the extent of the benefit that can be derived from the CAES for electric power system reliability improvement. The three scenarios considered can have varied applications in the electric power system. The ownership of the CAES is not enough, the right strategy in operating the CAES is

very important. The different strategies adopted for the operation the CAES will determine the extent of the benefit that can be derived for power system reliability improvement.

Chapter 5 considers the ownership of the CAES by a merchant and presents studies to analyze how the operation of a CAES affects the profit from energy arbitrage and the overall reliability of the electric power system. A merchant's objective is to make profit and he does this by exploiting short term difference in electricity prices by buying low and selling high. In the studies considered, the CAES motor/compressor is operated at its rated capacity for all the hours of the charging period with priority given to the wind resources to charge the storage. The 2-period used in Chapter 4 is modified to a 3-period in this chapter. The 3-period consists of a charging, discharging and an idle period. The merchant neither buys (charges) or sells (discharges) during the idle period because the price difference relative to the other two periods is not wide enough for him to make profit. Different studies were carried out to obtain the effect of the merchant activities on system reliability and the profit the merchant can make. First, the charging, discharging and idle periods were varied and four different period variations were considered using same motor and generator rating for all four scenarios. It was observed that the scenario that gave the best reliability improvement didn't give the best profit. A couple of factors account for this, the correlation between the load and the price is one factor, the amount of charging, discharging and idle hours available is another key factor. The difference in load level between the charging period and the discharge period also plays a significant role in the level of profits and reliability obtained. One scenario gave the best reliability improvement and a relatively high profit, this is due to the high correlation between the price and the load so that when the load is high, the price is high as well and when the load is at its lowest, and the price is at its lowest as well which leads to the maximum profit. In terms of the maximum reliability improvement, the merchant sells at these high load periods which leads to extra capacity available to meet the system load. The motor and generator size were varied to observe the effect on the overall system reliability. Study shows that the choice of the motor/compressor and generator size to be used will be informed by a combination of the reliability level and profit to be achieved.

Energy management of the CAES for an annual reliability evaluation was done in Chapter

5. The entire year was split into four seasons. The spring, summer and fall seasons were considered as off-peak season while the winter season was considered as peak season. This was based on the individual season's LOLE contribution to the annual LOLE. Energy management was done by transferring excess energy from the off-peak season to the peak season. There was a significant improvement in the system reliability after energy was transferred compared to when energy wasn't transferred. A right energy management strategy can lead to significant reliability improvement in the electric power system. The profit the merchant can make for the year however, was reduced after energy was transferred. An optimization tool can be used to address the opposing effect of energy transfer on the system reliability and profit and to obtain the right strategy to operate the CAES to get both an increase in reliability improvement and profit after energy transfer. Policies and incentives can also be introduced to ensure the merchant operating practices does not adversely affect the system reliability. The results obtained can serve as a good reference for utilities for long term planning purposes.

LIST OF REFERENCES

[1] R. Billinton and R. N. Allan, “Reliability evaluation of power systems”. Springer, 1996.

[2] R. Billinton, R. N. Allan, and L. Salvaderi, *Applied Reliability Assessment in Electric Power Systems*. New York: IEEE Press, 1991.

[3] R. N. Allan, R. Billinton, and S. H. Lee, “Bibliography of the Application of Probability Methods in Power System Reliability Evaluation 1977-1982,” *Power Eng. Rev. IEEE*, vol. PER-4, no. 2, pp. 24–25, 1984.

[4] R. N. Allan, R. Billinton, A. M. Breipohl, and C. H. Grigg, “Bibliography on the application of probability methods in power system reliability evaluation: 1987-1991,” *Power Syst. IEEE Trans.*, vol. 9, no. 1, pp. 41–49, 1994.

[5] R. Billinton, M. Fotuhi-Firuzabad, and L. Bertling, “Bibliography on the application of probability methods in power system reliability evaluation 1996-1999,” *Power Syst. IEEE Trans.*, vol. 16, no. 4, pp. 595–602, 2001

[6] R. N. Allan, R. Billinton, A. M. Breipohl, and C. H. Grigg, “Bibliography on the application of probability methods in power system reliability evaluation,” *Power Syst. IEEE Trans.*, vol. 14, no. 1, pp. 51–57, 1999

[7] R. Billinton, “Bibliography on the Application of Probability Methods In Power System Reliability Evaluation,” *Power Appar. Syst. IEEE Trans.*, vol. PAS-91, no. 2, pp. 649–660, 1972.

[8] M. Jaccard, “Renewable Portfolio Standard,” E.-C. C. J. Cleveland, Ed. New York; Elsevier, 2004, pp. 413-421.

[9] R. Karki, D. Dhungana, S. Shimu and R. Billinton, "Reliability evaluation incorporating the load following capability of wind generation," *2013 26th IEEE Canadian Conference on Electrical and Computer Engineering (CCECE)*, Regina, SK, 2013, pp. 1-4.

[10] SaskPower to develop wind, solar and geothermal power to meet up to 50% renewable target. [Online]. Available: http://www.saskpower.com/about-us/media-information/saskpower-targets-up-to-50-renewable-power-by-2030/ [Accessed: 29-Aug-2017].

[11] Global Wind Energy Council, “Global statistics” [Online]. Available: http://www.gwec.net/global-figures/graphs/ [Accessed: 29-Aug-2017].

[12] Canadian Wind Energy Association, Canwea, “Installed Capacity” [Online]. Available: http://canwea.ca/wind-energy/installed-capacity/ [Accessed: 29-Aug-2017].

[13] P. Hu, R. Karki and R. Billinton, “Reliability evaluation of generating systems containing wind power and energy storage” IET Generation Transmission and Distribution, vol. 3, pp. 783-791, August 2009.

[14] Z.Y. Gao and P. Wang, “Impacts of Energy Storage on Reliability of Power Systems with WTGs” in *IEEE International Conference on Probabilistic Methods Applied to Power Systems, 2010 IEEE 11th International Conference,* pp. 70-75, 2010.

[15] P. Giorsetto and K. F. Utsurogi, “Development of a new procedure for reliability modeling of wind turbine generators”, *IEEE Transactions on Power Apparatus and Systems*, Vol. 102, no. 1, January, 1983, pp. 134-143.

[16] X. Wang, H. Dai, and R. J. Thomas, “Reliability modeling of large wind farms and electric utility interface systems”, *IEEE Transactions on Power Apparatus and Systems*, Vol. 103, no. 3, March, 1984, pp. 569-575.

[17] R. Karki, P. Hu, “Wind power simulation model for reliability evaluation”, *Proceedings of the IEEE Canadian Conference on Electrical and Computer Engineering*, Saskatoon, May 1-4, 2005, pp. 541-544.

[18] R. Karki, P. Hu, R. Billinton, “A simplified wind power generation model for reliability evaluation”, *IEEE Transactions on Energy Conversion*, Vol. 21, no. 2, June, 2006, pp.533 – 540.

[19] R. Karki, P. Hu, R. Billinton, “Reliability evaluation of a wind power delivery system using an approximate wind model”, *41st International Universities Power Engineering Conference*, Newcastle, UK, September 6th-8th, 2006.

[20] P. B. Eriksen, T. Ackermann, et al., “System operation with high wind penetration”, *IEEE Power and Energy Magazine*, Vol. 3, no. 6, November/December, 2005, pp. 65-74.

[21] Energy Storage: [Online]. Available: http://energystorage.org/energy-storage [Accessed: 29-Aug-2017].

[22] J.W. Tester, E.M. Drake, M.J. Driscoll, M.W. Golay and W.A. Peters, “Sustainable Energy; Choosing among options”. The MIT Press, 2005.

[23] R. B. Schainker and M. Nakhamkin, “Compressed-Air Energy Storage (CAES): Overview, Performance and Cost Data for 25MW-220MW Plants,” *IEEE Transactions on power Apparatus and Systems,* Vol. PAS-104, pp. 791-795, 1985.

[24] Y. S. H. Najjar and M. S. Zaamout, “Performance analysis of compressed air energy storage (CAES) plant for dry regions,” *Energy Conversion Management*, Vol. 39, pp. 1503-1511, 1998.

[25] M. Ni, Z. Zhou and D. Osborn, “Economic and Operation benefits of Energy Storage- a Case Study of MISO,” *Power and Energy Society General Meeting, 2012 IEEE,* pp. 1-7, 2012.

[26] B. Cleary, M. Conlon, A. Duffy, V. Fthenakis and A. O'Connor, "Assessing the benefits of compressed air energy storage on the 2020 Irish power system," *Power Engineering Conference*

(UPEC), 2013 48th International Universities', Dublin, , pp. 1-6, 2013.

[27] H. Ibrahim, A. Bourji, M. Ghandour and A. Merabet, "Optimization of compressed air storage's volume for a stand-alone wind-diesel hybrid system," *Electrical Power & Energy Conference (EPEC), 2013 IEEE,* pp. 1-7, 2013.

[28] B. Bagen and R. Billinton, "Incorporating well-being considerations in generating systems using energy storage" *IEEE Transactions on Energy Conversion*, vol. 20, pp. 225-230, 2003.

[29] R. Billinton, Bagen and Y. Cui, "Reliability evaluation of small stand-alone wind energy conversion systems using a time series simulation model,*" IEE Proceedings- Generation, Transmission and Distribution*, vol. 150, pp. 96-100, 2003.

[30] B. Bagen and R. Billinton, "Impacts of Energy Storage on Power System Reliability Performance", *Electrical and Computer Engineering, 2005. Canadian Conference*, pp. 494-497, 2005.

[31] B. Bagen and R. Billinton, "Reliability Cost/Worth associated with wind energy and energy storage utilization in electric power systems", *International Conference on Probabilistic Methods Applied to Power Systems, 2008 IEEE 10th* pp. 1-7, 2008.

[32] X. Liu, S. Islam, A.A. Chowdhury and D.O. Koval, "Reliability Evaluation of a Wind-Diesel-Battery Hybrid Power System" *Industrial and Commercial Power Systems Technical Conference, 2008. ICPS 2008. IEEE/IAS,* pp. 1-8, 2008.

[33] R. Zheng and J. Zhong, "Generation Adequacy Assessment for Power Systems with Wind Turbine and Energy Storage", I*nnovative Smart Grid Technologies (ISGT), 2010,* pp. 1-6, 2010.

[34] Z.Y. Gao and P. Wang, "Reliability Evaluation of Power Systems with WTGs and Energy Storage", *IPEC Conference Proceedings,* pp. 654-659, 2010.

[35] P. C. Symons, "Opportunities for energy storage in stressed electricity supply systems," *2001 Power Engineering Society Summer Meeting. Conference Proceedings,* Vancouver, BC, Canada, vol.1, pp. 448-449, 2001.

[36] S. M. Schoenung and C. Burns, "Utility energy storage applications studies," in *IEEE Transactions on Energy Conversion*, vol. 11, no. 3, pp. 658-665, Sep 1996.

[37] H. Khani and R. Dadash Zadeh, "Energy storage in an open electricity market with contribution to transmission congestion relief," *2014 IEEE PES General Meeting, Conference & Exposition*, National Harbor, MD, 2014, pp. 1-5.

[38] H. T. Le, S. Santoso and T. Q. Nguyen, "Augmenting Wind Power Penetration and Grid Voltage Stability Limits Using ESS: Application Design, Sizing, and a Case Study," in *IEEE Transactions on Power Systems*, vol. 27, no. 1, pp. 161-171, Feb. 2012.

[39] Ha Thu Le and S. Santoso, "Increasing wind farm transient stability by dynamic reactive compensation: Synchronous-machine-based ESS versus SVC," *IEEE PES General Meeting*, Minneapolis, MN, pp. 1-8, 2010.

[40] Á. Ortega and F. Milano, "Generalized Model of VSC-Based Energy Storage Systems for Transient Stability Analysis," in *IEEE Transactions on Power Systems*, vol. 31, no. 5, pp. 3369-3380, Sept. 2016.

[41] T. Xia, L. He, N. An, M. Li and X. Li, "Electromechanical transient modeling research of energy storage system based on power system security and stability analysis," *2014 International Conference on Power System Technology*, Chengdu, pp. 221-226, 2014.

[42] S. Kahrobaee and S. Asgarpoor, "Optimum planning and operation of compressed air energy storage with wind energy integration," *2013 North American Power Symposium (NAPS)*, Manhattan, KS, pp. 1-6, 2013.

[43] M. Ghofrani, A. Arabali, M. Etezadi-Amoli and M. S. Fadali, "A Framework for Optimal Placement of Energy Storage Units Within a Power System With High Wind Penetration," in *IEEE Transactions on Sustainable Energy*, vol. 4, no. 2, pp. 434-442, April 2013.

[44] H. Lund, G. Salgi, B.Elmegaard, and A.N. Andersen, "Optimal Operation Strategies of Compressed Air Energy Storage (CAES) on Electricity Spot Markets with Fluctuating Prices," *Applied Thermal Engineering*, vol. 29, issues 5–6, pp 799-806, April 2009.

[45] B. Mauch, P. M.S. Carvalho, J. Apt, "Can a wind farm with CAES survive in the day-ahead market?" *Energy Policy*, issue 48, pp. 584– 593, 2012.

[46] R. Madlener, and J. Latz, "Centralized and Decentralized Compressed Air Energy Storage for Enhanced Grid Integration of Wind Power," *Institute for Future Energy Consumer Needs and Behavior (FCN)*, Sep. 2010.

[47] D. J. Swider, "Compressed Air Energy Storage in an Electricity System With Significant Wind Power Generation," in *IEEE Transactions on Energy Conversion*, vol. 22, no. 1, pp. 95-102, March 2007.

[48] J.B. Marean, "Compressed Air Energy Storage Engineering and Economic Study," report prepared for New York State Energy Research and Development Authority, Dec. 2009.

[49] S. Succar, and R.H. Williams, "Compressed Air Energy Storage: Theory, Resources, and Applications for Wind Power," Princeton Environmental Institute, Energy Systems Analysis Group, Apr. 2008.

[50] M. Raju, S. K. Khaitan, "Modeling and simulation of compressed air storage in caverns: A case study of the Huntorf plant," *Applied Energy* issue 89, pp. 474-481, 2012.

[51] R. Egidi, "Technical and Economic Analysis of Various Power Generation Resources

Coupled with CAES Systems," National Energy Technology Laboratory, DOE/NETL-2011/1472, May 2011.

[52] I. Arsie, V. Marano, G. Nappi, and G. Rizzo, "A Model of a Hybrid Power Plant with Wind Turbines and Compressed Air Energy Storage," *Proceedings of PWR2005,* Apr. 2005.

[53] E. Fertig, and J. Apt, "Economics of compressed air energy storage to integrate wind power: A case study in ERCOT," *Energy Policy,* issue 39 pp. 2330-2342, 2011.

[54] R. Billinton, "Criteria used by Canadian utilities in the planning and operation of generation capacity", *IEEE Transactions on Power Systems,* Vol. 3, no. 4, November, 1988, pp. 1488-1493.

[55] R. Billinton and R. N. Allan, *Reliability Assessment of Large Electric Power Systems.* Springer, 1988.

[56] A. Alferidi, "Evaluating the Reliability contribution of Photovoltaics in Electric Power Systems," University of Saskatchewan, Saskatoon, 2012.

[57] R. Billinton and R. N. Allan, *Reliability Evaluation of Engineering Systems: Concepts and Techniques.* Springer, 1992.

[58] R. N. Allan, A. M. L. da Silva, A. A. Abu-Nasser and R. C. Burchett, "Discrete Convolution in Power System Reliability," *Reliability, IEEE Transactions on,* vol. R-30, pp. 452-456, 1981.

[59] M. Mazundar and D. P. Gaver, "A Comparison of Algorithms for Computing Power Generating System Reliability Indices," *Power Apparatus and Systems, IEEE Transactions on,* vol. PAS-103, pp. 92-99, 1984.

[60] R. Billinton and W. Li, *Reliability Assessment of Electrical Power Systems Using Monte Carlo Methods,* Plenum Publishing, New York, 1994.

[61] P. Hu, "Reliability Evaluation of electric Power Systems Including Wind Power and Energy Storage", University of Saskatchewan, Saskatoon, 2009.

[62] Canadian Electricity Association-Equipment Reliability Information System (CEA-ERIS), "Generation Equipment States Annual Report", 1996.

[63] R. Billinton, H. Chen, and R. Ghajar, "Time-series models for reliability evaluation of power systems including wind energy," Microelectronics Reliability, vol. 36, no. 9, pp. 1253–1261, 1996.

[64] R. Billinton, R. Karki, Y. Gao, D. Huang, P. Hu and W. Wangdee, "Adequacy Assessment Considerations in Wind Integrated Power Systems," in *IEEE Transactions on Power Systems*, vol. 27, no. 4, pp. 2297-2305, Nov. 2012.

[65] R. Billinton and Y. Gao, "Multistate Wind Energy Conversion System Models for Adequacy Assessment of Generating Systems Incorporating Wind Energy," in *IEEE Transactions on Energy Conversion*, vol. 23, no. 1, pp. 163-170, March 2008.

[66] T. R. Oke, “Initial Guidance to Obtain Representative Meteorological Observations at Urban Sites,” Geneva, 2006.

[67] J. H. Seinfeld and S. N. Pandis, *Atmospheric Chemistry and Physics: From Air Pollution to Climate Change*, 2nd ed. Hoboken, New Jersey: WILEY, 2006.

[68] H. A. Sturges, “The choice of a class interval,” *J. Am. Stat. Assoc.*, vol. 21, no. 153, pp. 65–66, 1926.

[69] D. Dhungana, “Incorporating Correlation in the Adequacy Evaluation of Wind Integrated Power Systems,” University of Saskatchewan, Saskatoon, 2013.

[70] M. Padhee, “Incorporating wind power curtailment in reliability and wind energy benefit assessment,” University of Saskatchewan, Saskatoon, 2015.

[71] EPRI-DOE, "*Handbook of Energy Storage for Transmission and Distribution Applications*," EPRI, Palo Alto, CA, and the U.S. Department of Energy, Washington, DC, Tech. Rep. 1001834., Dec. 2003.

[72] Energy Storage Council, “Energy storage; the sixth dimension of the electricity production and delivery value chain.” [Online]. Available: http://assets.fiercemarkets.net/public/smartgridnews/sgnr_2008_0102.pdf [Accessed: 29-Aug-2017].

[73] Sandia Report, “DOE*/EPRI 2013 Energy Storage Handbook in Collaboration with NRECA*," Sandia National Laboratories, SAND2013-5131, July 2013.

[74] H. Chen, X. Zhang, J. Liu and C. Tan, “Compressed Air Energy Storage, Energy Storage - Technologies and Applications”, Dr. Ahmed Zobaa (Ed.), InTech, 2013.

[75] "Unlocking North Americas Vast Renewable Energy Potential Using Compressed Air Energy Storage. [Online]. Available: http://satl.ca/uploads/2/8/8/5/2885345/asist_-_september_17.pdf [Accessed: 29-Aug-2017].

[76] BBC Brown Boveri; Huntorf Air Storage Gas Turbine Power Plant. [Online]. Available: http://www.solarplan.org/Research/BBC_Huntorf_engl.pdf [Accessed: 29-Aug-2017].

[77] Underwater Compressed Air Energy Storage [Online]. Available: http://www.hydrostor.ca/ [Accessed: 29-Aug-2017].

[78] Toronto Hydro Pilots World's First Offshore Compressed-Air Energy Storage Project. [Online]. Available: http://www.greentechmedia.com/articles/read/toronto-hydro-pilots-worlds-first-offshore-compressed-air-energy-storage [Accessed: 29-Aug-2017].

[79] S. D. Lim, A. P. Mazzoleni, J. k. Park, P. I. Ro and B. Quinlan, "Conceptual design of ocean compressed air energy storage system," *2012 Oceans*, Hampton Roads, VA, 2012, pp. 1-8.

[80] EERA Technical report-CAES, X Luo and J Wang: Overview of current development on compressed air energy storage [Online]. Available: https://www.eera-set.eu/wp-content/uploads/Overview-of-Current-Development-on-Compressed-Air-Energy-Storage_EERA-report-2013.pdf [Accessed: 29-Aug-2017].

[81] B. Cleary, A. Duffy, A. O'Connor, M. Conlon and V. Fthenakis, "Assessing the Economic Benefits of Compressed Air Energy Storage for Mitigating Wind Curtailment," in *IEEE Transactions on Sustainable Energy*, vol. 6, no. 3, pp. 1021-1028, July 2015.

[82] J. Taylor and A. Halnes, "Analysis Of compressed air energy storage," *PCIC Europe 2010*, Oslo, 2010, pp. 1-5.

[83] Crotogino, Fritz & Mohmeyer, Klaus-Uwe and Scharf, Roland, "Huntorf CAES: More than 20 Years of Successful Operation". Nat Gas. 45. April 2001.

[84] S. Zunft, C. Jakiel, M. Koller, C. Bullough, "Adiabatic compressed air energy storage plants for the grid integration of wind power". *International Workshop on Large-Scale Integration of Wind Power and Transmission Networks for Offshore Windfarms.* 2006.

[85] C. Bullough, C. Gatzen, C. Jakiel, M. Koller, A. Nowi, S. Zunft, "Advanced adiabatic compressed air energy storage for the integration of wind energy". *Proceedings of the European Wind Energy Conference, EWEC, London.* 2004.

[86] National Energy Technology Laboratory (NETL), "Technical and economic analysis of various power generation resources coupled with CAES systems," DOE/NETL-2011/1472, 2011.

[87] R. B. Schainker, "Executive overview: energy storage options for a sustainable energy future," *IEEE Power Engineering Society General Meeting, 2004.* Denver, CO, Vol.2, pp. 2309-2314. 2004.

[88] V. Vongmanee and V. Monyakul, "A new concept of small-compressed air energy storage system integrated with induction generator," *2008 IEEE International Conference on Sustainable Energy Technologies*, Singapore, pp. 866-871. 2008.

[89] R. M. Ali, "Feasibility of compressed air energy storage to store wind on monthly and daily basis." Iowa State University, 2010.

[90] I. Arsie, V. Marano, G. Nappi, and G. Rizzo, A Model of a Hybrid Power Plant with Wind Turbines and Compressed Air Energy Storage, ASME Power, 2005.

[91] A. P. M. Subcommittee, “IEEE Reliability Test System,” *Power Appar. Syst. IEEE Trans.*, vol. PAS-98, no. 6, pp. 2047–2054, 1979.

[92] M. Milligan and K. Porter, “Wind capacity credit in the United States,” *2008 IEEE Power Energy Soc. Gen. Meet. - Convers. Deliv. Electr. Energy 21st Century*, pp. 1–5, Jul. 2008.

[93] S. Mishra, “Wind power capacity credit evaluation using analytical methods,” University of Saskatchewan, 2010.

[94] Understanding Electric Utility and De-regulation. Taylor & Francis Group, LLC. 2006.

[95] F. Graves, T. Jenkin, D. Murphy, “Opportunities for Electricity Storage in Deregulating Markets”, *The Electricity Journal*, Vol 12, Issue 8, pp. 46-56, October 1999.

[96] AESO Pool Price. [Online]. Available: http://ets.aeso.ca/ets_web/docroot/Market/Reports/HistoricalReportsStart.html [Accessed: 29-Aug-2017].